

ADDIS ABABA UNIVERSITY
ADDIS ABABA INSTITUTE OF TECHNOLOGY
DEPARTMENT OF CIVIL ENGINEERING

SHEAR MODULUS AND DAMPING RATIO VALUES OF SOILS COMMONLY FOUND IN HAWASSA

A THESIS SUBMITTED TO THE ADDIS ABABA INSTITUTE OF TECHNOLOGY, SCHOOL OF GRADUATE STUDIES, OF ADDIS ABABA UNIVERSITY

IN PARTIAL FULFILLMENT OF THE REQUIRMENT FOR THE DEGREE OF MASTER SCIENCE IN CIVIL ENGINEERING

BY
AYALEW GASHAW

ADVISOR
Dr. HADUSH SEGED

January 2012



ADDIS ABABA UNIVERSITY
SCHOOL OF GRADUATE STUDIES

SHEAR MODULUS AND DAMPING RATIO VALUES OF SOILS COMMONLY FOUND IN HAWASSA

By

Ayalew Gashaw

AAU, Institute of Technology

Approved by Board of Examiners

Dr. Hadush Seged Advisor	_____ Signature	_____ Date
Dr. Samuel Tadesse External Examiner	_____ Signature	_____ Date
Prof. Alemayehu Teferra Internal Examiner	_____ Signature	_____ Date
Ato. Zeru Belay Chairman	_____ Signature	_____ Date

DECLARATION

I hereby declare that the work which is being presented in this thesis entitles **"SHEAR MODULUS AND DAMPING RATIO VALUES OF SOILS COMMONLY FOUND IN HAWASSA"** is original work of my own, has not been presented for a degree in any other university and that all sources of material used for the thesis have been duly acknowledged.

---------- ----------

Ayalew Gashaw Date

(Candidate)

This is to certify that the above declaration made by the candidate is correct to the best of my knowledge.

---------- ----------

Dr. Hadush Seged Date

(Thesis Advisor)

ACKNOWLEDGEMENTS

First and for most, praise and thanks be to GOD almighty, for giving me the health and the strength to finish this work.

I am deeply indebted to my adviser Dr. Hadush Seged for his encouragement, supervision, and guidance he has provided me throughout my research. His critical comment and kind support gives me strength right from inception of the topic to the last minute of the research.

I would like to extend my gratitude to my instructors, Professor Dr. Ing. Alemayehu Teferra, Dr. Samuel Tadesse, and Dr. Messele Haile for giving me all the basics and their suggestions during progress reports.

I gratefully acknowledge to Hawassa municipality offices for their help during sample collection.

Last but not least, I would like to thank my course mate and AAiT Geotechnical Engineering laboratory people for their support, socialization, and help each other.

TABLE OF CONTENT

ACKNOWLEDGEMENTS i
TABLE OF CONTENT ii
SYMBOLS AND ABBREVIATION v
LIST OF TABLES vii
LIST OF FIGURES ix
LIST OF APPENDICES xiii
ABSTRACT xiv
CHAPTER 1- INTRODUCTION - 1
1.1 Background 1
1.2 Objective 2
1.2.1 General objective 2
1.2.2 Specific objectives 2
1.3 Materials and Methods 2
1.4 Scope of the study 3
1.5 Organization of the thesis 3
CHAPTER 2- LITERATURE REVIEW 4
2.1 Dynamic soil properties 4
2.1.1 General 4
2.1.2 Cyclic stress-strain behavior of soil 5
2.2 Some important properties of soil 7
2.2.1 Index properties 7
2.2.1.1 Particle shape 7
2.2.1.2 Specific gravity 7
2.2.1.3 Moisture content 8
2.2.1.4 Relative Density 8
2.2.1.5 In-situ unit weight 8

2.2.1.6 Consistency of clay soil 9
2.2.1.7 Grain size distribution 11
2.2.2 Soil compaction 11
2.2.3 Soil type 11
2.3 Shear modulus and damping ratio of soil 13
2.3.1 Method of determining shear modulus and damping ratio values of soil 13
2.3.2 Computation of Shear modulus and Damping ratio parameters 14
2.3.2.1 Shear modulus 14
2.3.2.2 Damping ratio 14
2.3.2.3 Maximum shear modulus 15
2.3.3 Factors affecting shear modulus and damping ratio values 18
2.3.4 Shear modulus and damping ratio values of soils 19
2.3.4.1 Sand 19
2.3.4.2 Clay 20
2.3.4.3 Other soil types 22
2.4 Cyclic simple shear testing system overview 24
CHAPTER 3- DATA COLLECTION AND TEST RESULTS 26
3.1 Sample collection 26
3.2 Description of the study area 27
3.2.1 Geographic and Climatic conditions 27
3.2.2 Geology and subsurface condition 27
3.2 Summary of some basic test results 29
3.3 Cyclic simple shear test 30
3.3.1 Specimen preparation 30
3.3.2 The compression stage 30
3.3.3 The cyclic simple shear stage 31
3.3.4 Presentation of cyclic shear test results 31
3.3.4.1 Axial loads and shear strain levels used 31
3.3.4.2 Shear stress and strain parameters 32

3.3.4.3 Hysteresis loops of test results 35
CHAPTER 4- DATA ANALYSIS AND DISCUSSION OF TEST RESULTS 39
4.1 Computation of shear modulus and damping ratio values 39
4.2 Effect of number of cycles 45
4.3 Shear modulus and Damping ratio values and curves 45
4.4 Effect of axial loads 49
4.5 Computation of maximum shear modulus 50
4.6 Modulus reduction (G/G_{max}) values 53
CHAPTER 5- COMPARISON OF TEST RESULTS WITH LITERATURE 55
5.1 Introduction 55
5.2 Shear modulus reduction 55
5.2.1 Comparison 55
5.2.2 Discussion 59
5.3 Damping ratio 59
5.3.1 Comparison 59
5.3.2 Discussion 63
CHAPTER 6- CONCLUSION AND RECOMMENDATION 64
6.1 Conclusion 64
6.2 Recommendation 65
LIST OF REFERENCES 66
APPENDICES 68
Appendix – A 69
Appendix – B 74
Appendix – C 78
Appendix – D 88
Appendix – E 92
Appendix – F 96

SYMBOLS AND ABBREVIATION

$a\ (k)$	parameter related to PI
AAiT	Addis Ababa Institute of Technology
A_{loop}	Area of hysteresis loop
ASTM	American Society for testing and Materials
e	Void ratio of soils
e_{max}	Maximum void ratio or void ratio in the loosest state
e_{min}	Minimum void ratio or void ratio in the densest state
G	Dynamic shear modulus
G_{max}	Maximum Dynamic shear modulus
G_s	Specific gravity of soil
MDD	Maximum dry density
OCR	Over consolidation ratio
OMC	Optimum moisture content
PI	Plastic index
V	Volume of the core-cutter
w	Moisture content of soil
W_1	Empty weight of core-cutter
W_2	Weight of core-cutter and the soil in the core-cutter

W_D	Dissipated energy
W_s	Maximum strain energy
γ	Shear strain
γ_s	Unit weight of soil
γ_c	Shear strain at the tip of hysteresis loop
γ_d	Dry unit weight of soil
γ_w	Unit weight of water
β	Damping ratio
ν_s	Shear wave velocity
ρ	Density of soil
σ	Normal stress
σ_m	Mean normal stress
τ	Shear stress
τ_c	Shear stress at the tip of hysteresis loop

LIST OF TABLES

Table 2.1: Specific gravities of some soil types.....7

Table 2.2: Range of plasticity index with its classification.....9

Table 2.3: Test procedures for measuring moduli and damping characteristics…….…...13

Table 3.1: Average high/low temperature in Hawassa……..27

Table 3.2: Average rain fall for Hawassa……...27

Table 3.3: Field and maximum densities, water contents and specific gravities……..……29

Table 3.4: Atterberg limits and Classification …….....29

Table 3.5: Summary of axial stresses and shear strains used in this study ……...32

Table 3.6: Shear stress and shear strain of pit 1 with 2.5 % strain and 400 KPa axial loads…….33

Table 4.1: Tabulation for shear modulus and damping ratio computation……40

Table 4.2: Typical calculation of shear modulus and damping ratio …….……...42

Table 4.3: Values of shear modulus and damping ratio for pit 1 with 400 KPa axial loads …….43

Table 4.4: Shear modulus and damping ratio values with 100 KPa axial pressures……..46

Table 4.5: Shear modulus and damping ratio values with 250 KPa axial pressures……..47

Table 4.6: Shear modulus and damping ratio values with 400 KPa axial pressures……..48

Table 4.7: *a* values with respect to plasticity index…….…….…….50

Table 4.8: Values of the parameters *PI*, a and e for all test pits .....…...51

Table 4.9: Typical G_{max} values of soils ……..……52

Table 4.10: : Computed G_{max} values with axial stresses of, *(a)* 100 kPa, *(b)* 250 kPa and*(c)* 400 kPa……..52

Table 4.11: Modulus ratio (G/G_{max}) values…….……...…….54

Table A-1: liquid limit and plastic limit test values of pit 1, 2 and 5…….……69

Table A-2: liquid limit tests of oven dried soils of pit 1 and 2…….……...71

Table C-1: Shear modulus values of pit 1…….…….78

Table C-2: Damping ratio values of pit 1…….....79

Table C-3: Shear modulus values of pit 2…….…….80

Table C-4: Damping ratio values of pit 2…….……..81

Table C-5: Shear modulus values of pit 3…….…….82

Table C-6: Damping ratio values of pit 3…….……..83

Table C-7: Shear modulus values of pit 4…….…….84

Table C-8: Damping ratio values of pit 4…….……..85

Table C-9: Shear modulus values of pit 5……..86

Table C-10: Damping ratio values of pit5…….…….……87

LIST OF FIGURES

Figure 2.1: Hysteretic stress-strain relationships at different strain amplitudes…….….6

Figure 2.2: Changes in soil properties with shear strain……..6

Figure 2.3: Modulus reduction and damping ratio curves of soils with different plasticity…....10

Figure 2.4: Hysteretic stress-strain response of soil subjected to cyclic loading……...15

Figure 2.5: Shear modulus reduction and damping ratio curves…….……..17

Figure 2.6: Variation of shear modulus with shear strain for sand……19

Figure 2.7: Damping ratio curve for sand……..20

Figure 2.8: Typical modulus reduction curves for saturated clay …….21

Figure 2.9: Damping ratio for saturated clay……..……..…….22

Figure 2.10: Shear modulus ratio vs. Shear strain of fine grained soil in South of Tehran ….....23

Figure 2.11: Damping ratio vs. Shear strain curve of fine grained soil in South Tehran ……..23

Figure 2.12: Cyclic simple shear test machine …….…….25

Figure 2.13: Visualization of the shearing stage of a specimen under cyclic simple shear test….25

Figure 3.1: Picture of test pit1……...…….26

Figure 3.2: Location of test pits……...…..... 26

Figure 3.3: The geology of the area containing Hawassa…….…….28

Figure 3.4: Sinusoidal wave shapes for 2.5 % strain and 1Hz and for two cycles…….…..34

Figure 3.5: Hysteresis loops of the 5th cycle of pit 1 at 400 KPa of axial stress for each strain level……36

Figure 3.6: Hysteresis loops of the 40 cycles of pit 1 at 400 KPa of axial stress for each strain level……37

Figure 3.7: Hysteresis loops for 5th cycle of each strain levels of pit 1……..38

Figure 4.1: The hysteresis loop plotted using table 4.1 stress and strain values……..…..……41

Figure 4.2: The shear modulus and damping ratio curve of the result in table 4.3 for selected cycles……..44

Figure 4.3: Shear modulus and damping ratio curves of table 4.4…….46

Figure 4.4: Shear modulus and damping ratio curves of table 4.5…….……47

Figure 4.5: Shear modulus and damping ratio curves of table 4.6…….48

Figure 4.6: Shear modulus and damping ratio curves of pit 1 with 100,250 and 400 KPa axial loads……49

Figure 5.1: Location of modulus reduction values of pit 1 as compared with curves developed for sand by Seed and Indriss (1970)…….……56

Figure 5.2: Location of modulus reduction values of pit 1 as compared with curves developed for saturated by Seed and Indriss (1970)…….56

Figure 5.3: Location of modulus reduction values of all test pits as compared with Abera's Gulelle area clay soils …….…….57

Figure 5.4: Location of modulus reduction values of all test results as compared with curves developed for sand by Seed and Indriss (1970)……...……..57

Figure 5.5: Location of modulus reduction values of all test results as compared with curves developed for saturated clay by Seed and Indriss (1970)…….…….58

Figure 5.6: Location of modulus reduction values of all test results as compared with curves developed by Vucetic and Dobry (1991) ……...……..58

Figure 5.7: Location of damping ratio values of pit 1 as compared with curves developed for sand by Seed and Indriss (1970)…….60

Figure 5.8: Location of damping ratio values of pit 1 as compared with curves developed for saturated by Seed and Indriss (1970)…….60

Figure 5.9: Location of damping ratio values of pit 1 as compared with Abera's Gulelle area clay soils ……..……..61

Figure 5.10: Location of damping ratio values of all test results as compared with curves developed for sand by Seed and Indriss (1970)……...……..61

Figure 5.11: Location of damping ratio values of all test results as compared with curves developed for saturated clay by Seed and Indriss (1970)……..62

Figure 5.12: Location of damping ratio values of all test results as compared with curves developed by Vucetic and Dobry (1991)……..62

Figure A-1: Liquid limit graphs of pit 1, 2 and 5 ……..…….70

Figure A-2: Liquid limit graphs of oven dried soils of pit 1 and 2……..…….…….71

Figures A-3: Grain size distribution curves of pit 1, 2 and 3…….72

Figures A-3: Grain size distribution curves of pit 4 and 5…….……....73

Figure B-1: Hysteresis loops of test pit 2 ……..……74

Figure B-2: Hysteresis loops of test pit 3……..75

Figure B-3: Hysteresis loops of test pit 4……..76

Figure B-4: Hysteresis loops of test pit 5……..77

Figure D-1: Shear modulus and Damping ratio curves of pit 2……..…88

Figure D-2: Shear modulus and Damping ratio curves of pit 3…….89

Figure D-3: Shear modulus and Damping ratio curves of pit 4…….……90

Figure D-4: Shear modulus and Damping ratio curves of pit 5…….……91

Figure E-1: Comparison of shear modulus ratio of pit 2 with literature values……92

Figure E-2: Comparison of shear modulus ratio of pit 3 with literature values……...…..…..…93

Figure E-3: Comparison of shear modulus ratio of pit 4 with literature values……..……94

Figure E-4: Comparison of shear modulus ratio of pit 5 with literature values……95

Figure F-1: Comparison of damping ratio of pit 2 with literature values……96

Figure F-2: Comparison of damping ratio of pit 3 with literature values……..97

Figure F-3: Comparison of damping ratio of pit 4 with literature values……..98

Figure F-4: Comparison of damping ratio of pit 5 with literature values……..99

LIST OF APPENDICES

Appendix-A Atterberg limit test results and Grain size distribution curves……...69

Appendix-B Hysteresis loop of the 5^{th} cycles of each test pits ……..…74

Appendix-C Shear modulus and Damping ratio values of selected cycles……78

Appendix-D Shear modulus and Damping ratio curves…….88

Appendix-E Comparison of Shear modulus ratio with literature values…….....92

Appendix-F Comparison of damping ratio with literature values……...96

ABSTRACT

The nature and distribution of earthquake damage is strongly influenced by the response of soils to cyclic loading. Design of geotechnical engineering problems that involve dynamic loading of soils and soil-structure interaction systems requires the determination of dynamic soil properties. The response of soil to cyclic loading is determined mainly by the shear modulus and damping characteristics of the soil. In Ethiopia, areas close to the Ethiopian rift valley are prone to damaging earthquakes. However, little experimental work has so far been done in assessing the dynamic properties of soils and only two researchers have attempted to experimentally measure dynamic properties of red clay soils found in Addis Ababa.

In this thesis, the shear modulus and damping ratio values of soils commonly found in Hawassa were determined using cyclic simple shear testing machine on remolded samples. The tests were conducted as a function of cyclic strain amplitude of 0.01 %, 0.1 %, 1 %, 2.5 %, and 5 % under the axial pressures of 100 kPa, 250 kPa and 400 kPa. The test results revealed that the shear modulus reduction values are in good agreement with well established literature values except at the lowest strain level (0.01 %). The damping ratio values of the tests are generally lower than the literature values except at the lowest strain level (0.01 %). This indicates that, the testing conditions appear to have significant effect on the damping ratio values but little effect on the shear modulus reduction values. Using the test results, the computed maximum shear modulus, $G_{max,}$ values for the soils considered in this work are within the range of 31,734 kPa to 98,084 kPa, which is acceptable for this soil type based on the literature.

CHAPTER 1
INTRODUCTION

1.1 Background

The biggest rift valley zone in East Africa passes through Ethiopia. The rift valley zone is a place where active volcanic eruptions are taking place and susceptible to earthquake. The ground motion due to earthquake may lead to permanent settlement, tilting of footing and, thus, failure of the structure supported by them [3]. Soil may liquefy leading to buildings sinking and lighter structures such as septic tank floating [3]. The nature and distribution of earthquake damage is strongly influenced by the response of soils to cyclic loading and design of geotechnical engineering problems that involve dynamic loading of soils and soil–structure interaction systems require the determination of dynamic soil properties. Soil properties that influence wave propagation include stiffness, damping, Poisson's ratio, and density [13]. Of these, the stiffness and damping characteristics of cyclically loaded soils are critical for the evaluation of many geotechnical engineering problems [13]. Even though Ethiopia is susceptible to earthquake particularly in the rift valley zone, little experiments have so far been done in the determination of the dynamic properties of soils in the country [7]. Our Geotechnical engineers have been using charts from literature for the determination of these parameters for design [7].

Hawassa is a city in Ethiopia, on the shores of Lake Hawassa in the Great Rift Valley. Hawassa is the capital of the Southern Nations, Nationalities and people region and one of the developing cities in the country where different infrastructures are being built dramatically. The proximity of significant earthquakes to the major population centers like Hawassa obviously leads to the question of how much damage will be sustained by the buildings and other infrastructures constructed or being constructed. Therefore, it is necessary to understand the ground responses of the soil deposits during the occurrences of earthquakes. In order to understand the ground responses of soil deposits, it is necessary to characterize the dynamic soil properties of the soil. In cases of ground response involving no residual soil displacements, the response is determined

mainly by the shear modulus and damping characteristics of the soil under cyclic loading conditions [16]. In this thesis, the shear modulus and damping ratio values of soils commonly found in Hawassa city have been characterized in the laboratory using the cyclic simple shear testing machine on remolded samples. In addition, some important properties of the soils have been determined for better characterization of the soils.

1.2 Objective

1.2.1 General objective

The main objective of this research is to determine the dynamic shear modulus and damping ratio values of soils found in Hawassa using cyclic simple shear testing machine and to make a comparison of the results with literature values.

1.2.2 Specific objectives

- To determine the index properties and classify the soils.
- To determine field density and maximum dry density of the soils.
- To determine shear modulus and damping ratio of specimens remolded to field conditions

1.3 Materials and Methods

To meet the above objectives, the following methodologies have been employed:

- Previous studies and papers related to dynamic properties of soils have been reviewed.
- In order to have more information about the area, the geology and environmental condition have been studied from available data.
- As soils in Hawassa are more of silt and silty clay type, disturbed soil samples have been collected from 2.5 m to 3 m depth from five selected test pits of the area.
- During collection of soil samples, the field densities were determined using core cutter method and also the field moisture contents of the soils have been determined.
- In the laboratory, samples have been remolded to field condition for cycling loading test and other tests which have been conducted to characterize the soils are:

- Atterberg limit
- Specific gravity
- Compaction
- Particle size analysis

- From cyclic simple shear machine test results, the shear stress is calculated simply by dividing the shear force by the area of the specimen base, and the shear strain is calculated by dividing the shear displacement by the height of the specimen.
- Shear modulus and damping ratio values of the soil then have been calculated.
- Finally the results have been compared to known literature values and discussed.

1.4 Scope of the study

Soils commonly found in Hawassa city are mostly silt and silty clay types. As it is difficult to collect undisturbed soil samples of these soils, disturbed soil samples have been collected from 5 test pits. Thus, this thesis is limited to the determination of cyclic shear modulus and damping ratio values for remolded soil specimens of the 5 test pits using cyclic simple shear machine.

1.5 Organization of the thesis

This thesis contains six Chapters and Appendices. The first Chapter contains background of the thesis, objectives, materials and methods and scope of the thesis. Chapter two covers a literature review which contain introduction about dynamic soil properties, some important properties of soil, shear modulus and damping ratio of soils and cyclic simple shear testing machine overview. The third Chapter is about sample collection and test results. It covers how samples are collected, description of the area and laboratory test results including cyclic simple shear tests. Chapter four is about data analysis and discussion of test results of cyclic simple shear test. In Chapter five, comparison of shear modulus reduction and damping ratio values with literature have been done. Chapter six contains conclusions and recommendations. Reference materials are appropriately sited and listed. The thesis ends with Appendices which contain test results and graphs.

CHAPTER 2
LITERATURE REVIEW

2.1 Dynamic soil properties

2.1.1 General

It is well known that the stress-strain properties of a soil and its behavior depend upon several factors and can be different in many ways under dynamic loading condition as compared to the case of static loading [3]. During an earthquake, a soil deposit is subjected to a complex system of stresses and strains resulting from the ground motion induced by the earthquake. In general, these stresses and strains will be cyclical due to the vibrational nature of the loading [4].

The behavior of soil subjected to dynamic loading is known as dynamic soil property [3]. The response of soil to cyclic loading is controlled mostly by the mechanical properties of the soil [14]. The mechanical properties associated with dynamic loading are: shear wave velocity, shear modulus, damping ratio and Poisson's ratio [14]. It has long been recognized that local soil conditions can significantly affect the ground response when seismic waves propagate upward through a soil profile [19]. The better understanding of the dynamic properties of some particular natural soils such as the Mexico city clays or the San Francisco Bay mud, together with the actual ground motion measurements during the Michoacan-1985 and the Loma-Prieta-1989 earthquakes, have greatly contributed to show the importance of local site conditions and especially the specific dynamic properties (G_{max}, strain dependent shear modulus and damping) of natural soils [15]. Thus, the shear modulus and damping characteristics of cyclically loaded soils are critical to the evaluation of Geotechnical Engineering problems at a wider strain level.

2.1.2 Cyclic stress-strain behavior of soil

Earthquake-induced stresses and strains that produce the most damage in soils are generally considered to be due to cyclic shearing of the soil [4]. Shear waves propagate primarily up ward near the ground surface [4]. Therefore, most geotechnical earthquake engineering analysis assumes that earthquake ground motions are generated by vertically-propagated shear waves [4]. The stress-strain response of soil to this type of cyclic loading is nonlinear and hysteretic and commonly characterized by a hysteresis loop [4]. The most common model used to represent the hysteretic behavior of soil in seismic analysis is the equivalent-linear model [4]. The equivalent-linear model represents non-linear hysteretic soil behavior using an equivalent shear modulus, G, equal to the slope of the line connecting the tips of the hysteresis loop and an equivalent damping ratio, β**,** proportional to the enclosed area of the loop [4].

Cyclic laboratory studies have shown that, the loading parameters which govern the cyclic response of saturated soils are those that govern the distortion (deformation) of the soil skeleton [23]. The main component of such distortion is relative displacement between soil particles, which can be expressed in terms of the shear strain, γ [23]. Such displacements are directly responsible for the breakage of particle bond, slippage at the particle contacts, and corresponding change of microstructural repulsion forces [23]. Thus, it is readily apparent that, the values of shear modulus and damping ratio will depend on the magnitude of the strain for which the hysteresis loop is determined (See Figure 2.1). Consequently, stiffness and damping characteristic of soils are strain-dependent and therefore, in this study, both shear moduli and damping factors have been determined as a function of the induced strain (strain-dependent test) in a soil specimen [16].

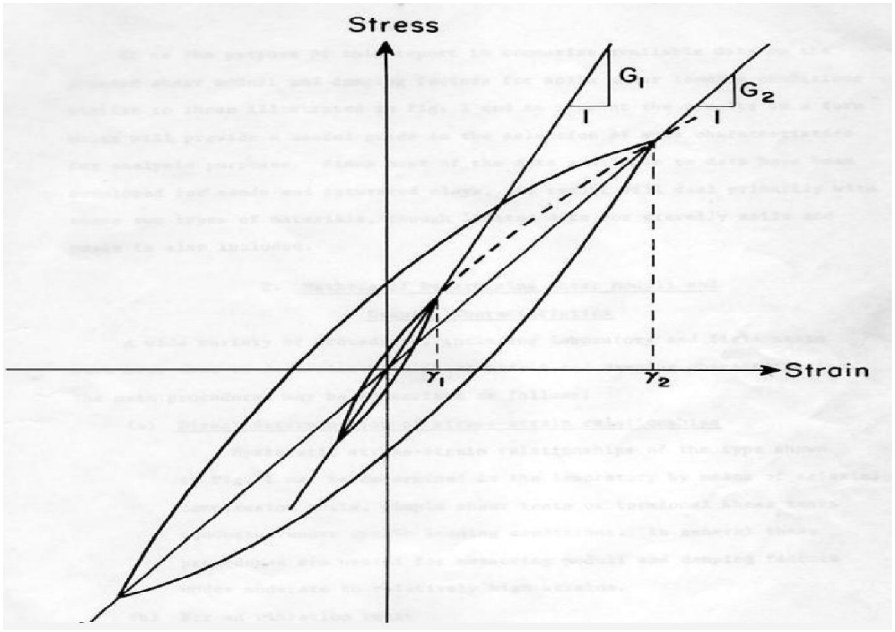


Figure 2.1: Hysteretic stress-strain relationships at different strain amplitudes [16]

It has been shown that the deformation characteristics of soils vary to a large extent depending upon the magnitude of shear strains to which soils are subjected [18]. Overall changes in soil behavior with changes in shear strain are illustrated in Figure 2.2, in which approximate ranges of the shear strain producing elastic, elasto-plastic, and failure states of stress are indicated [18].

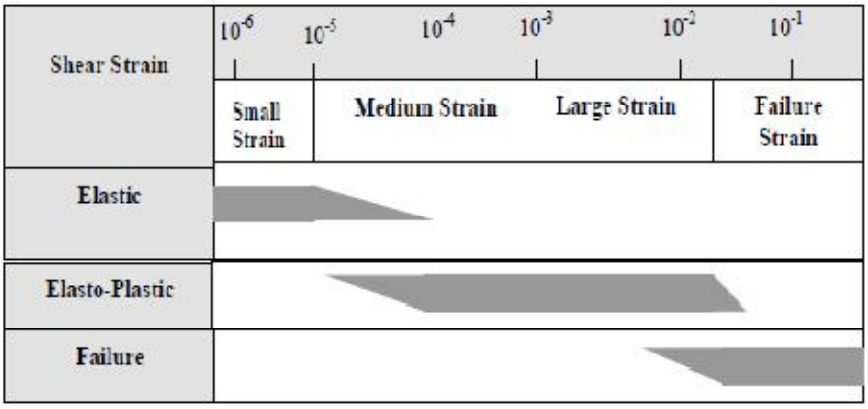


Figure 2.2: Change in soil properties with shear strain [18]

2.2 Some important properties of soil

2.2.1 Index properties

Those properties which help to assess the engineering behavior of a soil and which assist in determining its classification accurately are termed 'Index Properties'[22]. Some of the important physical properties, which may relate to the state of the soil or the type of the soil include: soil color, soil structure, texture, particle shape, grain specific gravity, water content, density index, in-situ unit weight, consistency limits, and particle size distribution, and related indices [22].

2.2.1.1 Particle shape

The particle shape of coarse-grained soils may be described as 'angular', 'sub-angular', 'sub-rounded', 'rounded' and 'well-rounded'. Silt particles rarely break down to less than 2μm size because of their mineralogical composition. Clay particles are invariably less than 2μm size. Microscopic studies of such soils reveal that the particle shape is flake-like or needle-like [22].

2.2.1.2 Specific gravity

Specific gravity of the soil solids is useful in the determination of void-ratio, degree of saturation. It is also useful in computing the unit weight of the soil under different conditions and also in the determination of particle size by wet analysis [22]. Table 2.1 shows the specific gravity value of some soil type.

Table 2.1: Specific gravities of some soil types [22]

S. No.	*Soil type*	*Grain specific gravity*
1	Quartz sand	2.64 - 2.65
2	Silt	2.68 - 2.72
3	Silt with organic matter	2.40 - 2.50
4	Clay	2.44 - 2.92
5	Bentonite	2.34
6	Loess	2.65 - 2.75
7	Lime	2.70
8	Peat	1.26 - 1.80

2.2.1.3 Moisture content

Moisture content of a soil has a direct bearing on its strength and stability particularly for fine-grained soils. The water content of a soil in its natural state is termed its 'Natural moisture content', which characterizes its performance under the action of load. The knowledge of water content is necessary in soil compaction control, in determining consistency limits of soil, and for the calculation of stability of all kinds of earth works and foundations [22]. The water content of soil can influence the behavior of cyclically loaded soil specimen, as it controls grain to grain slippage and pore water pressure development.

2.2.1.4 Relative Density

Relative density of a soil indicates the relative compactness of the soil mass. This is used in relation to coarse-grained soils or sands. In a dense condition, the void ratio is low whereas in a loose condition, the void ratio is high. Thus, the in-place void ratio may be determined and compared, with the void ratio in the loosest state and that in the densest state. It is an important parameter with respect to the potential for soil liquefaction and seismically-induced settlement of cohesionless soil [22]. Determination of relative density (D_r) is helpful in compaction of coarse grained soils and in evaluating safe bearing capacity in case of sandy soils [22].

$$D_r = \frac{e_{max} - e}{e_{max} - e_{min}} \text{----------2.1}$$

2.2.1.5 In-situ unit weight

The *in-situ* unit weight refers to the unit weight of a soil in the undisturbed condition of soil in-place. Determination of *in-situ* unit weight is made on borrow-pit soils so as to estimate the quantity of soil required for placing and compacting. In the laboratory test, it is standard practice to make *in-situ* unit weight of disturbed soil so as to resemble the field condition [22].

Two important methods for the determination of the *in-situ* unit weight are given below:

i. Sand-replacement method

The principle of the sand replacement method consists in obtaining the volume of the soil excavated by filling in the hole *in*-situ from which it is excavated, with sand, previously

calibrated for its unit weight, and thereafter determining the weight of the sand required to fill the hole [22].

ii. Drive-cylinder method

This test method covers the determination of in-place density of soil by obtaining a relatively undisturbed soil sample by driving a thin-walled cylinder. According to ASTM-D 2937-94, this test method is used to determine the in-place density of natural, inorganic soils which do not contain significant amount of particles coarser than 4.75 mm, and which can be readily retained in the drive cylinder. For this research, the Drive-cylinder method has been used to determine the field density of the soils in each test pits.

2.2.1.6 Consistency of clay soil

Consistency of a soil refers to the resistance offered by it against forces that tend to deform or rupture the soil aggregate [22]. Consistency of a soil can be expressed in terms of Atterberg limits [22]. Atterberg limit tests indicate the range of the plastic state (plasticity is defined as the property of cohesive soils which possess the ability to undergo changes of shape without rupture) and other states. The range of water content between the liquid and plastic limits, which is an important measure of plastic behavior, is called the plasticity index, I_p [22]. Table 2.2 below provides plasticity range of soils in terms of the plasticity index.

Table 2.2: Range of plasticity index with its classification [22]

Plasticity index	plasticity
0	non – plastic
1 to 5	slight
5 to 10	low
10 to 20	medium
20 to 40	high
> 40	very high

Plasticity index is one of the most significant index properties which strongly influence the cyclic shear parameters. As a result of a survey and analysis over numerous test data, Vucetic and Dobry (1991) proposed families of curves as shown in Figure 2.4 which are the averaged relations indicating the effect of the plasticity index on the strain-dependent modulus and damping of cohesive soils [11]. The modulus reduction curves show that the linear cyclic threshold shear strain is greater for highly plastic soils than for soils of low plasticity [13]. This characteristic is extremely important as it can strongly influence the manner in which soil deposit will amplify or attenuate earthquake motion [13]. The damping ratio curves show that the highly plastic soils have lower damping ratio values than soils of lower plasticity [13]. The charts also cover the behavior of saturated cohesionless non-plastic material such as sand, for which the corresponding curves is indicated by *PI = 0.*

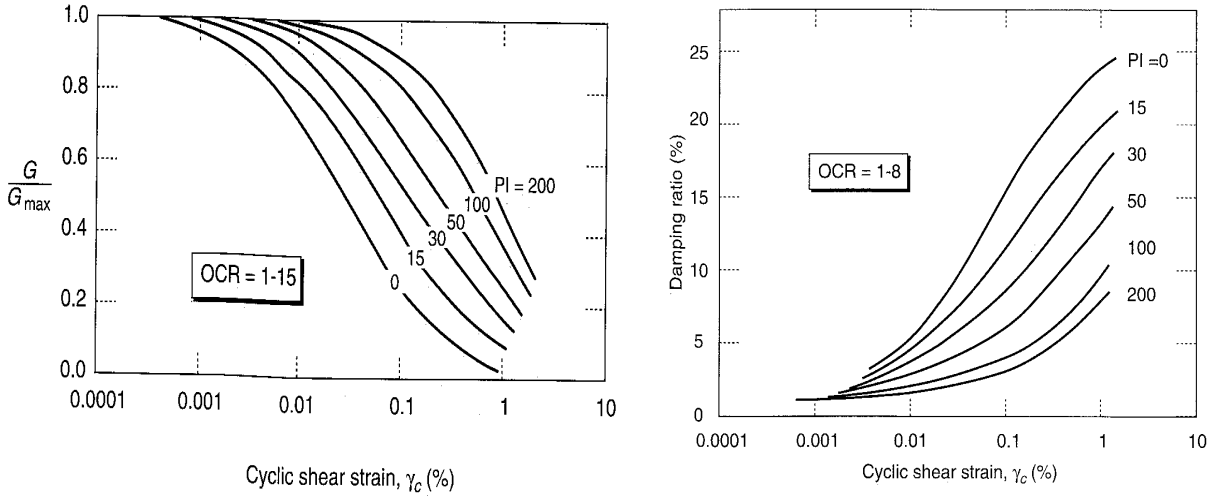


Figure 2.3: Modulus reduction and damping ratio curves of fine-grained soils of different plasticity [13]

2.2.1.7 Grain size distribution

The knowledge of grain size analysis of a soil is very useful in the present geotechnical world. It covers the quantitative determination of the distribution of particle sizes in soils. The distribution of particle sizes larger than 75 μm (retained on the No. 200 sieve) is determined by sieving, while the distribution of particle sizes smaller than 75 μm is determined by a sedimentation process, using a hydrometer [22]. Grain size distribution is one factor in seismically loaded soil deposit. Uniformly graded non-plastic soils tend to form more unstable particle arrangements and more susceptible to collapse and failure than well-graded soils. Well-graded soils have small particles that fill in the void space between large particles. This tends to reduce the potential contraction of the soil, resulting in less susceptible to loosing strength under dynamic loading [24].

2.2.2 Soil compaction

Compaction, in general, is the densification of soil by removal of air, which requires mechanical energy [2]. The degree of compaction of a soil is measured in terms of its dry unit weight. Moisture content has a strong influence on the degree of compaction achieved by a given soil. Besides moisture content, other important factors that affect compaction are soil type and compaction effort [2]. In this study, test specimens have been compacted to field density and moisture content for cyclic shear testing to replicate the natural state of the soil samples.

2.2.3 Soil type

Natural soil deposits are never homogeneous in character; wide variations in properties and behavior are commonly observed. Classification of soils is necessary since through it an approximate, but fairly accurate, idea of the average properties of a soil group or a soil type is obtained [22]. According to Unified soil classification system, USCS, soils are classified into three broad categories: [1]

- Coarse-grained soils up to 50% passing No.200 ASTM sieve
- Fine-grained soils with more than 50% passing No.200 ASTM sieve
- Fine-grained soil can be inorganic or organic soils

The first two categories can be distinguished by their plasticity characteristics. The third can be identified by its color, odor and a second liquid limit test shall be performed on a test specimen which has been oven dried at 110 ˚c to a constant weight, typically over night [1].

The seismic responses of different natural soil deposits reflect different dynamic soil properties [24]. The effect of soil type on seismic response can be explained by linking with USCS as summarized below.

- *Highly plastic soils like high plasticity clay*, have small damping and large range linearly elastic behavior, which are both prerequisite for a resonance to take place [23]. Soil failure due to cyclic degradation of stiffness and strength in this type of soil deposit is unlikely, because the degradation is small [23].
- *Fully saturated sand, silty clays and clayey silts,* exhibits a highly nonlinear behavior and considerable damage even at very small shear strain, during continuous cyclic loading their stiffness and strength degrade significantly [23]. The most critical aspect of the response of such soils is large drop in soil strength due to cyclic degradation, which may cause failure of foundation soil and collapse of supported structures [23].
- *Medium plasticity clay,* are somewhere in-between the two extreme cases described above [23].

2.3 Shear modulus and damping ratio of soil

2.3.1 Method of determining shear modulus and damping ratio values of soil

There are various procedures, including laboratory and field tests that have been used to determine shear modulus and damping characteristics of soils. A summary of the procedure and the approximate range of strain within which they have been used are presented in the Table 2.3 below [16]. There are different strain ranges for which the shear modulus and damping ratio are determined. These strain ranges are: very low strains ($\gamma \leq 10^{-3}$ percent), medium strains ($10^{-3} < \gamma < 10^{-1}$ percent) and large strains ($10^{-1} < \gamma < 5$ percent). From Table 2.3, the cyclic simple shear apparatus, which is used in this thesis work, enables one to determine shear modulus and damping ratio for cyclic strain range of $\gamma = 10^{-2}$ to $\gamma = 5$ percent. This range is the general range of strain encountered in the ground motion during seismic activities [3].

Table 2.3: Test procedures for measuring moduli and damping characteristics [16]

General procedure	Test condition	Approximate strain range	Properties can be determined
Determination of hysteretic stress-strain relationships	Triaxial compression	10^{-2} to 5 %	Modulus; Damping
	Simple shear	10^{-2} to 5 %	Modulus; Damping
	Tortional shear	10^{-2} to 5 %	Modulus; Damping
Forced vibration	Longitudinal vibration	10^{-4} to 10^{-2} %	Modulus; Damping
	Tortional vibration	10^{-4} to 10^{-2} %	Modulus; Damping
	Shear vibration-lab	10^{-4} to 10^{-2} %	Modulus; Damping
	Shear vibration-field	10^{-4} to 10^{-2} %	Modulus
Free vibration tests	Longitudinal vibration	10^{-3} to 1 %	Modulus; Damping
	Tortional vibration	10^{-3} to 1 %	Modulus; Damping
	Shear vibration-lab	10^{-3} to 1 %	Modulus; Damping
	Shear vibration-field	10^{-3} to 1 %	Modulus
Field wave velocity measurement	Compression wave	$\sim 5 \times 10^{-4}$ %	Modulus
	Shear wave	$\sim 5 \times 10^{-4}$ %	Modulus

2.3.2 Computation of Shear modulus and Damping ratio parameters

2.3.2.1 Shear modulus

The properties that are most important for dynamic analysis are the stiffness and material damping of the soil under dynamic loading. The parameters which can express these properties of soil are dynamic shear modulus and damping ratio. These parameters can be determined from the stress-strain behavior of soils under cyclic loading as expressed previously in section 2.1.2. The important utility of shear modulus is that it can be used as a varying parameter with respect to strain making the soil response represents the real modulus degradation in soil behavior [14].

Because most soils have curvilinear stress-strain relationships, the tangent shear modulus (G_{tan}) varies through a cycle of loading but, its average value over the entire loop can be approximated by the secant shear modulus, $\boldsymbol{G_{sec,}}$ which is commonly called equivalent shear modulus (G) [13]. Thus $\boldsymbol{G_{sec}}$ describes the general inclination of the hysteresis loop. Using the equivalent-linear analysis method, the secant shear modulus can be determined by the extreme points on the hysteresis loop (see Equation 2.2 and Figure 2.5 below).

$$G_{\text{sec}} = \frac{\tau_c}{\gamma_c} \quad \text{----------2.2}$$

Where: τ_c and γ_c are the shear stress and strain amplitudes at the tip, respectively

2.3.2.2 Damping ratio

Damping ratio represents the ability of a material to dissipate dynamic load or dampen the system [14]. As the soil elements loose stiffness with the amplitude of strain, its ability to dampen dynamic forces increases [14]. This is due to the energy dissipated in the soil by friction, heat or plastic yielding [14]. Thus, the breadth of the hysteresis loop is related to the area, which as a measure of energy dissipation, can conveniently be described by damping ratio [13]. From the hysteresis loop of Figure 2.5, damping ratio can be expressed in Equation 2.3 below.

$$\beta = \frac{\Delta W}{4\pi W} = \frac{A_{loop}}{4\pi A_{\Delta}} \text{ ----------2.3}$$

Where:

β is damping ratio

ΔW is the dissipated energy

W is maximum energy

A_{loop} is the area of hysteresis loop and

A_{Δ} is the area of triangle

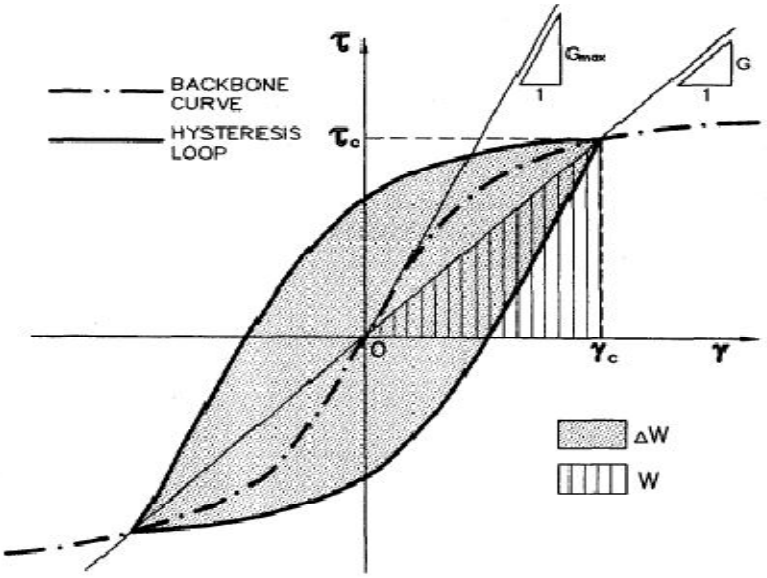


Figure 2.4: Hysteretic stress-strain response of soil subjected to cyclic loading [4].

2.3.2.3 Maximum shear modulus

Another way to represent shear modulus degradation with cyclic strain is by means of the modulus reduction curve. The modulus reduction value (G/G_{max}) normalizes the shear modulus

with respect to maximum shear modulus, G_{max} [14]. The locus of points corresponding to the tips of hysteresis loop of various cyclic strain amplitudes is called a backbone (or skeleton) curve. And its slope at the origin (zero cyclic strain amplitude) represents the largest value of the shear modulus, G_{max} (see Figure 2.5) [13]. Characterization of the shear modulus of an element of soils requires consideration of both G_{max} and the manner in which the modulus ratio, G/G_{max}, varies with cyclic strain amplitude and other parameters.

Since most seismic geophysical tests induce shear strains lower than about $3*10^{-4}$ %, the measured shear wave velocities can be used to compute G_{max} as [13]:

$$G_{\max} = \rho v_s^2 \quad \text{----------2.4}$$

Where ρ is the density of the soil deposit and

v_s is shear wave velocity

The use of measured shear wave velocities is generally the most reliable means of evaluating the in situ value of G_{max} for a particular soil deposit [13].

When shear wave velocity measurement are not available, G_{max} can be estimated in different ways. Laboratory test data suggest that, the maximum shear modulus can be expressed as [13]:

$$G_{\max} = 625F(e)(OCR)^k \, p_a^{1-n} (\sigma_m')^n \quad \text{----------2.5}$$

Some relationships were also presented to determine the value of maximum shear modulus (at essentially zero strain). The expression for evaluating the maximum shear modulus is [16]:

$$G_{\max} = 14760 \times \frac{(2.973 - e)^2}{1 + e} (OCR)^a (\sigma_m')^{1/2} \quad \text{----------2.6}$$

Where:

Hardin (1978), proposed that $F(e) = \frac{1}{(0.3+0.7e^2)}$ [13]

P_a is atmospheric pressure in the same unit as σ'_m

n is often equal to 0.5

OCR is over consolidation ratio of the soil

σ'_m is mean effective confining pressure

$a = k$ are parameters that depends on the plasticity index of the soil

e is void ratio of the soil

The modulus reduction and damping ratio values are described by modulus reduction and damping ratio curves as shown in Figure 2.6 below [4]. From this figure, it can be seen that, as shear strain increases, modulus reduction curve will decrease while damping ratio curve increases.

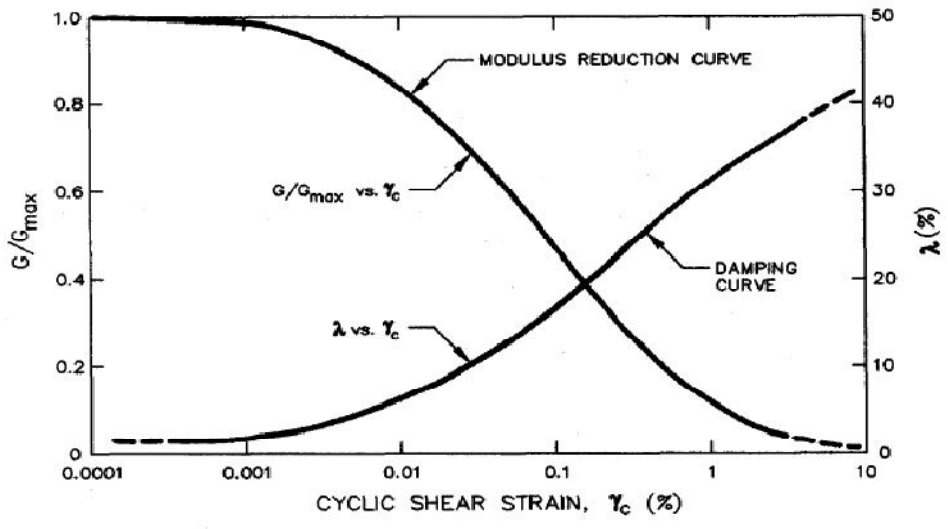


Figure 2.5: Shear modulus reduction and damping ratio curves [4]

2.3.3 Factors affecting shear modulus and damping ratio values

The seismic response of different natural soil deposits must reflect the different dynamic properties of soil material [13]. A comprehensive survey of the factors affecting the shear moduli and damping factors of soils and expressions for determining these properties have been presented by Hardin and Drnevich (1970) [16]. Laboratory tests have also shown similar factors affects these parameters [13]. Thus, the primary factors affecting shear modulus and damping ratio values of soils are:

- Strain amplitude
- Effective mean principal stress
- Void ratio (relative density)
- Number of cycles of loading
- Degree of saturation for cohesive soils.
- Plasticity index.

2.3.4 Shear modulus and damping ratio values of soils

2.3.4.1 Sand

All investigations have shown that modulus values for sands are strongly influenced by the confining pressures, the strain amplitude and the void ratio (relative density) [16]. A number of investigators, using different laboratory test procedures, have presented data on the relationship between these factors [17]. It is noted that if each of the relationships is plotted to show the variation with shear strain of the ratio of shear modulus at strain γ to shear modulus at a shear strain of 10^{-4} percent, the results fall within the relatively narrow band shown in Figure 2.7 [17]. Many other investigators have found results in the same general range [17]. Thus, Figure 2.7 below shows generally representative shear modulus reduction values of most sands [16].

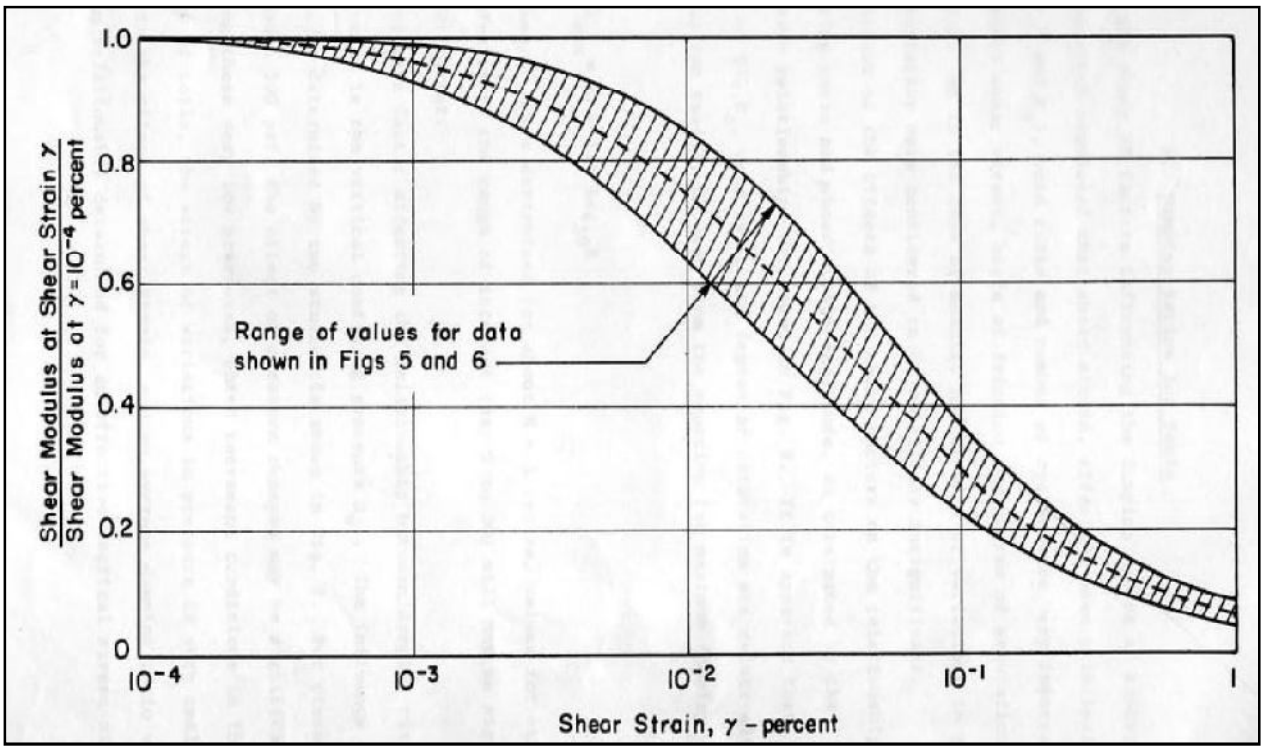


Figure 2.6: Variation of shear modulus with shear strain for sand [16]

From their study of factors influencing the damping ratio of sand, Hardin and Drnevich (1970) concluded that shear strain, effective mean principal stress, void ratio and number of cycles were very important [17]. Considering the potential scatter of test data for damping ratio (see Figure 2.8) even those obtained by the same investigator using the same test procedure, the adoption of such an average relationship may be even more justified [17]. This average relationship is likely to provide values of damping ratio with sufficient accuracy for many practical purposes [17].

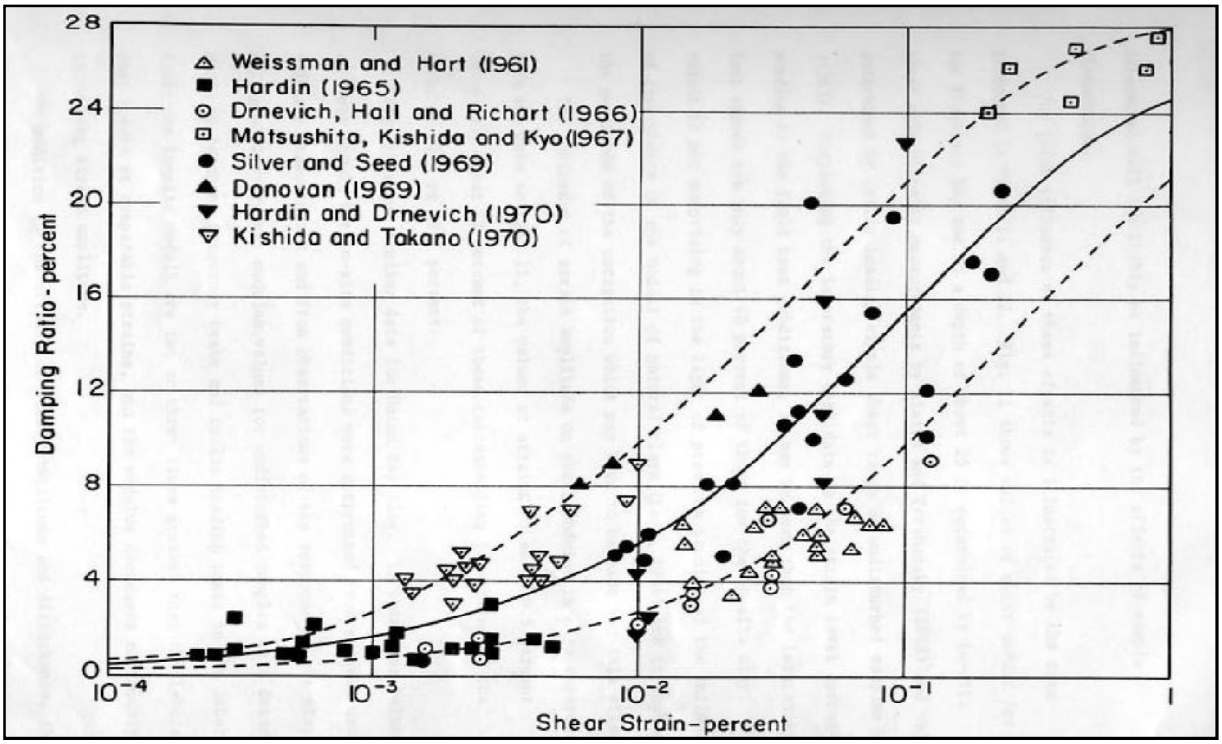


Figure 2.7: Damping ratio curve for sand [16].

2.3.4.2 Clay

Accurate determination of the shear modulus of saturated clays is enormously complicated by the large effects of strain amplitude and sample disturbance on modulus values [16]. The modulus reduction curves for clay show a much larger scatter and seem to be related to the characteristics of individual clay [19]. However, taste data at very low strain levels indicates an approximately

linear relationship between the shear modulus and shear strength for a number of clays [16]. It seems reasonable to expect that variations in clay characteristics might be taken into account by normalizing the shear modulus with respect to the undrained shear strength and expressing the relationship as a function of shear strain [16]. Alternatively, this relationship might be used to assess the influence of strain amplitude on the shear modulus of natural clays, by expressing the ordinate in terms of the ratio of shear modulus at shear strain γ to shear modulus at a shear strain 3×10^{-4} percent [16]. This ratio for the average values is plotted as a function of shear strain as shown in Figure 2.9.

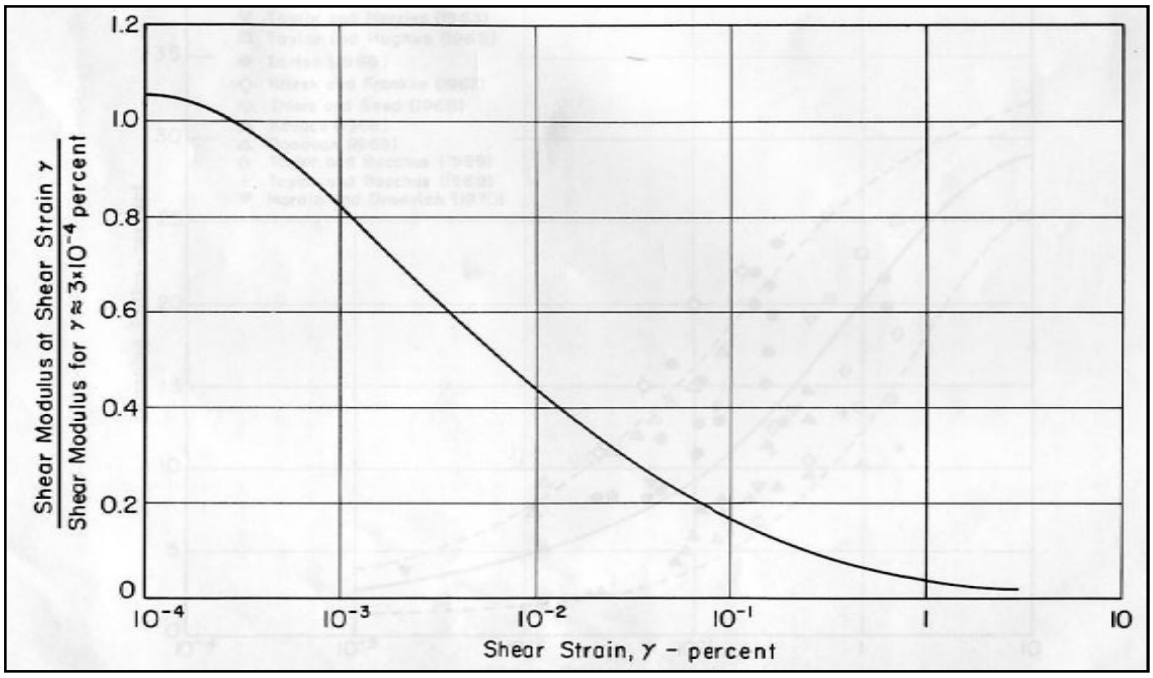


Figure 2.8: Typical modulus reduction curves for saturated clay [16]

Test data for damping ratios for saturated clays are limited and it is difficult to determine the main factors influencing the damping ratio of these soils [16]. The results of previous investigations of damping ratios for saturated clays are summarized in Figure 2.10 below [16]. This average relationship may well provide values of damping ratio with sufficient accuracy for many practical purposes [16].

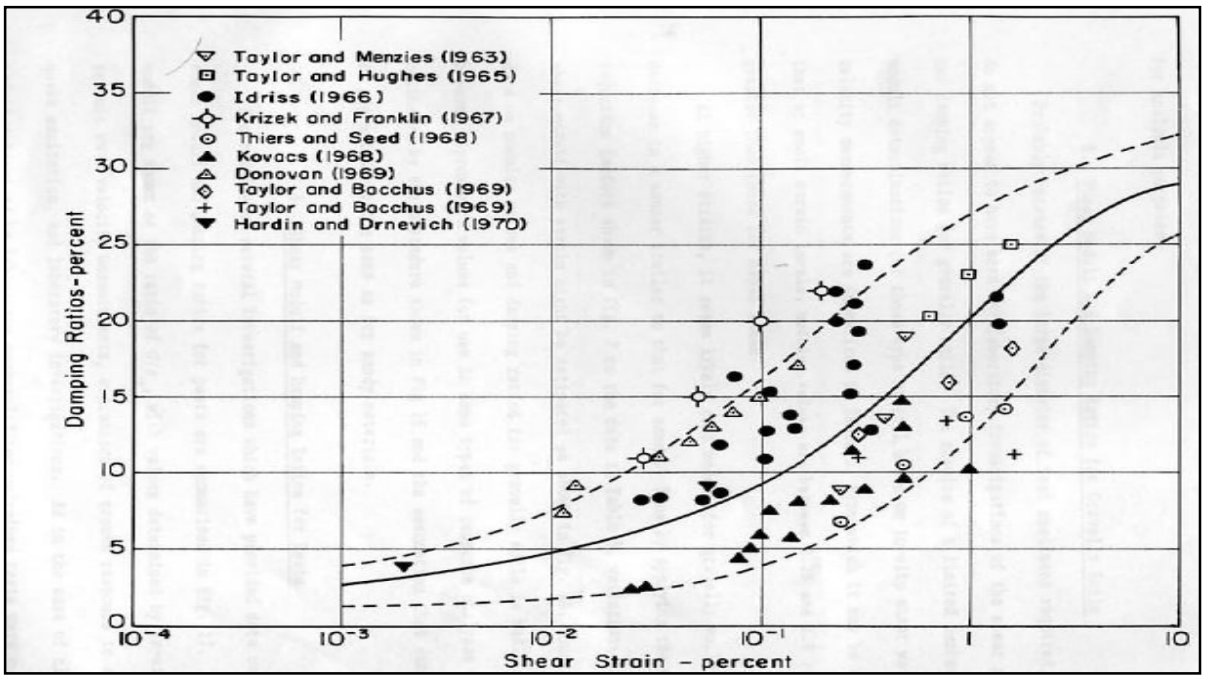


Figure 2.9: Damping ratio for saturated clay [16]

2.3.4.3 Other soil types

Since most researches about dynamic properties of soils were conducted on sands and clays type of soils, it would be difficult to get properly established curves for other soil types such as silts. As the soils used for this study are more of low plastic silts, it would be better to see if any similar soil type studied so far. Figure 2.11 and 2.12 show comparisons of soils in South of Tehran which is mainly silts with Vucetic and Dobry (1991) curves for plasticity indexes of 30, 15 and 0. The results show that, the location of shear modulus ratio values are comparable where as the damping ratio values are lower than that of Vucetic and Dobry curves. This may give us some indication about silt soil that it has lower damping ratio values as compared to literature.

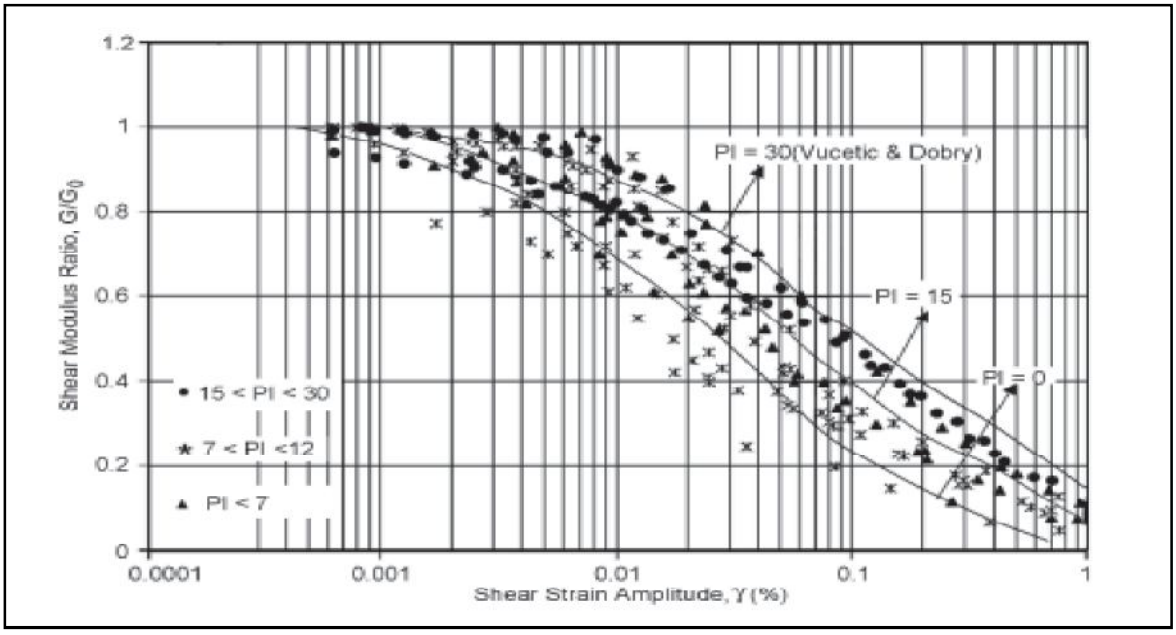


Figure 2.10: Shear modulus ratio vs. Shear strain curves of soils in South of Tehran as compared with Vucetic and Dobry (1991) curves [12].

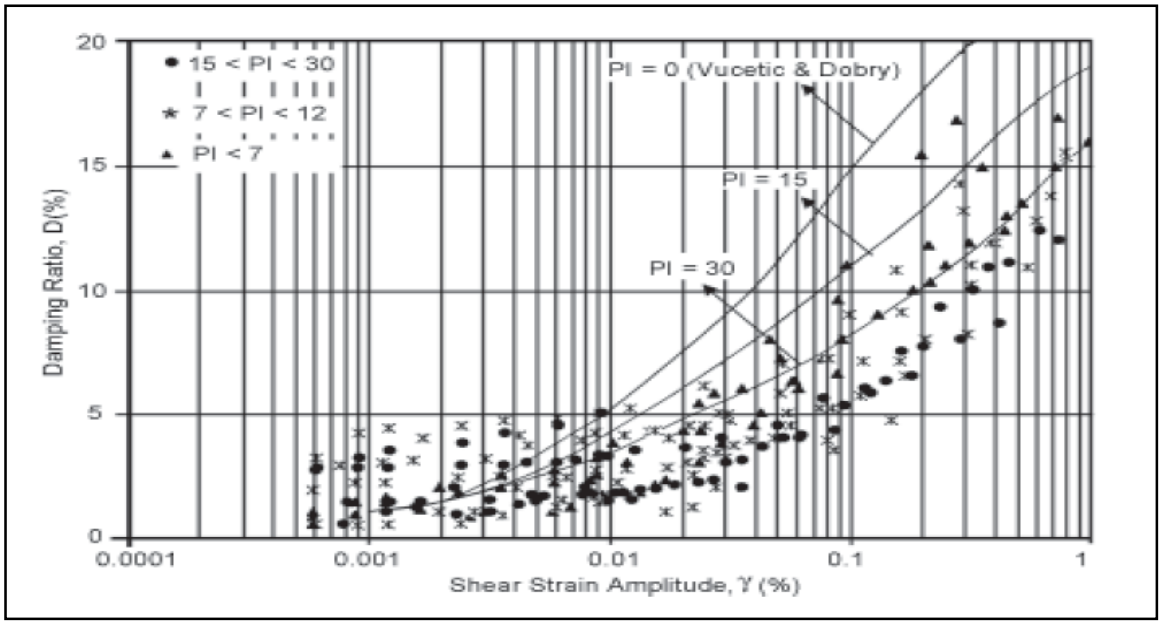


Figure 2.11: Damping ratio vs. Shear strain curves of soils in South Tehran as compared with Vucetic and Dobry (1991) curves [12].

2.4 Cyclic simple shear testing system overview

Laboratory testing for evaluation of cyclic stress-strain parameters of soils is appealing to many engineers because direct measurement can be made for the hysteresis stress-strain behavior of soils [4]. The cyclic direct simple shear test may provide the most accurate representation of the stress state resulting from a vertically propagating shear wave in a soil deposit of any laboratory test [4]. It also provides K_o condition for the lateral stress when the vertical stress is applied at the stage of consolidation [11]. In this research, the type of apparatus used is 31-WF7500 cyclic simple shear machine which is developed by the controls group-UK and the complete system is controlled by the UTS004 software application program. Figure 2.13 below shows a picture of the cyclic simple shear testing machine used in this study.

The system incorporates a two axis servo-controlled loading apparatus that allows control and measurement of axial and lateral stress and displacements applied to the specimen under test [21]. Specimen testing begins with a consolidation stage or compression stage (if it is the application of axial stress without saturation) which continues until testing paused by the operator at the end of consolidation. Loading may then be reinitiated for a cyclic shear testing stage. Shear strain is induced by horizontal movement at the bottom of the sample relative to the top [21]. Figure 2.14 shows the shearing stage of a specimen under test.

The apparatus uses a cylindrical test specimen. The specimen is supported laterally by a rubber membrane placed and secured with O-rings. To maintain a constant diameter throughout the test, the sample is supported by a series of slip rings [7]. The sample is set up in the machine, which has a rigidly fixed top half and a moving bottom half. The top half houses the vertical ram. This is housed in a linear bearing to allow vertical movement and prevent horizontal movement during consolidation test. The bottom half is mounted on roller bearings as in a standard shear box [7]. During cyclic shear stage, the vertical height of sample can be maintained at a constant height by the vertical displacement transducer and the rings maintain a constant sample diameter [21].



Figure 2.12: Cyclic simple shear test machine

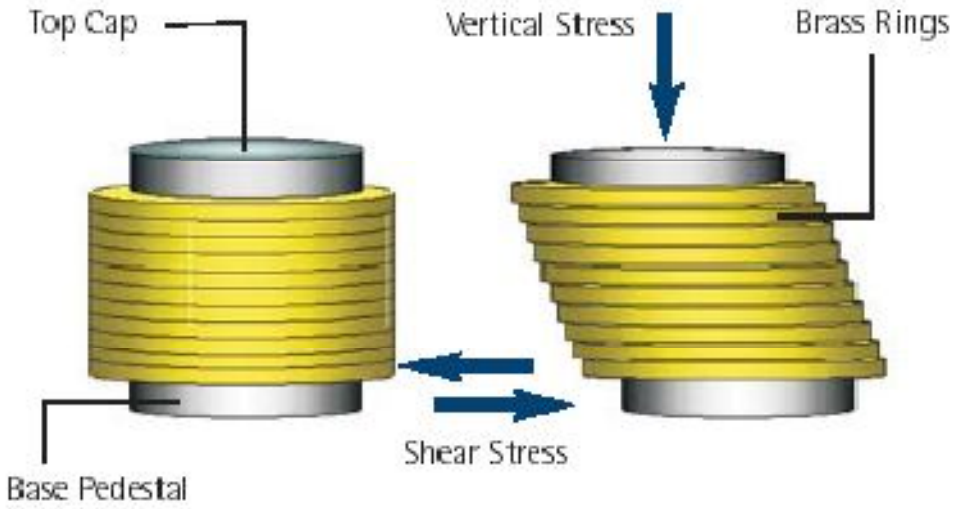


Figure 2.13: Visualization of the shearing stage of a specimen under cyclic simple shear test

CHAPTER 3

DATA COLLECTION AND TEST RESULTS

3.1 Sample collection

During the field work, five convenient places were selected in the city and from each sites disturbed samples were collected. As the foundations of most superstructures like buildings are placed around 2.5m to 3m, samples were collected within these depths. Figure 3.1 shows a typical test pit and the location of all test pits are shown in Figure 3.2 below. Using core cutter method, the field densities and natural moisture contents of the samples were determined.



Figure 3.1: Picture of test pit1

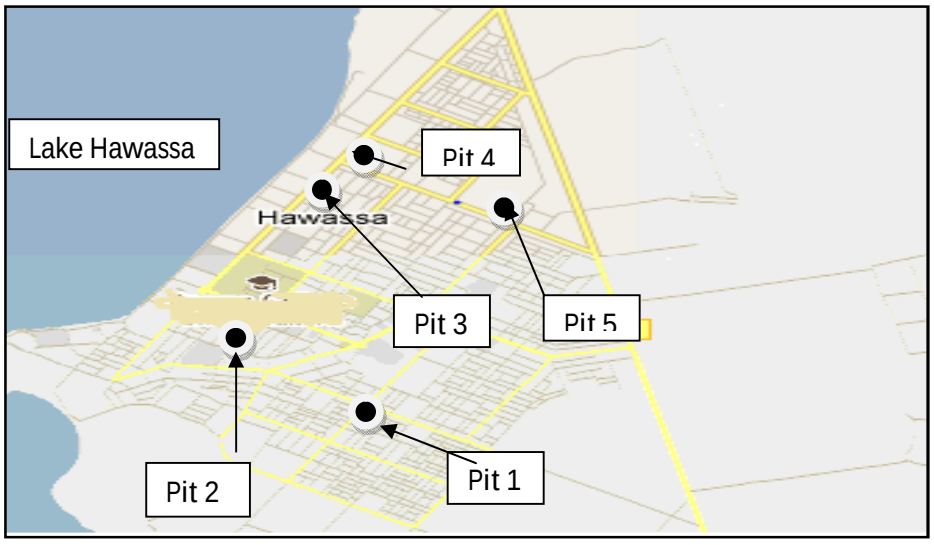


Figure 3.2: location of test pits

3.2 Description of the study area

3.2.1 Geographic and Climatic conditions

Hawassa is the capital of the Southern Nations, Nationalities and people region. The city is located in the Sidama Zone 270 km south of Addis Ababa and 1125 km north of Nairobi with a latitude and longitude of 7°3′N 38°28′E7.05°N 38.467°E and an elevation of 1708 m above sea level [9]. The city is surrounded by flat and slightly slopping lands, escarpments and hills [24].

The climate in the area is dry to sub-humid [24]. Table 3.1 and table 3.2 below show the average high/low temperature and average rain fall for Hawassa respectively.

Table 3.1: Average high/low temperature in Hawassa [10]

Month	Jan	Feb	Mar	Apr	May	Jun	Jul	Aug	Sep	Oct	Nov	Dec
Average high temp	21°c	20°c	23°c	21°c	20°c	19°c	19°c	19°c	21°c	21°c	22°c	21°c
Average low temp	10°c	10°c	12°c	13°c	13°c	13°c	13°c	13°c	12°c	11°c	9°c	10°c

Table 3.2: Average rain fall for Hawassa [10]

Month	Jan	Feb	Mar	Apr	May	Jun	Jul	Aug	Sep	Oct	Nov	Dec
Average precipitation	12mm	27mm	54mm	84mm	75mm	84mm	69mm	90mm	90mm	45mm	15mm	9mm
Average rainfall days	3	9	15	15	14	13	15	16	19	11	6	4

3.2.2 Geology and subsurface condition

Hawassa is situated within the Ethiopian Rift Valley. Because of the rifting activity, a series of NE and N trending faults associated with volcanically deposited lithologies have been developed. The Lake Hawassa is situated in the middle of a caldera like structure marking the center of a major fault zone that formed a number of associated narrow long linear ridges, valleys and

plateaus [20]. According to existing literatures, the essential geological formations developed in Hawassa and its surrounding areas are pyroclastic deposits of mainly pumiceous pyroclastics, ash, tuff and ignimbrite [20]. Figure 3.3 shows the geology of Hawassa according to the geological survey of Ethiopia.

These pyroclatics were deposited during a series of volcanic eruptions separated by some period of aerial weathering and deposition. This is confirmed by the alternation of different pyroclastic deposits separated by oxidized zones, deposits of sandy clay and clay soils derived from altered pyroclastic parent material. Around Lake Hawassa these pyroclastics grade into lacustrine deposits of silt, clay and silty clay composite soils derived from the alternation and decomposition of volcanic ash, tuff, pumice and ignimbrite [20]. The youngest deposit overlying the whole series is a thin layer of volcanic tiff deposit. This layer is underlain by oxidized and at places, literized pumiceous pyroclastics forming red surface [20]. Clay soils developed on the pyroclastic are mainly grayish in color [20].

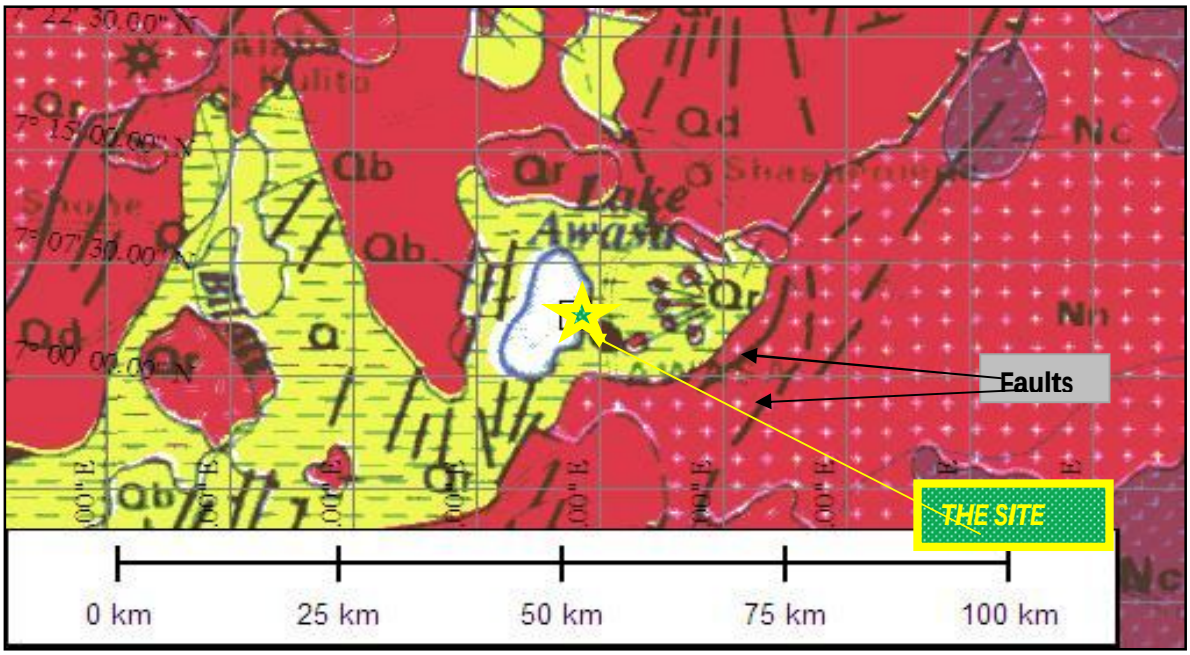


Figure 3.3: The geology of the area containing Hawassa as clipped from the Geological Map of Ethiopia obtained from the Geological Survey of Ethiopia.

3.2 Summary of some basic test results

Some basic laboratory tests were conducted according to ASTM-1998 standards for better understanding of some important properties of the soils under consideration. Table 3.3 and 3.4 below summarize results of basic laboratory and field tests including field density, field moisture content, compaction, Atterbeg limit and grain size tests.

Table 3.3: Field and maximum densities, water contents and specific gravities

Station	field density in g/cm3	field moisture content in %	field dry density	Specific gravity	MDD	OMC (%)	Maximum bulk density
Pit 1	1.51	25.33	1.2	2.547	1.28	30	1.664
Pit 2	1.71	34.1	1.27	2.518	1.305	32	1.72
Pit 3	1.55	27.72	1.21	2.461	1.28	29	1.651
Pit 4	1.55	33.42	1.16	2.418	1.247	34.5	1.722
Pit 5	1.45	31.38	1.104	2.519	1.286	31.5	1.69

Table 3.4: Atterberg limits and Classification

Test pit no	**1**	**2**	**3**	**4**	**5**
Test pit name	**Stadium**	**Enjory**	**BMN**	**Electric**	**Silasse Church**
LL	46	49	-	-	42
PL	35	35	-	-	35
PI	11	14	0	0	7
% passing 4.75mm sieve	99	99.4	96.4	97.4	99.4
% passing 0.075mm sieve	83.8	80.8	60	53.8	68.6
Percent silt size (0.075-0.005 mm) - ASTM	66.57	59.64	52.32	42.8	59.05
Percent clay size (≤ 0.005 mm) -ASTM	17.23	21.16	7.68	11.0	9.55
USCS Classification	Silt (ML)	Silt (ML)	Sandy silt (ML)	Sandy silt (ML)	Silt (ML)

Due to the lower values of the density and specific gravity observed in the results, an additional simple test was conducted to check whether the soils are organic or not. For this reasons, 'ASTM D2487 _98' method of determining organic content of soils has been used to check the presence of organic matter in the soils. According to ASTM D2487 _ 98, a soil is an organic silt or organic clay if the liquid limit after oven drying is less than 75 % of the liquid limit of the original specimen determined before oven drying. However, the test results for test pit1 and test pit 2 soils indicate that the LL ratio is 88.8 % and 88 % respectively. These values are greater than the 75 % boundary indicating that the soils are inorganic silts.

3.3 Cyclic simple shear test

3.3.1 Specimen preparation

In order to conduct the cyclic simple shear test, the disturbed soil samples have been remolded to field condition (at field density and water content) to replicate the natural state. The specimen is cylindrical in shape with 20 mm height and 70 mm diameter. Once the specimen is prepared, it will be mounted on the cyclic simple shear test machine for testing.

3.3.2 The compression stage

This stage is simply the application of a static axial loading stress to the specimen while the lateral loading (shear) axis is held stationary Since the testing machine doesn't have means of saturation during the application of axial load, the specimen is compressed under its natural moisture content condition. Axial stress and specimen displacements (axial and lateral) are measured over time and logged by the system. The logged data are also displayed to the operator in the form of charts and tables as the test stage proceeds. This stage is manually terminated once compression of the specimen is complete [21]. End of compression can be observed from the chart plotted continuously with axial strain against time on a semi-log scale as the test proceeds. When the axial strain against time curve is closing to be horizontal indicates, compression is ended and testing will be paused by the operator.

3.3.3 The cyclic simple shear stage

The cyclic shear stage of the test applies a lateral cyclic shear force, or optionally a displacement, to the specimen, while the axial axis is either maintained at the specified stress, or optionally, the specimen height is maintained [21]. Dynamic loading like earthquake occurs so rapidly that, excess pore pressure does not have time to dissipate for except in the case of very coarse, clean gravel soils [23]. This is because the presences of fines, especially clay, in the soil inhibit the dissipation of excess pore water pressure [23]. It is also observed that, dynamic loading will usually last for such a short time that the soil's response will be essentially undrained [23]. In this research, the cyclic shear test conducted is strain-dependent which allows a lateral cyclic displacement (shear strain value) to be selected to the specimen. The maximum and minimum levels of this displacement allow the amplitude and offset of the displacement to be specified. The specimen height is maintained constant during cyclic shear test so that, the test is conducted under constant volume condition. Both lateral force and specimen displacements are measured for each loading cycle. Measured data is obtained from 50 sample points captured over a single cycle period [21].

3.3.4 Presentation of cyclic shear test results

3.3.4.1 Axial loads and shear strain levels used

The cyclic simple shear testing machine enables one to conduct cyclic shear test within the strain levels of 10^{-2} percent to 5 percent. This test can also be conducted with different axial stress, which enables one to see its effect on the values of shear modulus and damping ratio. In this study, axial loads of 100 kPa, 250 kPa and 400 kPa were used. Table 3.5 below summarizes the axial stress and shear strain values used in this thesis. It should be noted here that, preparations of specimens and testing have been done for each strain level and axial load for a sample from one test pit and repeated to samples from all test pits.

Table 3.5: Summary of axial stresses and shear strains used in this study

Test pit	Sample type	Axial stress (kPa)	Shear strain (%)				
1	Remolded to field condition	100	0.01	0.1	1	2.5	5
		250	0.01	0.1	1	2.5	5
		400	0.01	0.1	1	2.5	5
2	Remolded to field condition	100	0.01	0.1	1	2.5	5
		250	0.01	0.1	1	2.5	5
		400	0.01	0.1	1	2.5	5
3	Remolded to field condition	100	0.01	0.1	1	2.5	5
		250	0.01	0.1	1	2.5	5
		400	0.01	0.1	1	2.5	5
4	Remolded to field condition	100	0.01	0.1	1	2.5	5
		250	0.01	0.1	1	2.5	5
		400	0.01	0.1	1	2.5	5
5	Remolded to field condition	100	0.01	0.1	1	2.5	5
		250	0.01	0.1	1	2.5	5
		400	0.01	0.1	1	2.5	5

3.3.4.2 Shear stress and strain parameters

During the cyclic shear stage of the test both lateral force and specimen displacements are measured for each loading cycle with time. Measured data can be displayed to the operator on Microsoft Excel spreadsheet. From the lateral force and displacement recorded data, one can calculate the shear stress (τ) and shear strain (γ) values. Using the specimen height after consolidation (< 20 mm) and its diameter, 70 mm, the shear stress and shear strain of the specimen can be calculated as shown in Equation 3.1 and 3.2 below:

$$\tau = \frac{force}{area} = \frac{shearforce}{(\pi \times 35^2)} \times 10^3 \quad \text{(MPa)} \quad \text{----------3.1}$$

$$\gamma = \frac{\Delta l}{l} = \frac{displacement}{height, afterconsolidation} \quad \text{----------3.2}$$

Table 3.6 below shows sample tabulation of shear strain and shear stress from the lateral force and specimen displacement taken from the 5th cycle test result of pit1 with peak-to-peak cyclic strain amplitude of 0.025 (2.5 %). The loading frequency used in this study is 1 Hz, which is commonly used in laboratory tests. From the predefined shear shape option such as, sinusoidal, triangular etc, the loading cycle shape has been selected to be sinusoidal (see Figure 3.4 below) as it is the most common type of seismic wave shape for analysis [3].

Table 3.6: Shear stress and shear strain values of the 5th cycle test result of pit 1 with 2.5 % strain and with 400 kPa axial loads.

Cycle No	Time (sec)	Lateral displacement (mm)	Shear force(kN)	γ=disp/18.194	$\tau=(F/(\pi*35^2))10^3$ (MPa)
5	0.000	-0.165	0.016	-0.0091	0.0041
	0.019	-0.051	0.056	-0.0028	0.0147
	0.038	0.026	0.080	0.0014	0.0209
	0.057	0.059	0.115	0.0032	0.0298
	0.076	0.100	0.163	0.0055	0.0424
	0.095	0.152	0.228	0.0084	0.0593
	0.114	0.202	0.288	0.0111	0.0749
	0.133	0.251	0.345	0.0138	0.0897
	0.152	0.297	0.396	0.0163	0.1029
	0.171	0.338	0.438	0.0186	0.1138
	0.19	0.386	0.466	0.0212	0.1211
	0.209	0.422	0.484	0.0232	0.1257
	0.228	0.437	0.494	0.024	0.1284
	0.247	0.453	0.497	0.0249	0.1291
	0.266	0.464	0.506	0.0255	0.1314
	0.285	0.470	0.511	0.0258	0.1327
	0.304	0.474	0.513	0.0261	0.1332
	0.323	0.476	0.511	0.0262	0.1329
	0.342	0.475	0.505	0.0261	0.1313
	0.361	0.471	0.493	0.0259	0.1281
	0.38	0.463	0.469	0.0255	0.1220
	0.399	0.446	0.424	0.0245	0.1102
	0.418	0.414	0.350	0.0228	0.0909
	0.437	0.371	0.258	0.0204	0.0669
	0.456	0.318	0.160	0.0175	0.0417
	0.475	0.255	0.065	0.014	0.0168
	0.494	0.152	-0.002	0.0084	-0.0006
	0.513	0.013	-0.051	0.0007	-0.0131
	0.532	-0.008	-0.063	-0.0004	-0.0164
	0.551	-0.043	-0.091	-0.0024	-0.0236
	0.57	-0.094	-0.148	-0.0052	-0.0385
	0.589	-0.145	-0.208	-0.008	-0.0540
	0.608	-0.198	-0.268	-0.0109	-0.0697

	0.627	-0.251	-0.328	-0.0138	-0.0851
	0.646	-0.302	-0.383	-0.0166	-0.0995
	0.665	-0.359	-0.410	-0.0197	-0.1066
	0.684	-0.389	-0.423	-0.0214	-0.1100
	0.703	-0.409	-0.441	-0.0225	-0.1146
	0.722	-0.425	-0.462	-0.0234	-0.1201
	0.741	-0.445	-0.487	-0.0244	-0.1264
	0.76	-0.461	-0.504	-0.0253	-0.1310
	0.779	-0.470	-0.511	-0.0258	-0.1328
	0.798	-0.474	-0.513	-0.026	-0.1332
	0.817	-0.476	-0.511	-0.0262	-0.1327
	0.836	-0.475	-0.506	-0.0261	-0.1314
	0.855	-0.471	-0.496	-0.0259	-0.1288
	0.874	-0.464	-0.477	-0.0255	-0.1239
	0.893	-0.448	-0.437	-0.0247	-0.1136
	0.912	-0.419	-0.368	-0.023	-0.0957
	0.931	-0.378	-0.282	-0.0208	-0.0732

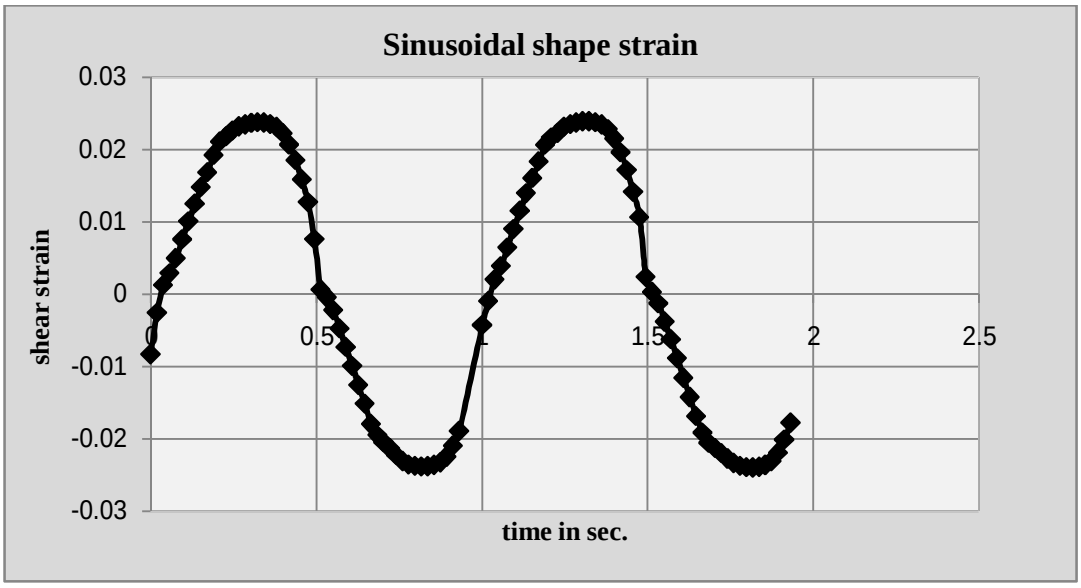


Figure 3.4: Sinusoidal wave shapes of 2.5 % strain of pit 1 for two cycles

3.3.4.3 Hysteresis loops of test results

The hysteresis loop of each cycle can be plotted using the results of shear strains and shear stresses that can be computed and presented with excel program. In most seismic events, the number of significant cycles is likely to be less than 20 [2]. For all practical purposes, the values determined at 5^{th} cycles likely to provide reasonable values [3]. Figure 3.5 below shows the hysteresis loops of the 5^{th} cycle plotted for each strain level of test pit1 tested under 400 kPa axial stresses. In this study, the number of cycles used in a taste is 40 and Figure 3.6 shows the hysteresis loops of 40 cycles together in each strain levels of test pit 1 tested with 400 kPa. It has been shown in section 2.1.2 that the deformation characteristics of soils vary to a large extent depending upon the magnitude of shear strains to which the soils are subjected. And also the values of shear modulus and damping ratio will depend on the magnitude of the strain for which the hysteresis loop is determined. Figure 3.7 shows the hysteresis loops of the 5^{th} cycles for each strain level test together and it shows how the value of shear strain affects the shape and size of the hysteresis loops. The effect of shear strain level can be explained as; when the shear strain increase, the line connecting the tips of the hysteresis loop rotate clockwise implying the shear modulus decreases. The width of the hysteresis loop becomes wider as the shear strain value increases. As a result, the damping effect of the soil increases.

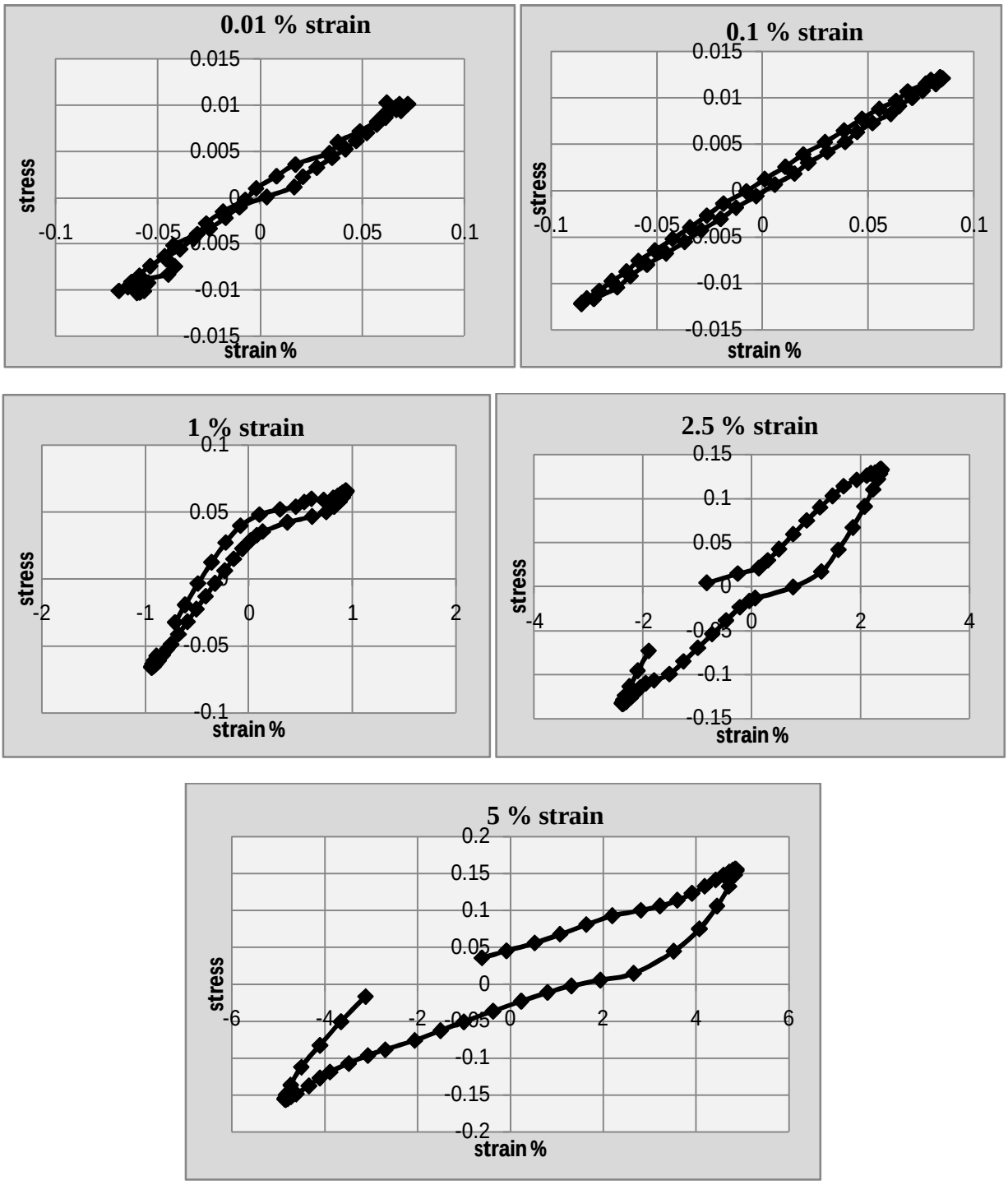


Figure 3.5: Hysteresis loops of the 5th cycle of pit 1 under 400 kPa of axial stress test for each strain level.

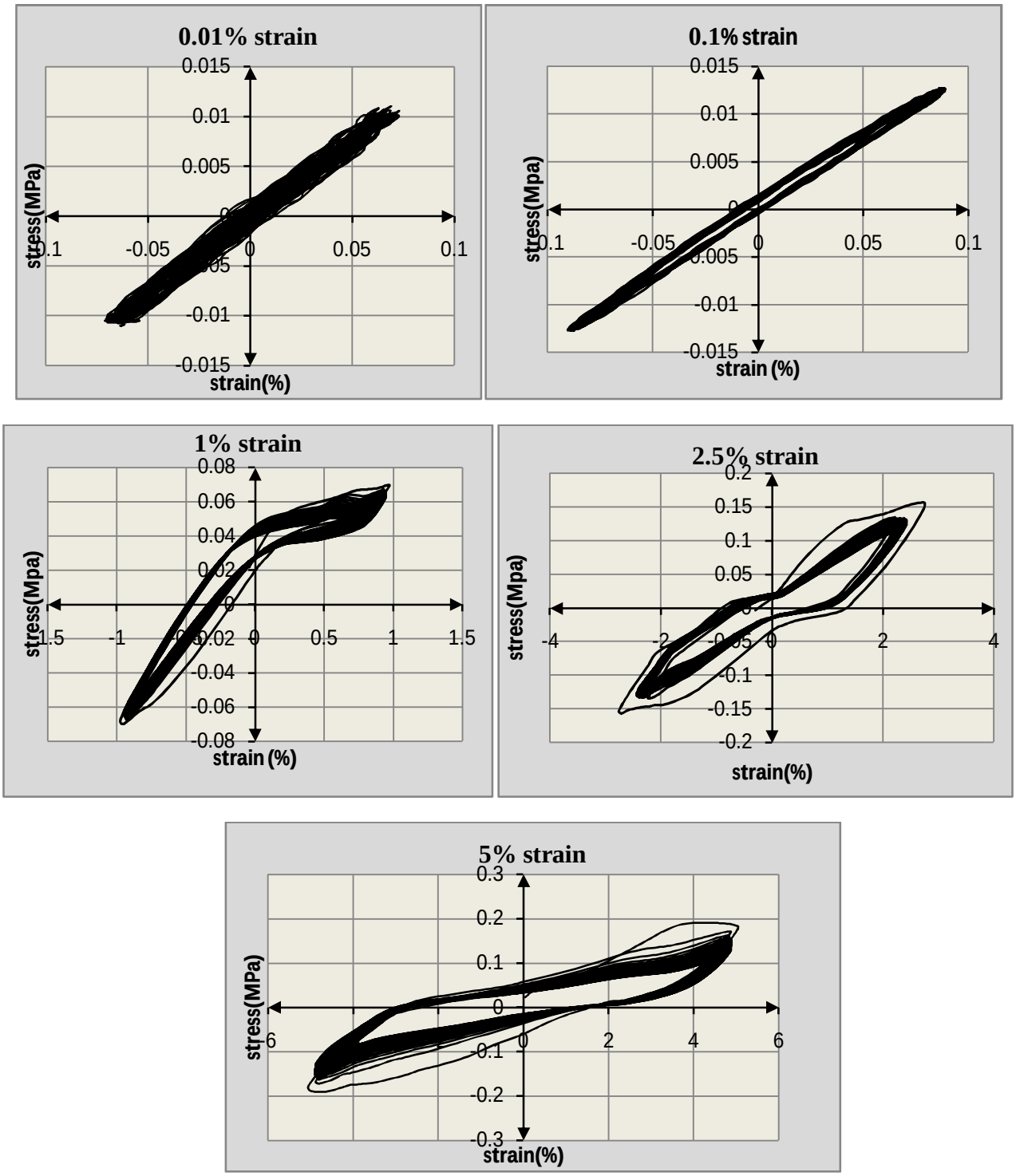
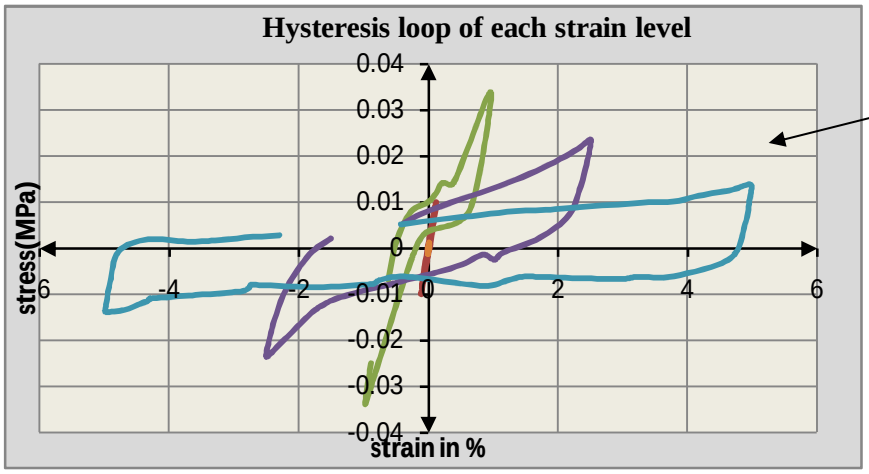
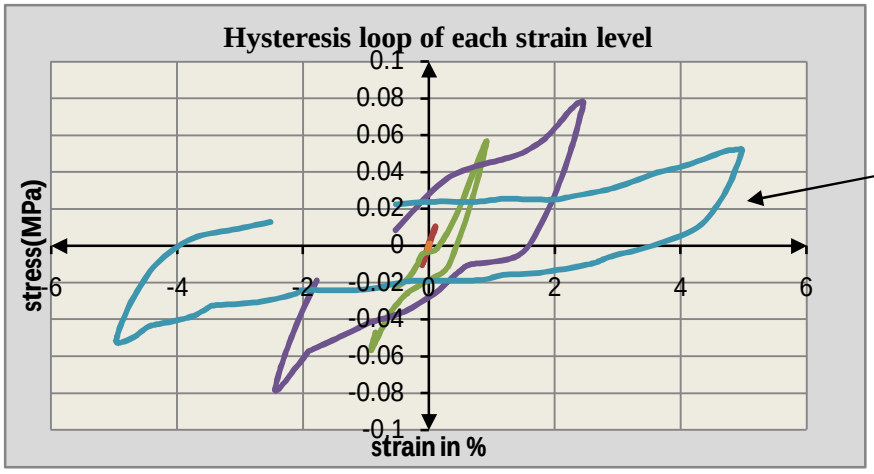


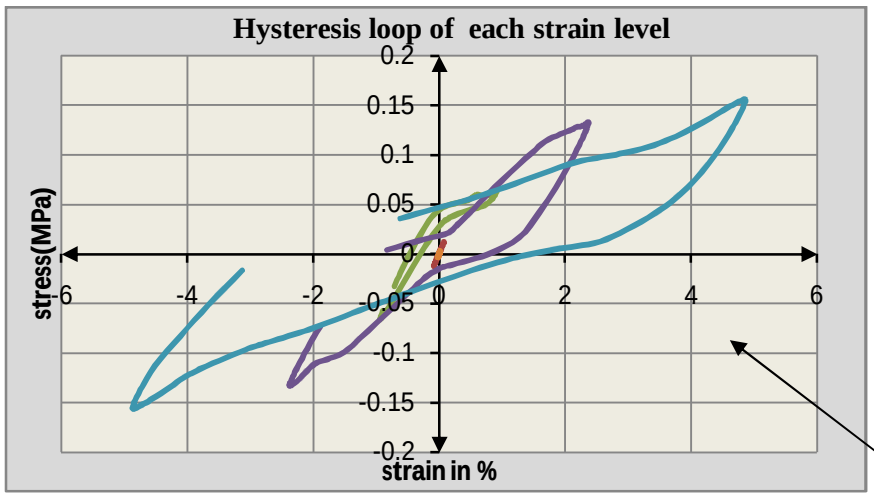
Figure 3.6: Hysteresis loops of the 40 cycles of pit 1 under 400 kPa of axial stresses



100 kPa axial loads



250 kPa axial loads



400 kPa axial loads

Figures 3.7: Hysteresis loops of the 5th cycle of pit 1 with strain levels of 0.01, 0.1, 1, 2.5 and 5 (all in percent).

CHAPTER 4

DATA ANALYSIS AND DISCUSSION OF TEST RESULTS

4.1 Computation of shear modulus and damping ratio values

Direct determination of stress-strain relationships are used for obtaining shear modulus and damping ratio by using cyclic simple shear test. As we have seen in section 3.3.4, the measured values of shear force and lateral displacement have been translated to shear stress and shear strain. And the hysteresis loops of each cycle can be plotted using the shear stress and strain values obtained from 50 sample points in a cycle. These 50 sample point's shear stress and shear strain values in a cycle have been analyzed for the determination of shear modulus and damping ratio values of the hysteresis loop. For the determination of shear modulus, *G*, and damping ratio, β, a typical calculation is presented below.

$$G = \frac{\tau}{\gamma} \quad \text{----------4.1}$$

$$\beta = \frac{W_D}{4\pi W_s} = \frac{A_{loop}}{4\pi A_\Delta} \quad \text{----------4.2}$$

$$A_{loop} = 0.5 \times \sum(\tau_i - \tau_{i+1}) \times (\gamma_i + \gamma_{i+1}) \quad \text{----------4.3}$$

$$A_\Delta = 0.5 \times X \times Y \quad \text{----------4.4}$$

Where: $X = \gamma_{\max} - \gamma_{center}$ and $Y = \tau_{\max} - \tau_{center}$

Since, the center of the hysteresis loop is at the origin; both the stress and strain value at center is zero.

To determine the shear modulus and damping ratio values of a cycle using the above equations, consider Table 3.6 again. Adding values of the expression $(\tau_i - \tau_{i+1}) \times (\gamma_i + \gamma_{i+1})$ to the right side, we can have Table 4.1 below and the values of shear modulus and damping ratio can be computed based on the values in this table and presented in Table 4.2.

Table 4.1: Tabulation for shear modulus and damping ratio computation

Cycle No	Time (sec)	γ=disp/18.194	$\tau=(F/(\pi*35^2))10^3$ (MPa)	$(\tau_i-\tau_{i+1})*(\gamma_i+\gamma_{i+1})$
5	0.000	-0.0091	0.0041	0.000126
	0.019	-0.0028	0.0147	$8.68*10^{-06}$
	0.038	0.0014	0.0209	$-4.1*10^{-05}$
	0.057	0.0032	0.0298	-0.00011
	0.076	0.0055	0.0424	-0.00023
	0.095	0.0084	0.0593	-0.0003
	0.114	0.0111	0.0749	-0.00037
	0.133	0.0138	0.0897	-0.0004
	0.152	0.0163	0.1029	-0.00038
	0.171	0.0186	0.1138	-0.00029
	0.190	0.0212	0.1211	-0.0002
	0.209	0.0232	0.1257	-0.00013
	0.228	0.024	0.1284	$-3.4*10^{-05}$
	0.247	0.0249	0.1291	-0.00012
	0.266	0.0255	0.1314	$-6.7*10^{-05}$
	0.285	0.0258	0.1327	$-2.6*10^{-05}$
	0.304	0.0261	0.1332	$1.57*10^{-05}$
	0.323	0.0262	0.1329	$8.37*10^{-05}$
	0.342	0.0261	0.1313	0.000166
	0.361	0.0259	0.1281	0.000314
	0.38	0.0255	0.1220	0.00059
	0.399	0.0245	0.1102	0.000913
	0.418	0.0228	0.0909	0.001037
	0.437	0.0204	0.0669	0.000955
	0.456	0.0175	0.0417	0.000784
	0.475	0.014	0.0168	0.00039
	0.494	0.0084	-0.0006	0.000114
	0.513	0.0007	-0.0131	$9.9*10^{-07}$
	0.532	-0.0004	-0.0164	$-2*10^{-05}$
	0.551	-0.0024	-0.0236	-0.00011
	0.570	-0.0052	-0.0385	-0.0002
	0.589	-0.008	-0.0540	-0.0003
	0.608	-0.0109	-0.0697	-0.00038
	0.627	-0.0138	-0.0851	-0.00044
	0.646	-0.0166	-0.0995	-0.00026
	0.665	-0.0197	-0.1066	-0.00014
	0.684	-0.0214	-0.1100	-0.0002
	0.703	-0.0225	-0.1146	-0.00025
	0.722	-0.0234	-0.1201	-0.0003
	0.741	-0.0244	-0.1264	-0.00023
	0.760	-0.0253	-0.1310	$-9.2*10^{-05}$
	0.779	-0.0258	-0.1328	$-2.1*10^{-05}$
	0.798	-0.026	-0.1332	$2.61*10^{-05}$
	0.817	-0.0262	-0.1327	$6.8*10^{-05}$
	0.836	-0.0261	-0.1314	0.000135
	0.855	-0.0259	-0.1288	0.000252

	0.874	-0.0255	-0.1239	0.000517
	0.893	-0.0247	-0.1136	0.000854
	0.912	-0.023	-0.0957	0.000986
	0.931	-0.0208	-0.0732	0.001523

Using the shear strain and damping ratio values of Table 4.1, the hysteresis loop of the cycle and the triangle with *X* and *Y* side dimensions are plotted in Figure 4.1. Thus, Figure 4.1 is used to visualize computation of shear modulus and damping ratio values of the cycle.

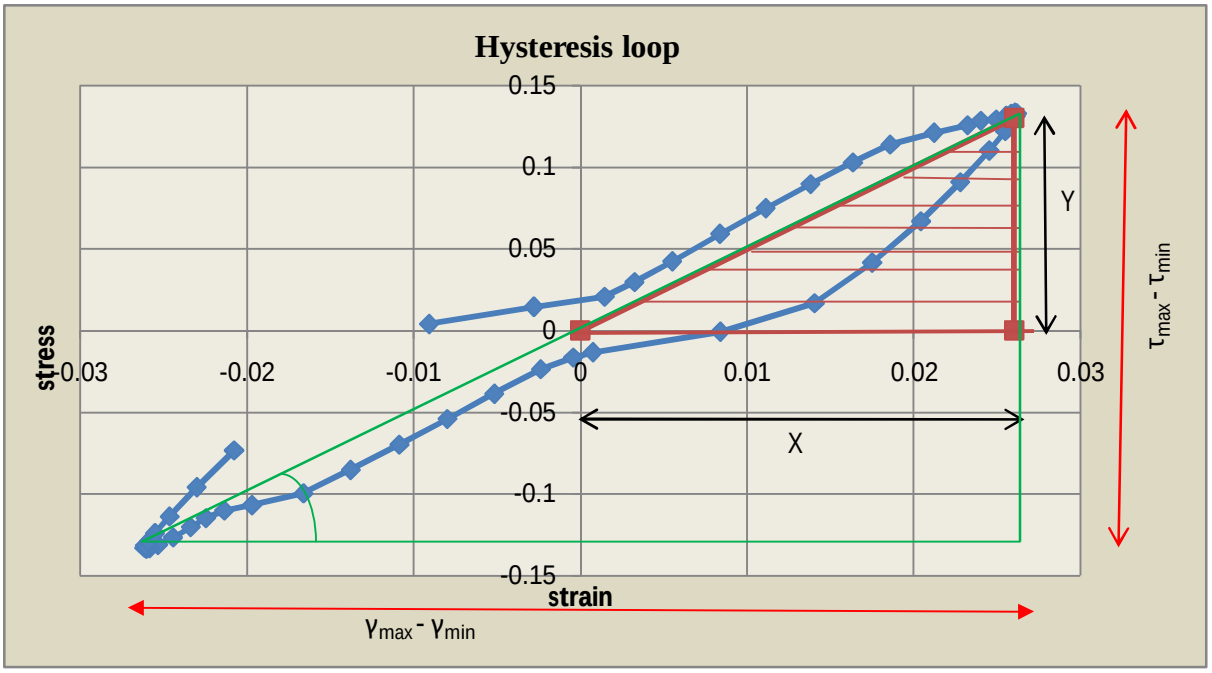


Figure 4.1: The hysteresis loop and triangle plotted using table 4.1 stress and strain values.

In order to determine the shear modulus and damping ratio values of a hysteresis loop, consider the following procedure:

To determine the equivalent (secant) shear modulus, the maximum and minimum shear stresses and shear strains are obtained from the cycle. Then, the magnitude of the difference between the maximum and minimum shear stresses and shear strains are determined. Thus, the equivalent shear modulus of the hysteresis loop will be calculated by using Equation 4.5 below.

$$G = \frac{(\tau_{max} - \tau_{min})}{(\gamma_{max} - \gamma_{min})} \quad \text{----------4.5}$$

To determine the damping ratio value of the hysteresis loop, the area of the loop and the triangle should be first determined. The loop area is calculated as the total sum of the values of the expression like the last column of Table 4.1 multiplied by 0.5 as shown in Equation 4.6 below.

$$A_{loop} = 0.5\left(\Sigma(\tau_i - \tau_{i+1}) \times (\gamma_i + \gamma_{i+1})\right) \quad \text{----------4.6}$$

The area of the triangle is calculated using the maximum values of shear stress and strain as:

$$A_{\Delta} = 0.5 \times X \times Y \quad \text{----------4.7}$$

Then, the damping ratio value is calculated as:

$$\beta = \frac{A_{loop}}{4\pi A_{\Delta}} \quad \text{----------4.8}$$

Using the above procedure a typical calculation of shear modulus and damping ratio for the cycle in Table 4.1 is presented in Table 4.2 below.

Table 4.2:Typical calculation of shear modulus and damping ratio using Figure 4.1 and Table 4.1

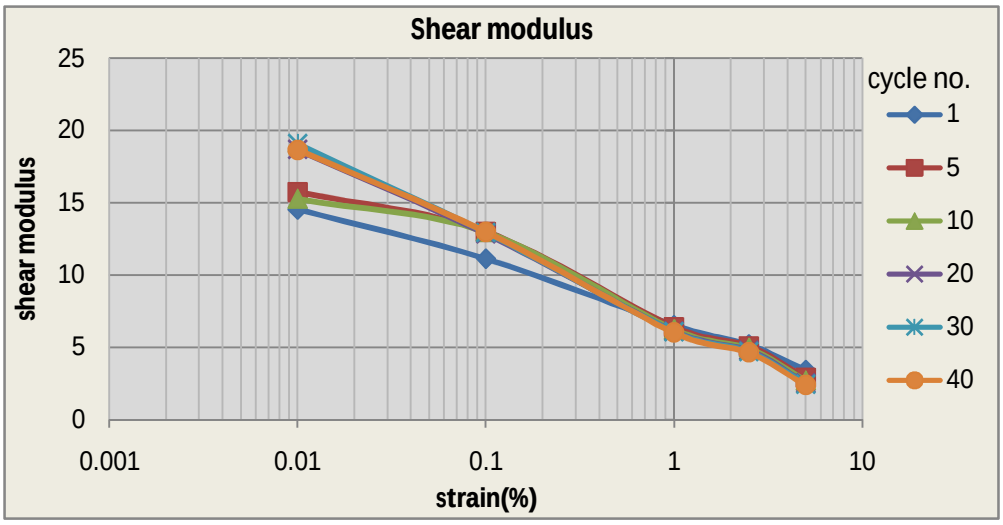
<table>
<tr><td colspan="2">Calculation of shear modulus</td><td colspan="2">Calculation of damping ratio</td></tr>
<tr><td>Calculation</td><td>Value</td><td>Calculation</td><td>Value</td></tr>
<tr><td>τ_{max}</td><td>0.1332</td><td>Area of hysteresis loop (A_{loop}) = $0.5*\sum(\tau_i - \tau_{i+1})*(\gamma_i + \gamma_{i+1})$</td><td>0.002498</td></tr>
<tr><td>τ_{min}</td><td>-0.1332</td><td rowspan="2">Area of triangle (A_{Δ}) = 0.5* X * Y = 0.5*0.0262*0.1332</td><td rowspan="2">0.001745</td></tr>
<tr><td>$\tau_{max} - \tau_{min}$</td><td>0.2664</td></tr>
<tr><td>γ_{max}</td><td>0.0262</td><td rowspan="2">$\beta = \frac{A_{loop}}{4\pi A_{\Delta}}$</td><td rowspan="2">0.1139</td></tr>
<tr><td>γ_{min}</td><td>-0.0262</td></tr>
<tr><td>$\gamma_{max} - \gamma_{min}$</td><td>0.0524</td><td rowspan="2">β (%)</td><td rowspan="2">11.39</td></tr>
<tr><td>$G = (\tau_{max} - \tau_{min})/(\gamma_{max} - \gamma_{min})$</td><td>5.084 (MPa)</td></tr>
</table>

Based on Table 4.2, the values of shear modulus and damping ratio of each cycle in a test can be determined. In this study, a single specimen was tested up to 40 cycles and Table 4.3 below shows shear modulus and damping ratio values of each cycle of pit 1 tested with 400 kPa axial loads.

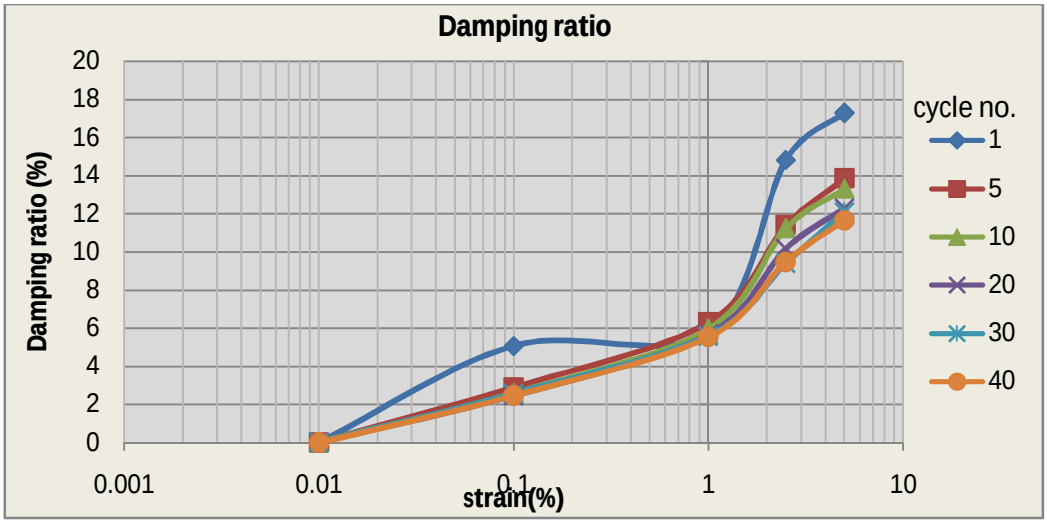
Table 4.3: Values of shear modulus and damping ratio for pit 1 tested with 400 KPa axial loads

Strain level	0.01%	0.1%	1%	2.5%	5%	0.01%	0.1%	1%	2.5%	5%
No cycle	G (MPa)					β (%)				
1	14.5453	11.1253	6.5176	5.1881	3.4113	0.032	5.0815	5.7586	14.836	17.309
2	14.0821	13.935	6.5544	5.5106	3.1947	0.0046	2.7515	7.0628	9.4231	15.9393
3	13.9766	13.138	6.4993	5.2496	3.0569	0.0191	3.4598	6.7603	10.921	15.1724
4	12.2503	13.1491	6.453	5.1853	2.9841	0.067	2.8952	6.5602	10.978	14.3119
5	15.739	12.9975	6.4042	5.0938	2.9184	0.022	2.8952	6.3113	11.411	13.8704
6	15.3935	13.0205	6.3689	5.0364	2.8671	0.0483	2.7599	6.2916	11.411	13.8248
7	14.6843	12.9038	6.3257	4.9866	2.8357	0.0719	2.8025	6.137	11.189	13.3489
8	14.2004	12.9222	6.2946	4.934	2.7937	0.0141	2.7477	6.1309	11.189	13.4319
9	15.5524	12.9106	6.2656	4.891	2.7544	0.0152	2.6171	5.9528	11.357	13.1637
10	15.2946	12.9976	6.2483	4.9705	2.7144	0.0531	2.5994	5.9678	11.246	13.3263
11	16.4147	13.1131	6.226	4.8762	2.6935	0.0356	2.4981	5.8965	11.407	12.9544
12	15.578	13.3018	6.2114	4.8709	2.6802	0.0288	2.5884	5.8838	10.354	12.9885
13	16.0567	12.9939	6.1894	4.8294	2.6613	0.031	6.7403	5.8579	10.992	12.8012
14	18.598	13.1166	6.189	4.8718	2.6386	0.0501	2.5377	5.7634	10.633	12.8874
15	16.7812	12.9213	6.1777	4.8648	2.6149	0.0133	2.5583	5.7592	10.861	12.7602
16	17.9577	12.9119	6.1646	4.8326	2.5981	0.0636	2.5338	5.7555	10.323	12.5615
17	16.7734	12.9761	6.157	4.8192	2.5831	0.0111	2.6781	5.745	10.122	12.6686
18	17.0271	13.1332	6.1486	4.8038	2.5707	0.0189	2.5523	5.7121	10.296	12.4208
19	18.0664	13.0121	6.1379	4.7646	2.5564	0.0128	2.6391	5.7297	10.076	12.5575
20	18.6919	12.8594	6.1172	4.7882	2.5459	0.0249	2.4635	5.6888	10.182	12.3079
21	16.9593	13.0131	6.1239	4.7558	2.537	0.008	2.6333	5.7072	10.274	12.4213
22	16.9593	13.0216	6.1103	4.7752	2.518	0.055	2.4996	5.6609	9.9679	12.3019
23	19.8994	13.0409	6.107	4.7722	2.5102	0.006	2.3605	5.6225	10.259	12.3775
24	17.7247	12.9207	6.0915	4.7616	2.5053	0.0249	2.6088	5.6829	9.8441	12.1987
25	19.64	13.0685	6.1024	4.7522	2.4933	0.0195	2.9205	5.6	9.7126	12.2548
26	18.5705	13.0264	6.0858	4.7515	2.4817	0.037	2.6833	5.6334	9.6903	12.2135
27	18.3744	13.0839	6.084	4.742	2.471	0.009	2.4864	5.6314	9.6687	12.0019
28	17.6274	12.9496	6.0808	4.7341	2.4738	0.025	2.4953	5.6575	9.5224	12.1318
29	17.2751	12.9436	6.0747	4.7251	2.4738	0.0441	2.573	5.5999	9.6512	11.9546
30	19.0848	12.9522	6.0745	4.7206	2.4626	0.031	2.5928	5.6127	9.4269	12.1082
31	17.3398	12.873	6.0699	4.7081	2.4548	0.005	2.2118	5.5929	9.5483	11.99
32	17.18	12.9646	6.0668	4.7037	2.4445	0.0251	2.5234	5.621	9.3703	12.0582
33	18.0167	12.8951	6.0538	4.6915	2.442	0.0283	2.504	5.5664	9.4228	11.9059
34	17.8384	13.0284	6.0614	4.6859	2.4378	0.0082	2.504	5.5293	9.2728	12.0275
35	19.2269	12.9073	6.0438	4.6788	2.4235	-0.017	2.5556	5.586	9.3899	11.9208
36	17.1137	13.0599	6.0525	4.6696	2.4199	0.019	2.4155	5.5301	9.3181	11.9777
37	17.6229	13.0327	6.0404	4.6615	2.4128	0.0053	2.3818	5.5961	9.3144	11.9173
38	17.9265	12.794	6.0404	4.649	2.4101	0.0268	2.5576	5.5421	9.3	11.7875
39	17.1746	13.0736	6.0427	4.6505	2.4041	0.0276	2.4732	5.5881	9.2964	11.9079
40	18.666	12.9916	6.0256	4.6381	2.3972	0.0061	2.4732	5.537	9.4952	11.6648

Using the values of shear modulus and damping ratio, the shear modulus and damping ratio curves can be plotted. Figure 4.2 below shows the shear modulus and damping ratio curves for some selected cycles from Table 4.3.



(*a*)



(*b*)

Figures 4.2: (*a*) shear modulus curves and (*b*) damping ratio curves of the results in Table 4.3 for selected cycles

4.2 Effect of number of cycles

The effect of number of cycles on the value of especially shear modulus in most soils subjected to cycling loading is observed up to 10 cycles, since strength degradation would occure from cycle to cycle as cycling loading continues. However, the effect of number of cycles on the soil used in this thesis is insignificant. These can be seen from Figure 3.7 which shows the hysteresis loops of 40 cycles for each strain level test have almost similar size and shape. As a result, the effect of number of cycles didn't show significant difference on the shear modulus and damping ratio values (see Table 4.3). Alternatively, this effect can also be seen in Figure 4.2 for some selected cycles. A similar effect has been observed for all other tests conducted in this study.

4.3 Shear modulus and Damping ratio values and curves

Shear modulus and damping ratio values of the 5^{th} cycles for all test pits and their graphs are presented below. Tables 4.4, 4.5 and 4.6 show the values of shear modulus and damping ratio of each test pits tested under the axial loads of 100 kPa, 250 kPa and 400 kPa respectively. Similarly Figures 4.3, 4.4 and 4.5 show the curves of shear modulus and damping ratio values taken from Tables 4.4, 4.5 and 4.6 respectively.

From Figures 4.3, 4.4 and 4.5, the curves of shear modulus and damping ratio show the closeness of the values of all test pits especially for higher strain levels. Eventhough, there is some difference from one test pit to the other, they didn't show a consistent value difference as one moves from one strain level to another. This makes difficult to compare one test pit curve with the other. The reasons for this may be, the similarity in soil type of the test pits, the narrow range of their PI values difference and other unknown factors.

The shear modulus and damping ratio values of some selected cycles of all test pits are presented in Appendix C.

Table 4.4: Shear modulus and damping ratio values with 100 kPa axial pressures

Strain (%)	0.01	0.1	1	2.5	5	0.01	0.1	1	2.5	5
	G (MPa)					β (%)				
Pit 1	10.3344	7.8377	3.2379	0.8747	0.2583	3.2221	8.7943	13.3656	17.2072	30.4857
Pit 2	7.0855	3.8776	3.0813	0.9057	0.4806	11.6735	11.613	18.3424	31.4454	39.3304
Pit 3	8.3221	6.8423	2.8903	0.6835	0.4438	4.5085	6.2642	10.6537	16.1719	18.1014
Pit 4	10.4429	8.3775	4.1512	1.814	0.4699	7.7097	11.4699	12.9492	24.6915	33.7001
Pit 5	6.769	4.9638	2.396	0.8661	0.4023	6.0378	11.7361	12.5878	16.0178	28.2749
average	8.5908	6.3798	3.1513	1.0288	0.411	6.6303	9.9755	13.5797	21.1068	29.9785

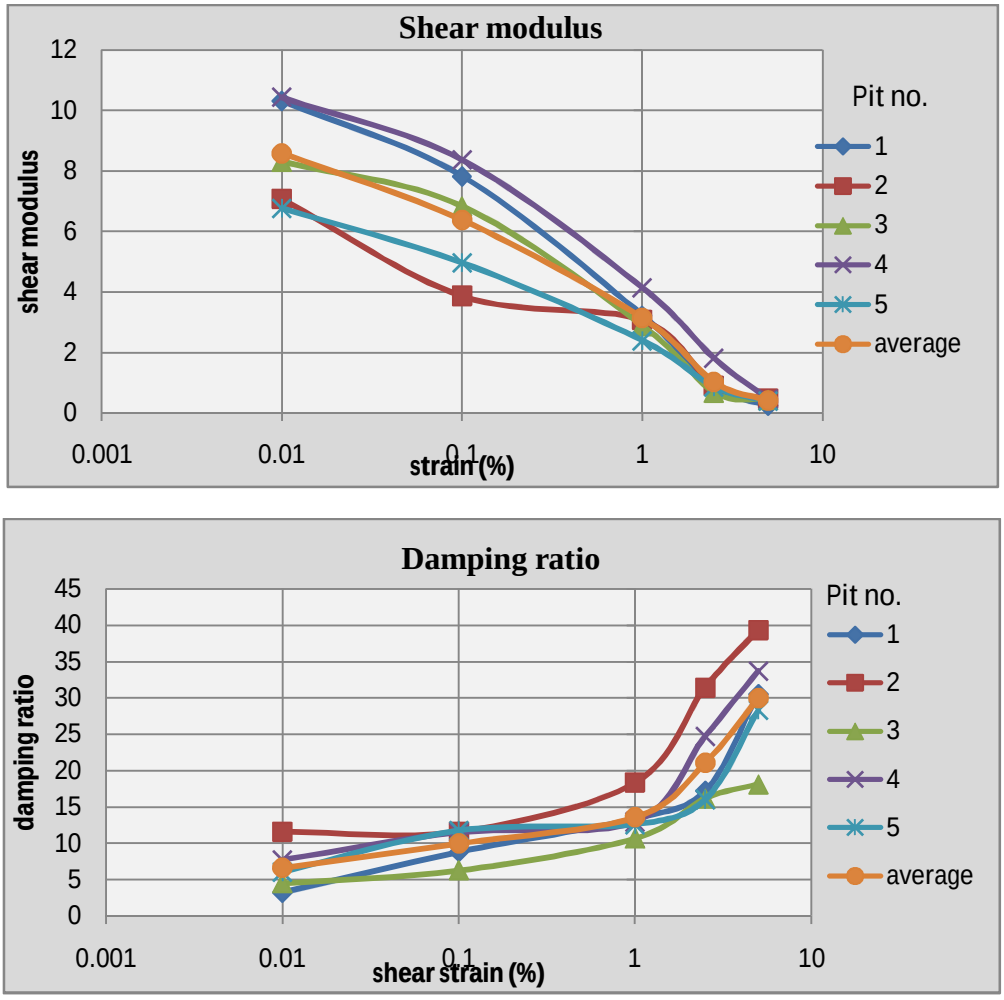
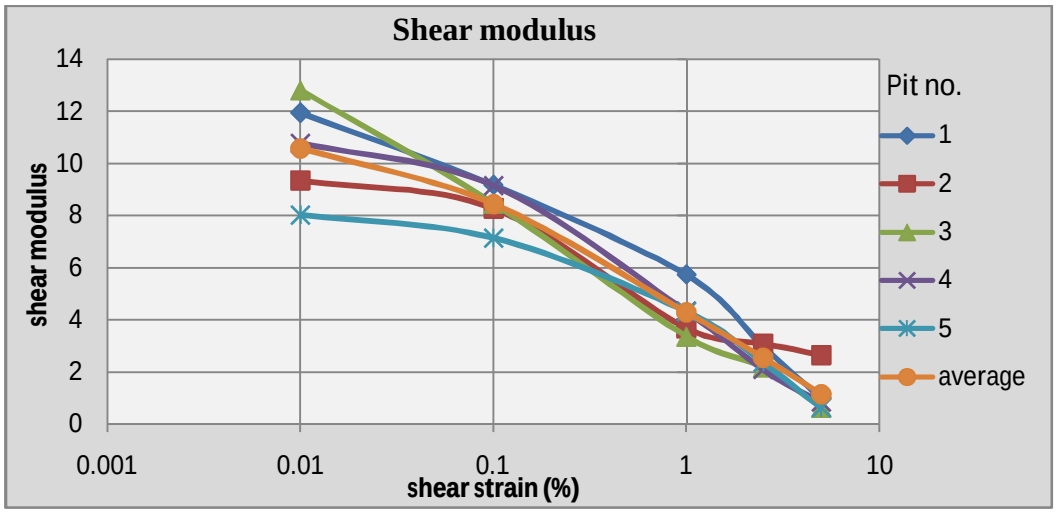


Figure 4.3: Shear modulus and damping ratio curves of Table 4.4

Table 4.5: Shear modulus and damping ratio values with 250 kPa axial pressures

Strain (%)	0.01	0.1	1	2.5	5	0.01	0.1	1	2.5	5
	G (MPa)					β (%)				
Pit 1	11.9353	9.1668	5.7271	2.971	0.9824	2.6779	7.6377	9.5277	12.752	22.8231
Pit 2	9.343	8.2755	3.6753	3.0837	2.6412	7.4936	9.8315	13.4919	22.3562	25.6675
Pit 3	12.8141	8.4653	3.3598	2.1765	0.6301	3.9148	5.8483	10.5729	14.4167	15.7919
Pit 4	10.7795	9.1505	4.3175	2.083	0.8334	6.5125	7.2869	10.4674	20.2461	27.7545
Pit 5	8.0207	7.1348	4.3138	2.3501	0.6142	5.4812	9.4008	8.5903	15.5255	20.5472
Average	10.5785	8.4386	4.2787	2.5329	1.1403	5.216	8.001	10.53	17.0593	22.5168



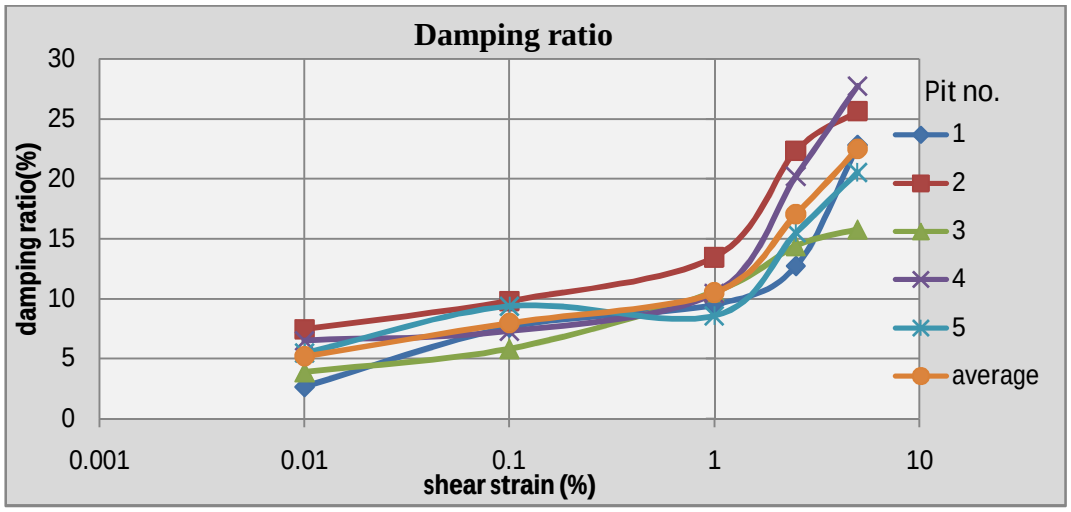


Figure 4.4: Shear modulus and damping ratio curves of Table 4.5

Table 4.6: Shear modulus and damping ratio values with 400 kPa axial pressures

Strain (%)	0.01	0.1	1	2.5	5	0.01	0.1	1	2.5	5
	G (MPa)					β (%)				
Pit 1	15.739	12.9975	6.4042	5.0938	2.9184	0.0219	2.8952	6.3113	11.411	13.8704
Pit 2	12.2432	10.3493	4.6262	4.1141	3.2939	2.9025	3.4011	7.2043	13.4418	15.8636
Pit 3	13.972	13.5101	5.5919	2.5689	1.0423	1.9527	3.1082	7.965	12.5884	13.7754
Pit 4	12.7693	10.2595	5.9683	2.9079	1.5489	5.7226	5.735	9.394	16.8174	19.6194
Pit 5	9.5725	8.5949	5.5686	3.3679	1.6541	3.1917	5.6256	8.0203	12.8188	15.6103
average	12.8592	11.1423	5.6318	3.6105	2.0915	2.7583	4.153	7.779	13.4155	15.7478

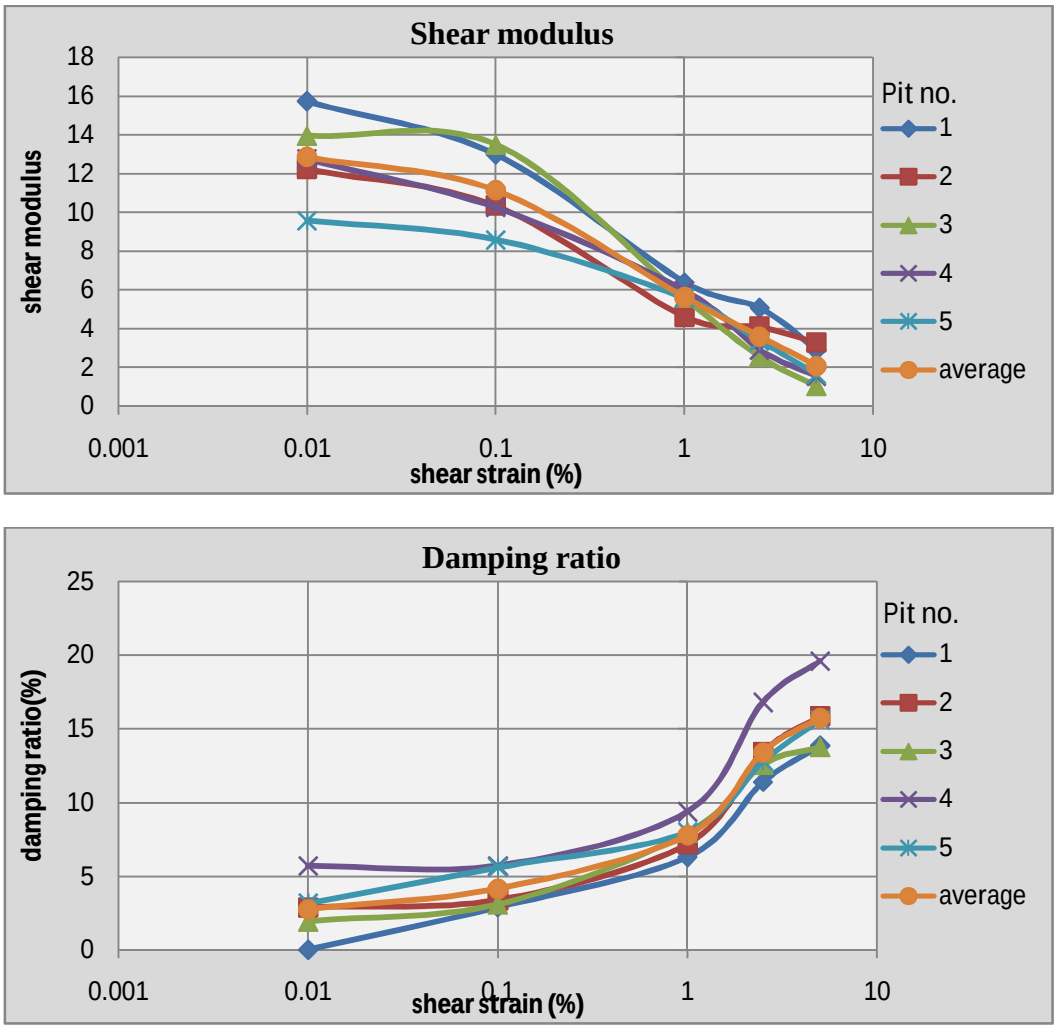
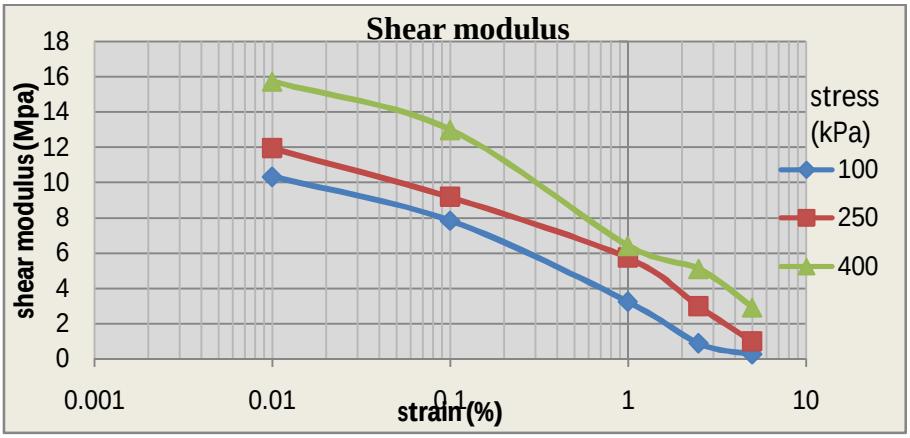


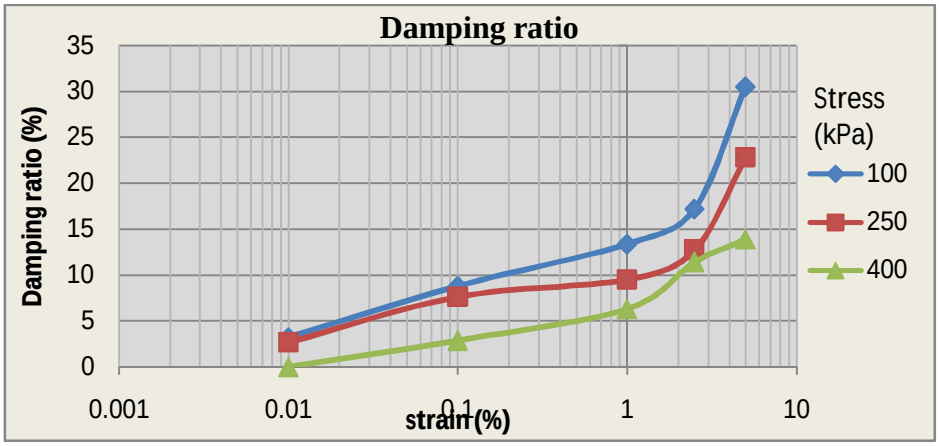
Figure 4.5: Shear modulus and damping ratio of Table 4.6

4.4 Effect of axial loads

Effective normal stresses can influence the values of shear modulus and damping ratio particularly for soils of low plasticity. In this study specimens were compressed under axial stresses of 100 kPa, 250 kPa and 400 kPa and their effect can be seen in Figure 4.6 below. From Figure 4.6 *a*, it can be seen that the higher the axial stress the higher the value of shear modulus. Similarly, Figure 4.6 *b*, shows the value of damping ratio decrease as the axial stress increase. This is true for all other test results (see Appendix D). This effect is also similar with literature and it can be explained from the fact that the dependency of soil strength on normal stresses.



(a)



(b)

Figure 4.6: (*a*) Shear modulus curves and (*b*) damping ratio curves of pit 1 with axial loads.

4.5 Computation of maximum shear modulus

Parameters describing the cyclic soil properties required for a dynamic analysis include the maximum shear modulus, and the modulus reduction and damping curves for the soil. The maximum shear modulus can be obtained from low strain seismic geophysical test which involves the measurements of body wave velocities which can be easily related to low-strain soil moduli or by using empirical correlations with index properties. In this study, computation of G_{max} is done using the expression in Equation (2.6) and presented below.

$$G_{\max} = 14760 \times \frac{(2.973 - e)^2}{1 + e} (OCR)^a (\sigma'_m)^{1/2} \quad \text{----------4.9}$$

Where G_{max} is the maximum shear modulus (lb/ft^2)

e is void ratio of the soil and equal to:

$$e = \frac{G_s \gamma_w}{\gamma_d} - 1 \quad \text{----------4.10}$$

a is a parameter that depend on the plasticity index of the soil and determined using Table 4.7 below.

Table 4.7: values of *a* with respect to plasticity index [15]

PI	*a*
0	0
20	0.18
40	0.30
60	0.41
80	0.48
≥100	0.5

From Table 4.7, the value of a ranges from 0 to 0.18 as the *PI* value goes from 0 to 20. Linear interpolation was used for the determination of *a* for each test pit (see Table 4.8 below).

Table 4.8: Values of the parameters *PI*, a and e for all test pits

Parameter	*Pit 1*	*Pit 2*	*Pit 3*	*Pit 4*	*Pit 5*
PI	11.664	14.082	0.000	0.000	6.990
a	0.105	0.127	0.000	0.000	0.063
e	1.120	0.980	1.030	1.080	1.280

The overconsolidation ratio (*OCR*) of soil is expressed as:

$$OCR = \frac{\sigma'_c}{\sigma'_p} \qquad \text{----------4.11}$$

Where σ_c' is preconsolidation pressure of a specimen

σ_p' is present effective vertical pressure

The term $(OCR)^a$ in the equation has little effect on the value of G_{max} since the value of *a* is zero for test pit 3 and 4 and also closer to zero in the others test pits.

σ_m' is mean principal effective stress (lb/ft^2) and it can be determined from the expression:

$$\sigma'_m = (\sigma_1 + \sigma_2 + \sigma_3)/3 \qquad \text{----------4.12}$$

Where σ_1 is the axial stress and $\sigma_2 = \sigma_3$ are the lateral confining stresses

Using K_0 loading condition, lateral stresses can be determined from the applied axial stress as:

$$\sigma_2 = \sigma_3 = K_0\sigma_1 \qquad \text{----------4.13}$$

K_0 is coefficient of earth pressure at rest and estimated reasonably to 0.5 for these silt soils.

Computation of G_{max} has been made for all test pits using the above procedures and tabulated in Table 4.10. Table 4.9 shows typical G_{max} values for different soil types and the computed values of G_{max} can be compared with this table. The G_{max} computed for the soils under study indicate that, the values are under acceptable range.

Table 4.9: Typical G_{max} values of soils [4].

Type of soil	*Initial shear modulus, G_{max} (kPa))*
Soft clays	2750 - 13750
Firm clays	6900 - 34500
Silty sands	27600 - 138000
Dense Sands and Gravel	69000 - 345000

Table 4.10: Computed G_{max} values with axial stresses of, *(a)* 100 kPa, *(b)* 250 kPa and *(c)* 400 kPa

Axial loads	*100 kPa*				
Test pit	*Pit 1*	*Pit 2*	*Pit 3*	*Pit 4*	*Pit 5*
σ_m' *(lb/ft^2)*	1392.37	1392.37	1392.37	1392.37	1392.37
OCR	0.5	0.5	0.5	0.5	0.5
G_{max} *(lb/ft^2)*	829412.38	1011771.13	1024267.16	948858.77	662792.92
G_{max} *(kPa)*	**39712.26**	**48443.60**	**49041.91**	**45431.35**	**31734.52**

(a)

Axial loads	*250 kPa*				
Test pit	*Pit 1*	*Pit 2*	*Pit 3*	*Pit 4*	*Pit 5*
$\sigma_m'(lb/ft^2)$	3480.92	3480.92	3480.92	3480.92	3480.92
OCR	0.2	0.2	0.2	0.2	0.2
$G_{max}(lb/ft^2)$	1191122.71	1424011.82	1619507.42	1500276.37	989184.58
$G_{max}(kPa)$	**57030.95**	**68181.68**	**77542.01**	**71833.23**	**47362.15**

(b)

Axial loads	*400 kPa*				
Test pit	*Pit 1*	*Pit 2*	*Pit 3*	*Pit 4*	*Pit 5*
$\sigma_m'(lb/ft^2)$	5569.48	5569.48	5569.48	5569.48	5569.48
OCR	0.125	0.125	0.125	0.125	0.125
$G_{max}(lb/ft^2)$	1434115.76	1696878.16	2048534.32	1897717.55	1214725.31
$G_{max}(kPa)$	**68665.46**	**81246.52**	**98083.82**	**90862.71**	**58161.04**

(c)

4.6 Modulus reduction (G/G_{max}) values

Modulus reduction values are used to plot the modulus reduction curves. Modulus reduction curves are the most widely used way of characterizing the modulus of soil under cyclic loading. The modulus reduction values can be determined using the values of table 4.10 for G_{max}. Table 4.11 below shows the modulus reduction (ratio) values determined using the G values of table 4.4, 4.5 and 4.6 with G_{max} values of table 4.10.

Tables 4.11: Modulus ratio ($\mathbf{G/G_{max}}$) values.

Axial load	100 kPa				
Shear strain (%)	0.01	0.1	1	2.5	5
	$\mathbf{G/G_{max}}$				
Pit 1	0.26023	0.19736	0.08153	0.02203	0.0065
Pit 2	0.14626	0.08004	0.06361	0.0187	0.00992
Pit 3	0.16969	0.13952	0.05894	0.01394	0.00905
Pit 4	0.22986	0.1844	0.09137	0.03993	0.01034
Pit 5	0.2133	0.15642	0.0755	0.02729	0.01268

(a)

Axial load	250 kPa				
Shear strain (%)	0.01	0.1	1	2.5	5
	$\mathbf{G/G_{max}}$				
Pit 1	0.20928	0.16073	0.10042	0.05209	0.01723
Pit 2	0.13703	0.12137	0.0539	0.04523	0.03874
Pit 3	0.16525	0.10917	0.04333	0.02807	0.00813
Pit 4	0.15006	0.12739	0.0601	0.029	0.0116
Pit 5	0.16935	0.15064	0.09108	0.04962	0.01297

(b)

Axial load	400 kPa				
Shear strain (%)	0.01	0.1	1	2.5	5
	$\mathbf{G/G_{max}}$				
Pit 1	0.22921	0.18929	0.09327	0.07418	0.0425
Pit 2	0.15069	0.12738	0.05694	0.05064	0.04054
Pit 3	0.14245	0.13774	0.05701	0.02619	0.01063
Pit 4	0.14053	0.11291	0.06568	0.032	0.01705
Pit 5	0.19028	0.17085	0.11069	0.06695	0.03288

(c)

CHAPTER 5
COMPARISON OF TEST RESULTS WITH LITERATURE

5.1 Introduction

Modulus reduction and damping ratio curves for sand and saturated clay soil types have been developed by some reserachers. The most represenetative and widely used curves for these type of soils are those established by Seed and Indriss,(1970). Vucetic and Dobry (1991) have also developed a set of curves that depend on the plasticty index, *PI*, of the soil (see Figure 2.3). In these curves, the curves plotted for *PI* equal to zero apply to cohesionless soil. For this study, the curves developedby Seed and Indrisss (1970), Vucetic and Dobry (1991) (for *PI* values of 0, 15and 30) and curves from test results of Abera for Gulelle area clay soils are used to compare the test results of soils under study.

5.2 Shear modulus reduction

5.2.1 Comparison

The shear modulus reduction values of Table 4.11 can be plotted and compared with literature values. Figure 5.1, 5.2, show locations of test pit 1 test results as compared with literature curves. And Figure 5.3 shows comparison with Abera's Gulelle area clay soils result curves. Figure 5.4, 5.5 and 5.6 show locations of the whole test results as compared with literature curves. Comparison for the others test pits are presented in Appendix-E.

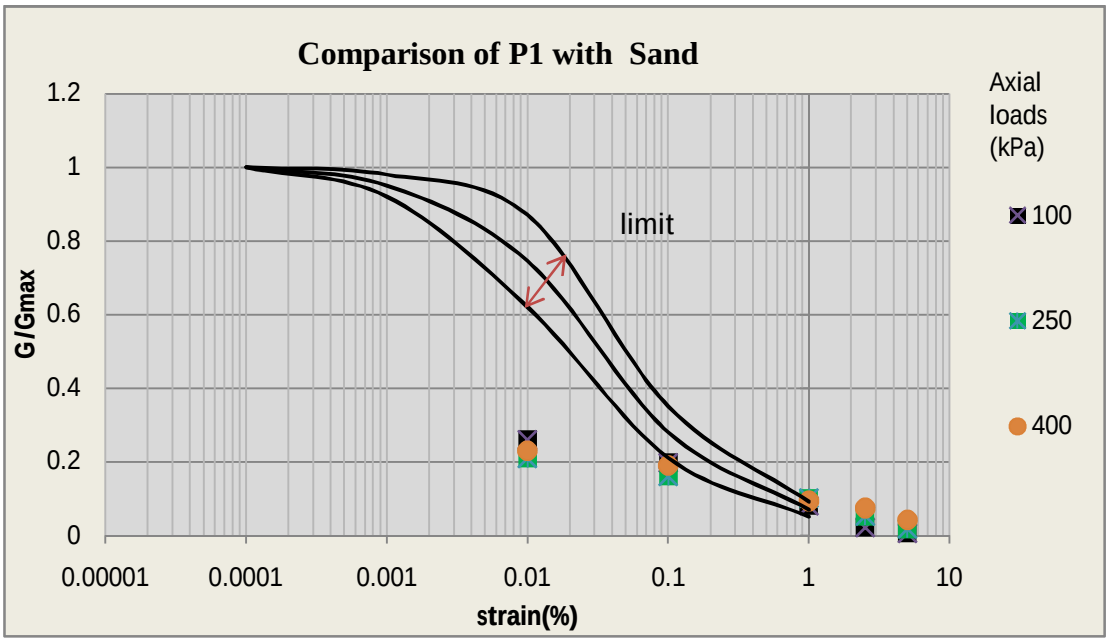


Figure 5.1: location of modulus reduction values of pit 1 as compared with curves developed for sand by Seed and Indriss (1970)

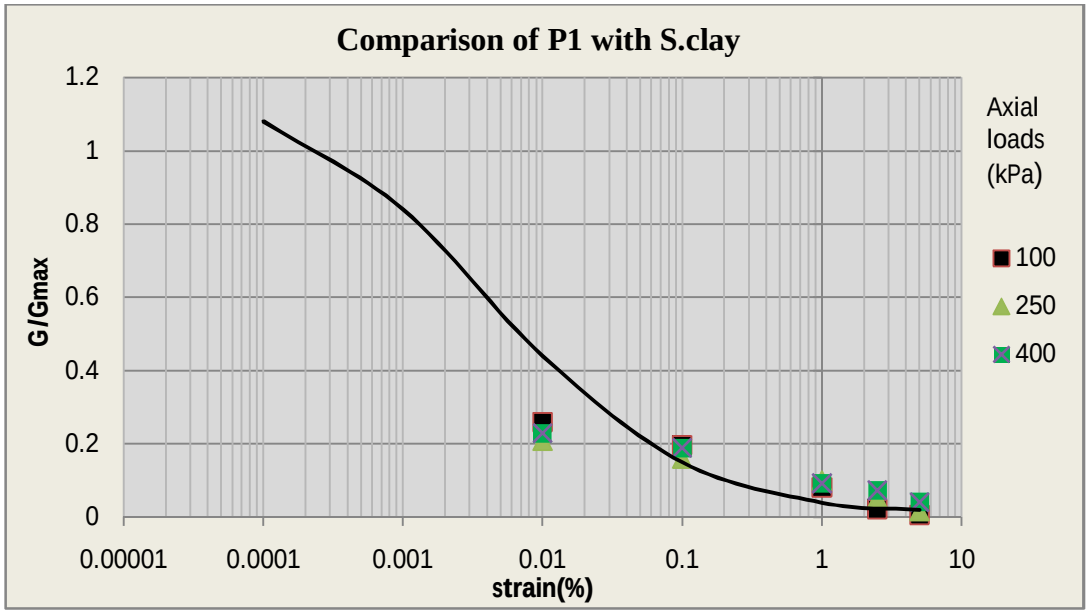


Figure 5.2: Location of modulus reduction values of pit 1 as compared with curves developed for saturated clay by Seed and Indriss (1970)

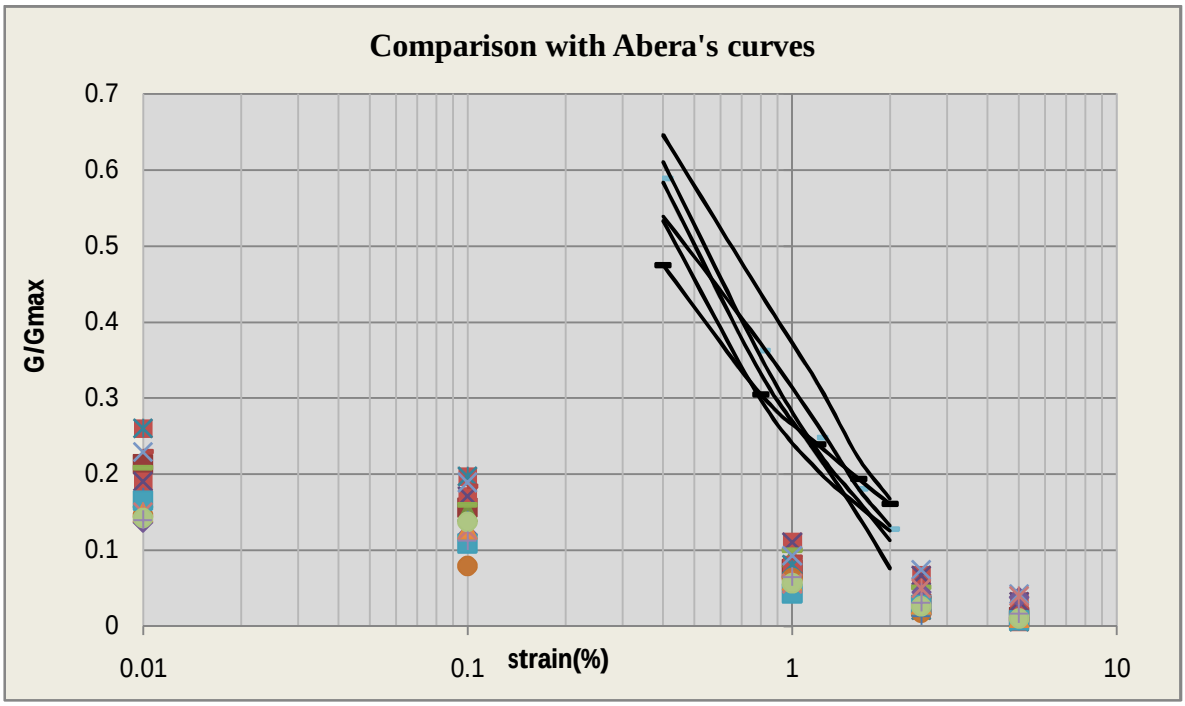


Figure 5.3: Location of modulus reduction values of all test results as compared with Abera's curves for Gulelle area clay soils

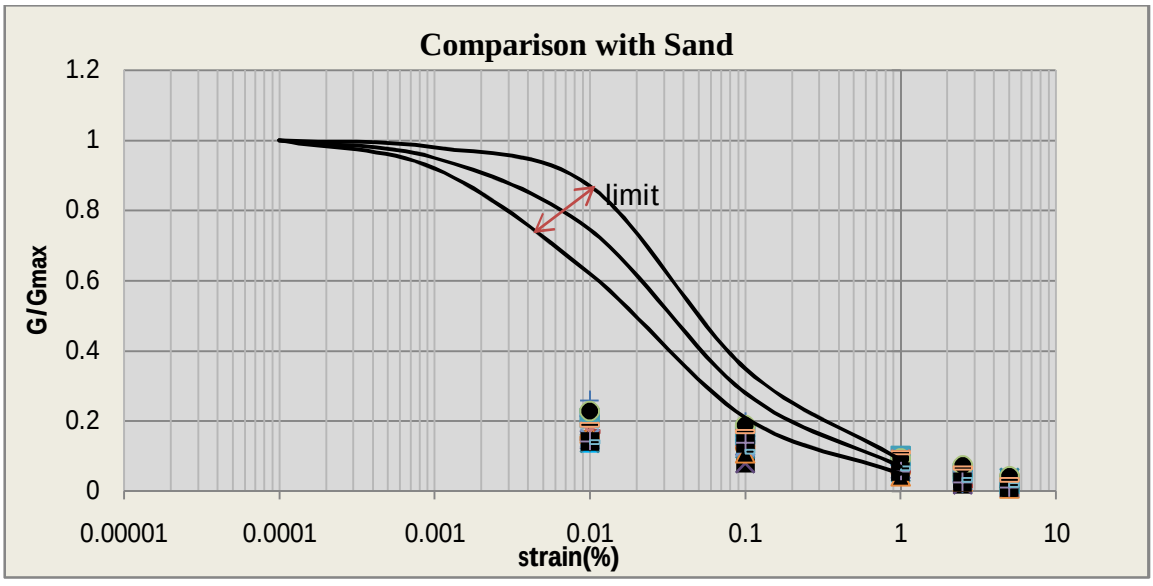


Figure 5.4: Location of modulus reduction values of all test results as compared with curves developed for sand by Seed and Indriss (1970)

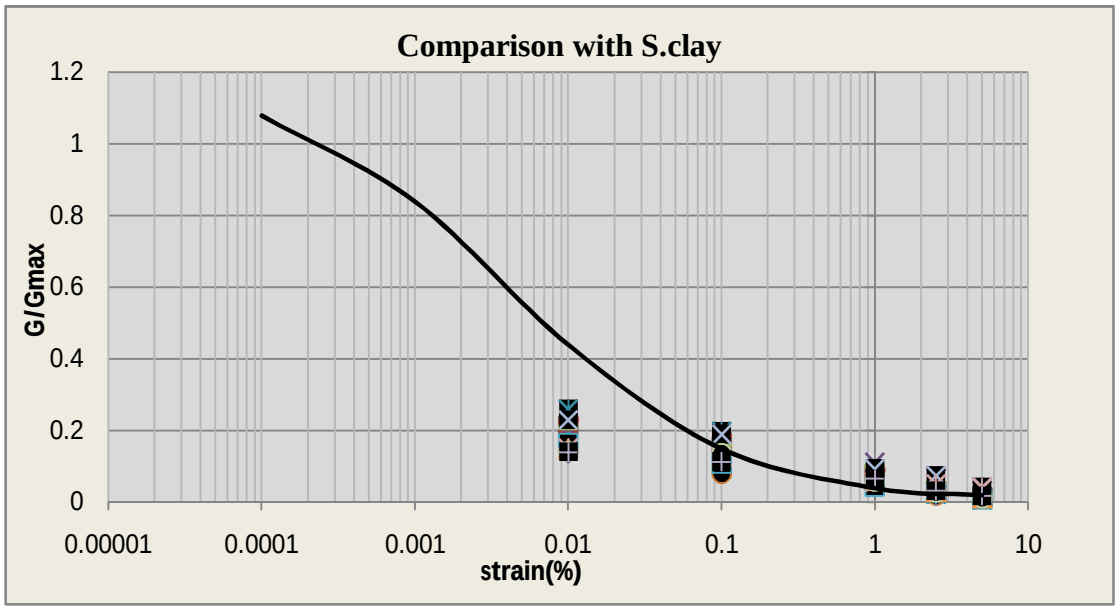


Figure 5.5: Location of modulus reduction values of all test results as compared with curves developed for saturated clay by Seed and Indriss (1970)

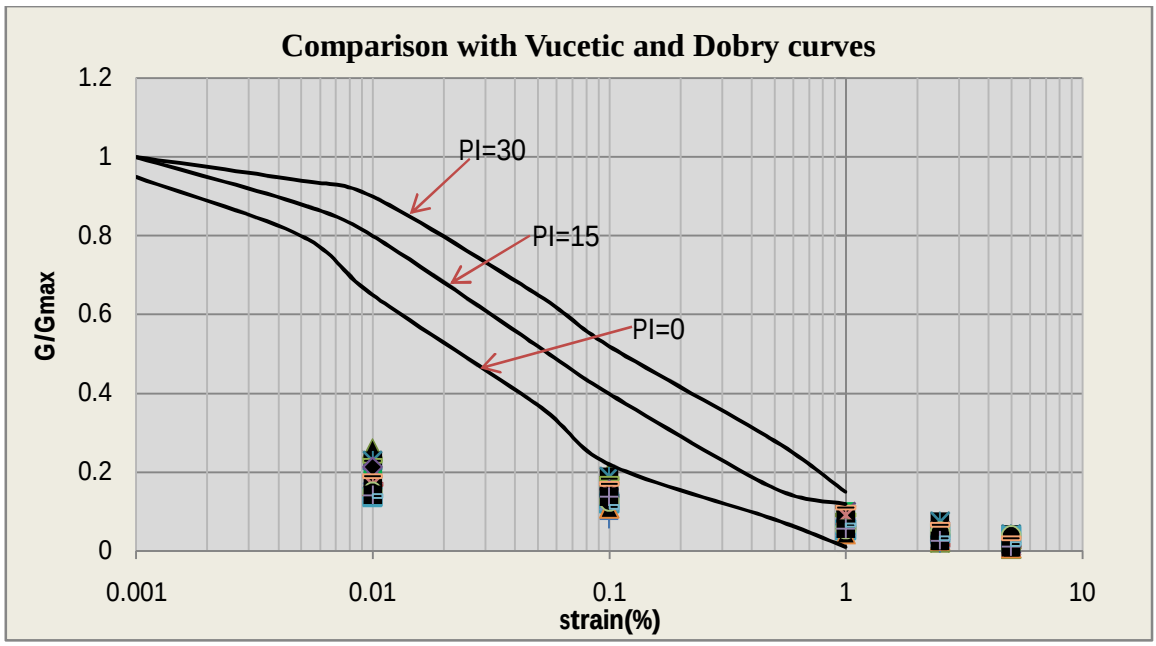


Figure 5.6: Location of modulus reduction values of all test results as compared with curves developed by Vucetic and Dobry (1991)

5.2.2 Discussion

- Figures 5.1, 5.2, 5.3, 5.4, 5.5 and 5.6 show that, the shear modulus reduction values of the soil under study at lower strain (0.01 percent) are lower than literature values.
- The shear modulus reduction values at 0.1 percent strain are lower than that of Vecetic and Dobry curves for sand but are comparable with saturated clay curve.
- The shear modulus reduction values for the other strains (1, 2.5 and 5 percents) are comparable with all litrature values since, the values for all types of soils approach to zero as strain levels increase.
- In general, it can be said that the results of shear modulus reduction values of the soils in this study are comparable with literature values except for lower stain level. This shows that the effect of testing conditions on shear modulus is minimal compared to literature results.

5.3 Damping ratio

5.3.1 Comparison

The damping ratio values of Tables 4.4, 4.5 and 4.6 can be plotted and compared with literature curves. Figures 5.7 and 5.8, show location of test pit 1 test results as compared with literature curves. Figure 5.9 shows total test result cerves as compared with Abera's Gulelle area clay soils. Figures 5.10, 5.11 and 5.12, show locations of the whole test results as compared with literature curves. Comparison for the others test pits are presented in Appendix-E.

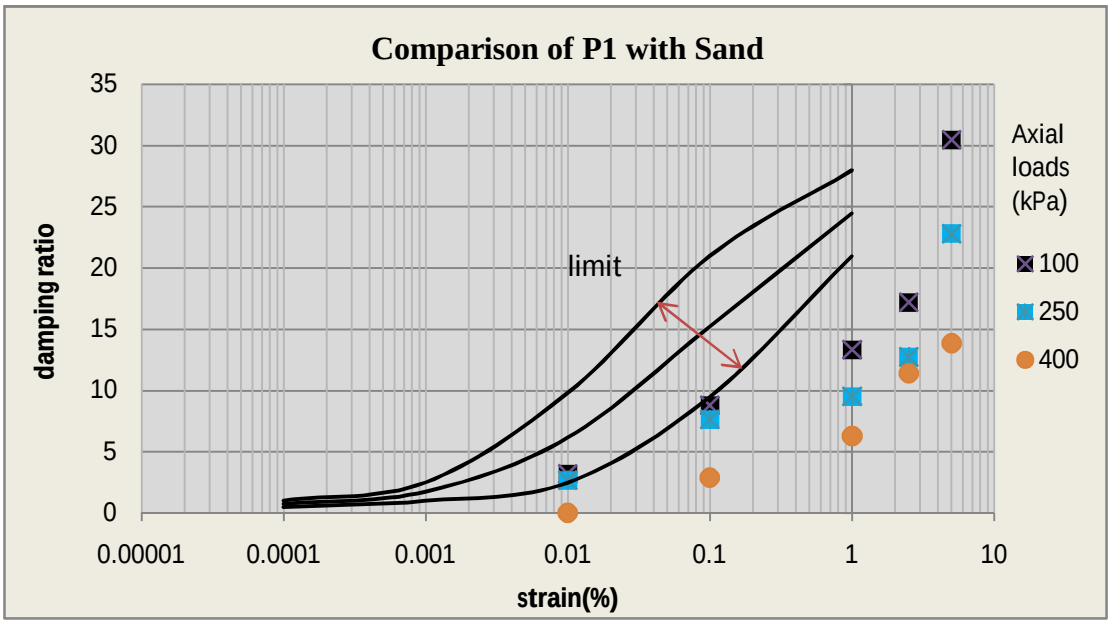


Figure 5.7: Location of damping ratio values of pit 1 as compared with curves developed for sand by Seed and Indriss (1970)

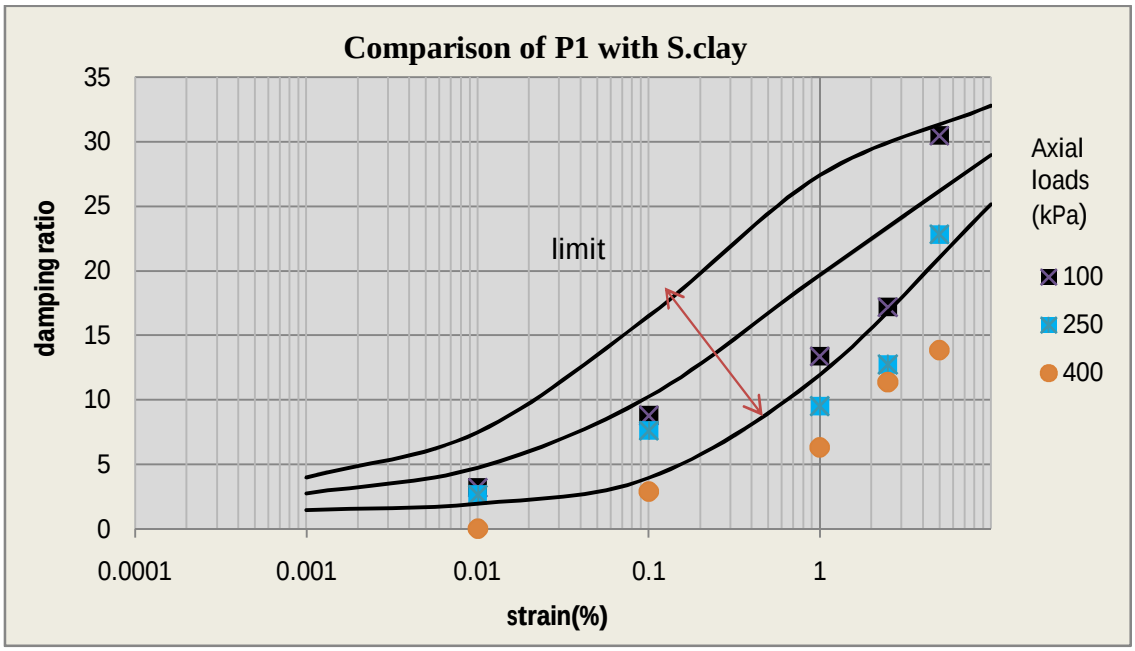


Figure 5.8: Location of damping ratio values of pit 1 as compared with curves developed for saturated clay by Seed and Indriss (1970)

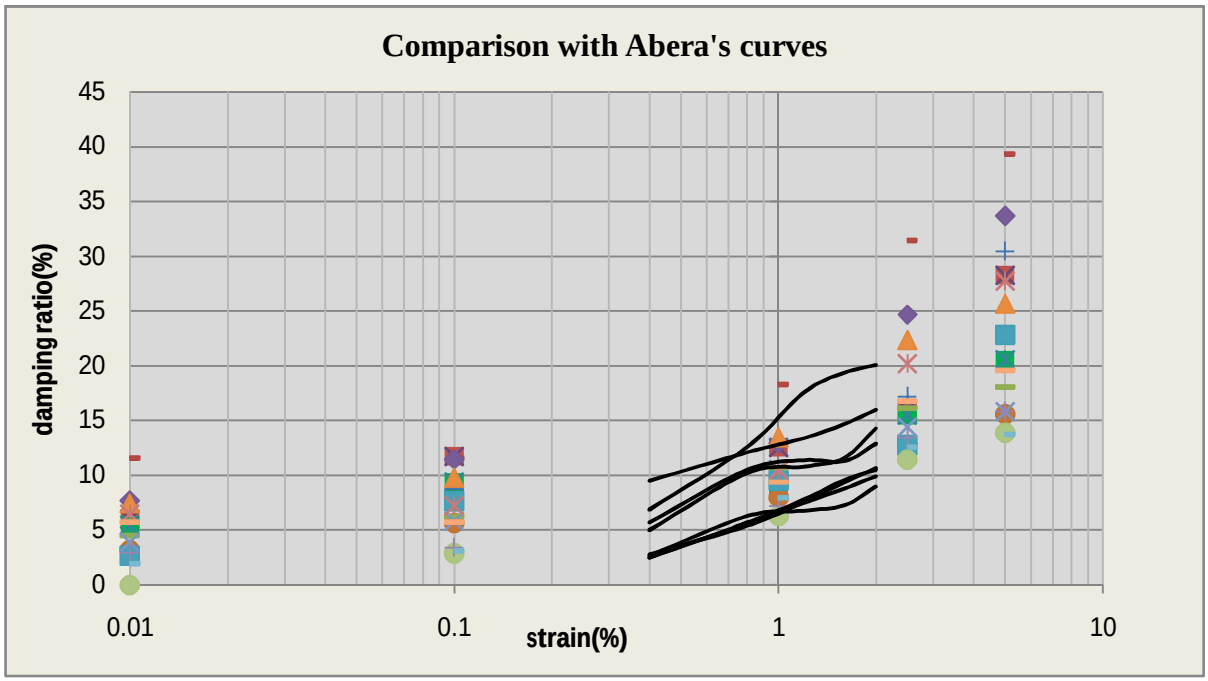


Figure 5.9: Location of damping ratio values of total test results as compared with Abera's curves for Gulelle area clay soils

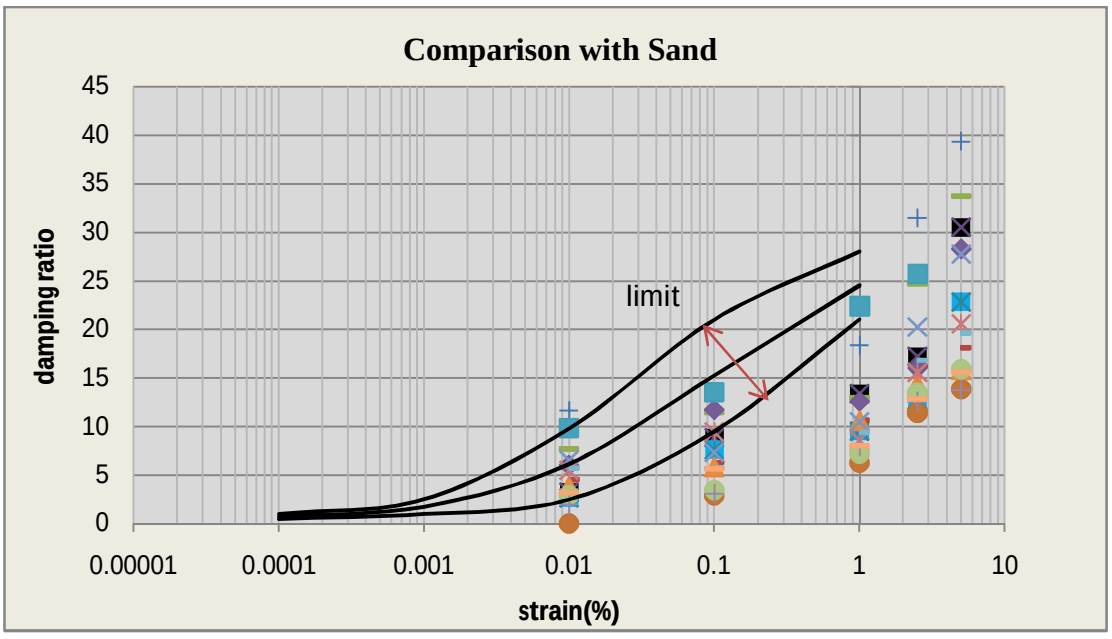


Figure 5.10: Location of damping ratio values of all test results as compared with curves developed for sand by Seed and Indriss (1970)

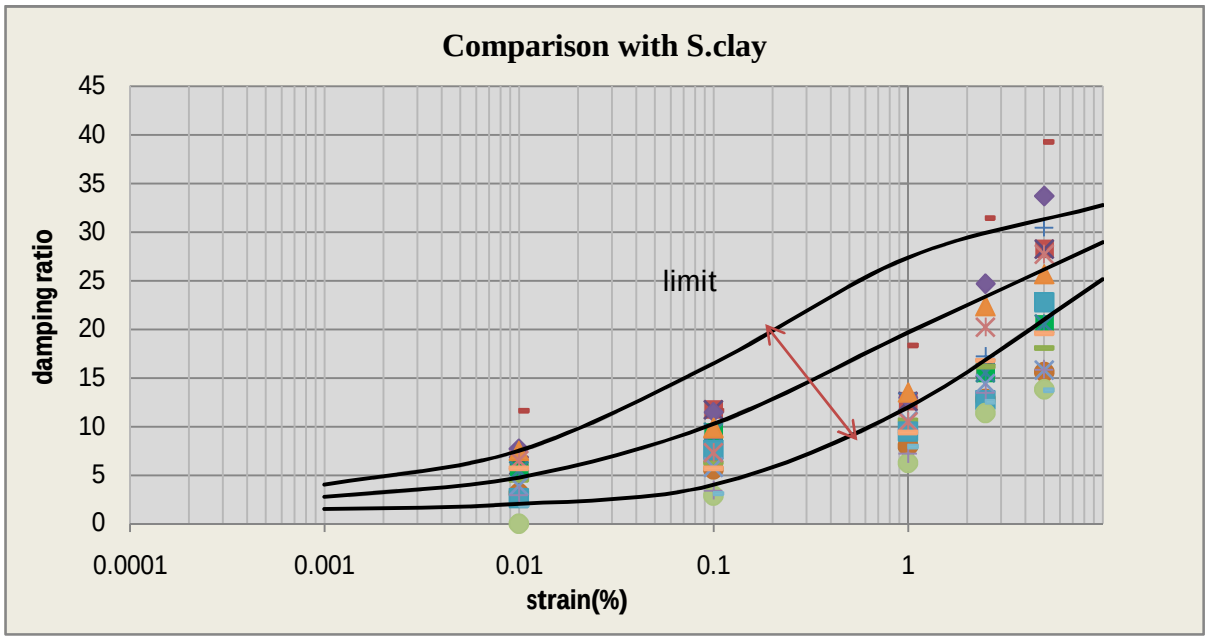


Figure 5.11: Location of damping ratio values of all test results as compared with curves developed for saturated clay by Seed and Indriss (1970)

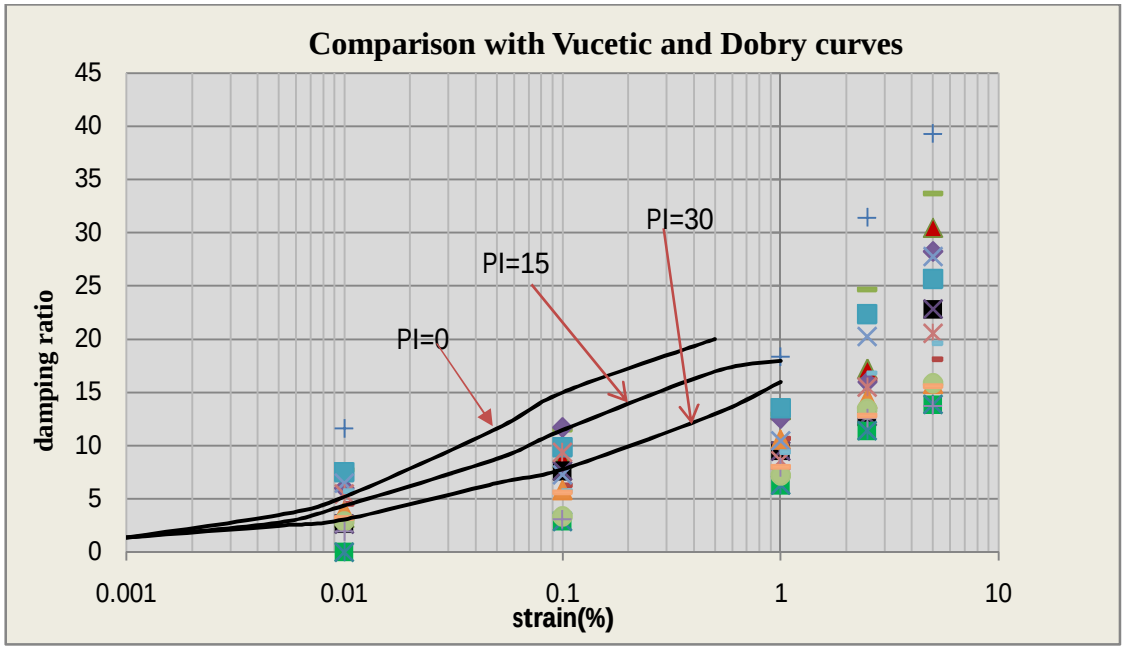


Figure 5.12: Location of damping ratio values of all test results as compared with curves developed by Vucetic and Dobry (1991)

5.3.2 Discussion

- It is known that, the damping effects for saturated clay is small as compared to cohesionless soils which exhibits considerable damping. Figures 5.10, 5.11 and 5.12 show that,the damping ratio of the soils under study have lower values as compared to the literature curves except for the lower strain (0.01 %) at which the result is moderate to all curves. However, the damping ratio results of these soils are comparable with Abera's Gulelle area clay soils.
- The values of the test results are positioned below the curve for sand and around the lower side of the curve for saturated clay. Eventhough, there is no curves developed for silt type of soils, the position of test results for this type of soil would be expected to be in between the curve for sand and for clay. But this is not the case for the silt soil considered in this study as the test results lie around the lower side of the clay. The reasons for this may be:
    - ✓ All samples considered in this thesis are remolded to field density and moisture content different to the conditioned of the soil in the literature.
    - ✓ The difference in testing conditions, as it was not possible to fully saturate the soil during consolidation.
    - ✓ As most previous tests were conducted using cyclic triaxial testing machine, the type of the testing machine may have its own effect on the values.
    - ✓ And other unknown factors .
- In general, unlike the shear modulus, the damping ratio results are lower than literature results except for the lower strain. This shows that the values of damping ratio have been affected by the above and other factors and their resultant effect is to lower the values.

CHAPTER 6
CONCLUSION AND RECOMMENDATION

6.1 Conclusion

This thesis has investigated the shear modulus and damping ratio values of soils commonly found in Hawassa using cyclic simple shear testing machine. Remolded soil specimen, which were taken from five test pits in the city, were used in the determination of these parametes. The index properties tests conducted in the laboratory show that the soils are mainly silt. For cyclic shear tests, specimens were remolded to field conditions so as to replicate some natural state like, density and moisture content.

The cyclic simple shear tests were conducted for the strain values of 0.01, 0.1, 1, 2.5 and 5 percents and under the axial stresses of 100, 250 and 400 kPa. From the test results of this study the following can be conclude:

- The computed maximum shear modulus, $G_{max,}$ values are within the range of 31.7 to 98 MPa which is acceptable for this soil type based on the literature.
- The shear modulus and damping ratio curves show similar shape and behavior comparing with the curves presented in the literature.
- The shear modulus reduction values are in good agreement with well established literature values except at the lowest strain level (0.01 %).
- The damping ratio values of the tests are generally lower than the literature values except at the lowest strain level(0.01 %).
- In comparison to literature values, the testing conditions appear to have significant effect on the damping ratio curves but little effect on the shear modulus reduction curves.

6.2 Recommendation

From this thesis, the following recommendation can be made:

- In addition to cyclic simple shear testing machine, cyclic triaxial testing machine should also be used. Since using cyclic triaxial testing machine, various testing procedures can be followed to have a better understanding and characterization of the dynamic proprties of the soils.

LIST OF REFERENCES

[1] ASTM, "American society for testing and materials", Annual Book of ASTM Standards, 1998.

[2] Das, B.M., "Principle of Geotechnical Engineering", California state University, Sacramento, 2006.

[3] Das, B.M., "Principles of Soil Dynamics", California State University, Scramento: Brooks/Cole ltd, 1993.

[4] Design Guidance, "Geotechnical Earthquake Engineering for Highways", Volume I, US department of transportation, Geotechnical Engineering Circular No.3,Washington, 1997.

[5] Dfaz-Rodriguez, I.A., "Dynamic properties of Mexico city for wide strain range", Earthquake Engineering, tenth world conference, 1992.

[6] Elia, B.D., Lanzo, G. and Pagliaroli, A., "Small-strain stiffness and Damping of soils in a direct simple shear device", pacific conference on Earthquake Engineering, 2003.

[7] Girmachew Yimer, "Shear modulus and Damping ratio of dry koka sand using cyclic simple shear test", Addis Ababa University, Addis Ababa,2010.

[8] Hobson, Y., "Liquefaction of sand in simple shear condition", Tokyo metropolitan University, Tokyo, Japan.

[9] http://en.wikipedia.org/wiki/Awasa

[10] http://www.worldweatheronline.com/weatheraverages/Ethiopia/707000/Awassa/708785/info.aspx

[11] Ishihara, K., "Soil behavior in Earthquake Geotechnics", department of civil Engineering, Science University of Tokyo, by Oxford University Presss Inc.,NewYork, 1996.

[12] Jafari[1], M.K., Shafiee[2], A. and RaZmkhah[3], A., 'Dynamic properties of fine grained soils in South of Tehran", Iran. JSEE: Spring 2002, Volume 4, 2002.

[13] Kramer.L., "Geotechnical Earthquake Engineering", New Jersey:Printice-Hall,Inc, 1996.

[14] Luna, R., and Jadi, H., "Determination of dynamic soil properties using Geophsical methods", department of Civil Engineering, University of Missouri-Rolla, 2000.

[15] Pitilakis, K.D., Anastassiais, A. and Raptakis, D., "Field and laboratory determination of Dynamic properties of natural soil deposits", Earthquake engineering, tenth world conference, 1992.

[16] Seed, H.B. and Idriss, I.M., "Soil Moduli and Damping factors for dynamic response analyses", EERC/70-10, College of Engineering university of California, Berkeley, 1970.

[17] Seed, H.B., Wong, T.R., Indriss, I.M. and Tokimatsu, K., "Moduli and Damping factors for Dynamic analysis of cohesionless soils", USB/EERC-84/14, collage of Engineering ,university of California, Berkeley, 1984.

[18] Sitharam, T.G., Raju, L.G. and Sridharan, A., "Dynamic properties and liquefaction potential of soils, department of civil Engineerin", India,Institute of Science, Bangalore 560012,India.

[19] Sun, I.J., Golesorkhi, R. and Seed, H.B., "Dynamic moduli and Damping factors for cohesive soils", USB/EERC-88/15, collage of Engineering ,university of California at Berkeley,1988.

[20] "The Geological Survey of Ethiopia", revised from the original edition Compiled by Mengesha Tefera, Tadiwos Chernet and Workineh Haro, Regional Geology Department EIGS, 1990.

[21] UTS004, "Simple shear test software reference", Universal testing system, IPC Global limited, 2003.

[22] Venkatramaiah, C., "Geotechnical Engineering, department of civil Engineering", revised third edition, S.V.University College of Engineering Tirupati, India, 2006.

[23] Vicetic, M., "Soil properties and seismic response", Earthquake Engineering, tenth world conference, Balkema, Rotterdam.University of California at Los Angeles, 1992.

[24] Yemaneh Gebreeziabher, "Assessment of the water balance of Lake Hawassa catchment", Ethiopia, International institute for Geo-Information science and earth observation enschede, the Netherland, 2004.

APPENDICES

Appendix – A

Atterberg limit test results and Grain size distribution curves

Table A-1: liquid limit and plastic limit test values of pit 1, 2 and 5

pit 1	***Liquid Limit***				***Plastic Limit***	
Trial No	*1*	*2*	*3*	*4*	*1*	*2*
No of blows	*16*	*17*	*36*	*29*	------	------
Water content, %	*46.861*	*46.5*	*45.652*	*46.0785*	*35.07*	*34.123*
Average %	*For 25 blow------**46.26***				***34.60***	
PI = LL – PL	*46.26-34.60=**11.66***					

pit 2	***Liquid Limit***				***Plastic Limit***	
Trial No	*1*	*2*	*3*	*4*	*1*	*2*
No of blows	*24*	*27*	*37*	*20*	------	------
Water content, %	*48.5*	*47.5*	*46.2*	*50.8*	*34.675*	*34.661*
Average %	*For 25 blow------**48.75***				***34.67***	
PI = LL – PL	*48.75-34.668 =**14.08***					

pit 5	***Liquid Limit***				***Plastic Limit***	
Trial No	*1*	*2*	*3*	*4*	*1*	*2*
No of blows	*14*	*18*	*30*	*20*	------	------
Water content, %	*44.2*	*43.8*	*41.3*	*42.5*	*35.26*	*35.05*
Average %	*For 25 blow------**42.10***				***35.16***	
PI = LL – PL	*42.1– 35.16=**6.94***					

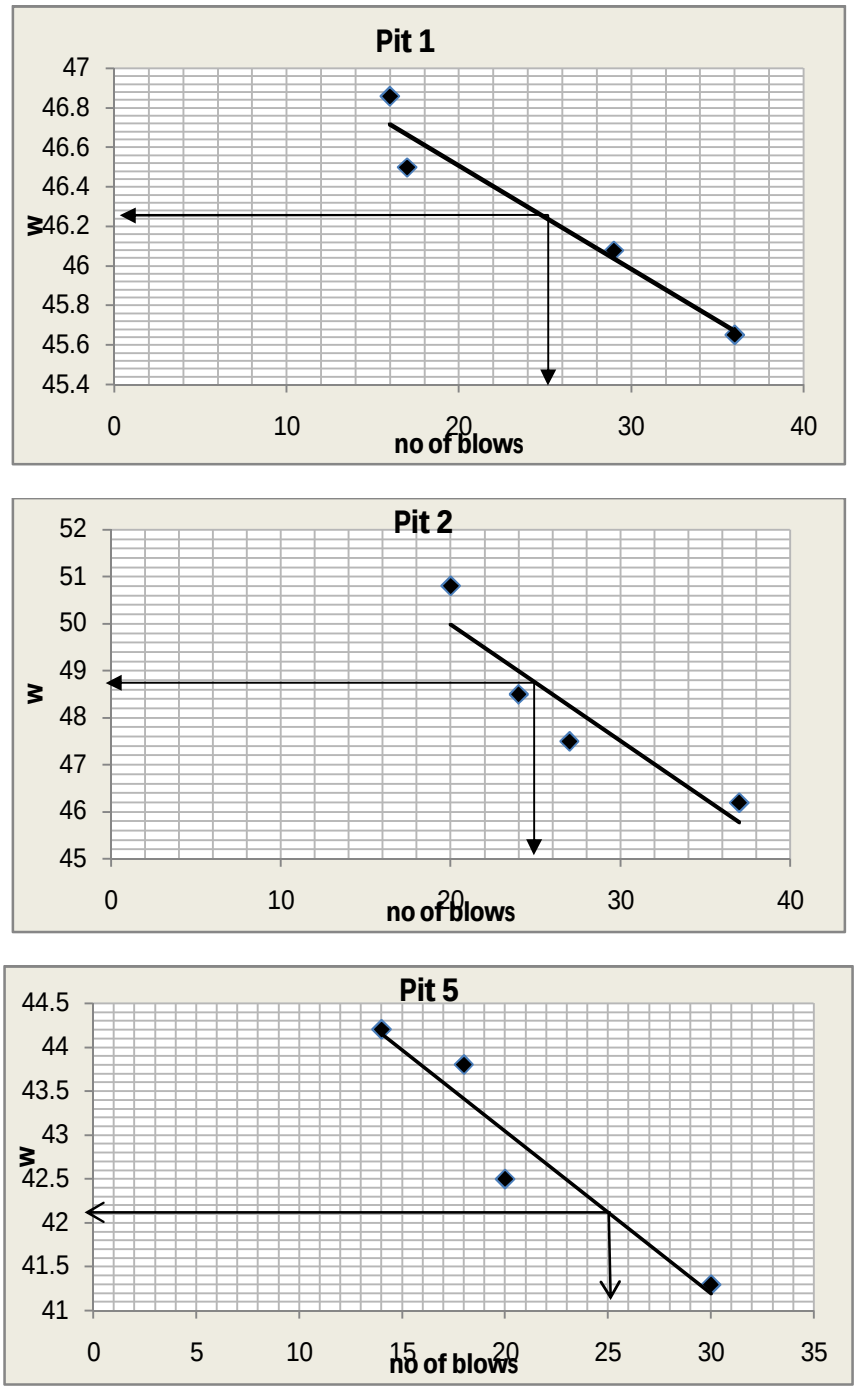


Figure A-1: Liquid limit graphs of pit 1, 2 and 5

Table A-2: Liquid limit tests of oven dried soils of pit 1 and 2

Pit 1	***Liquid Limit***		
Trial No	*1*	*2*	*3*
No of blows	*13*	*23*	*34*
Water content, %	*41.8325*	*41.459*	*40.456*
Average %	*For 25 blow------**41.06***		

Pit 2	***Liquid Limit***		
Trial No	*1*	*2*	*4*
No of blows	*34*	*31*	*15*
Water content, %	*41.8*	*42.5*	*43.8315*
Average %	*For 25 blow------**42.9***		

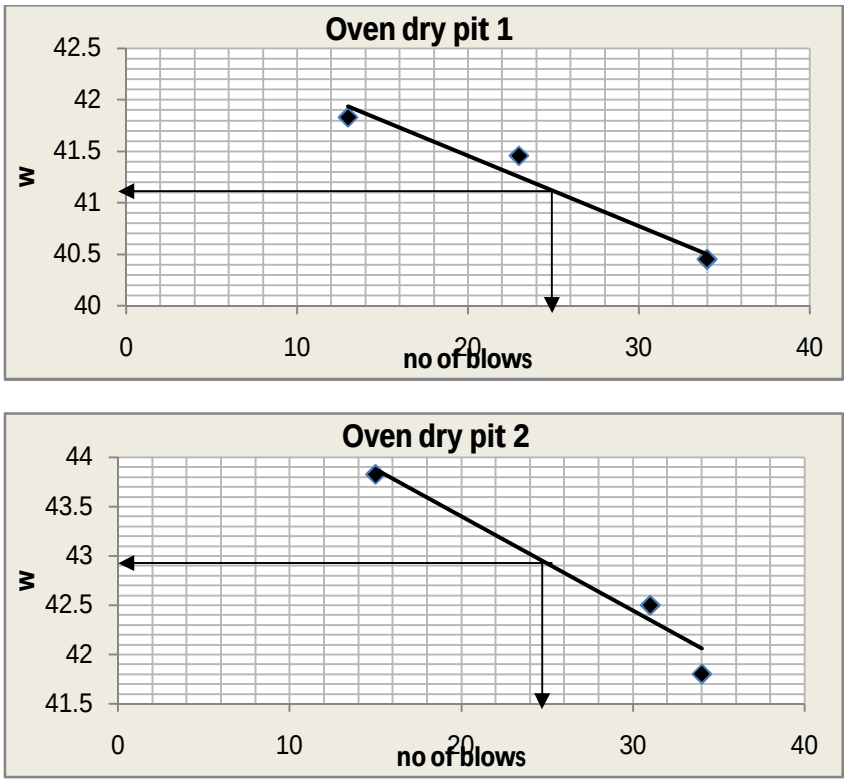
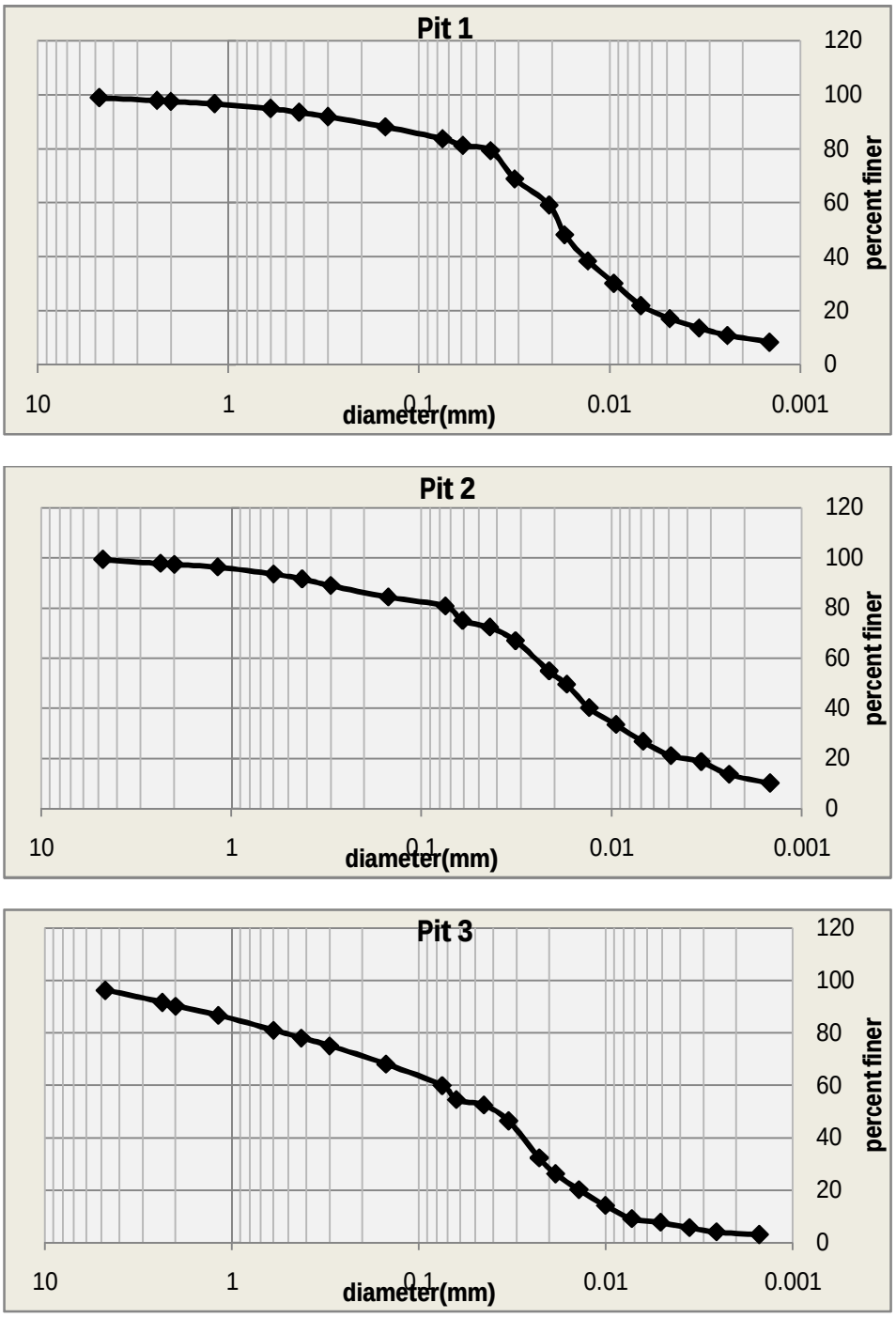
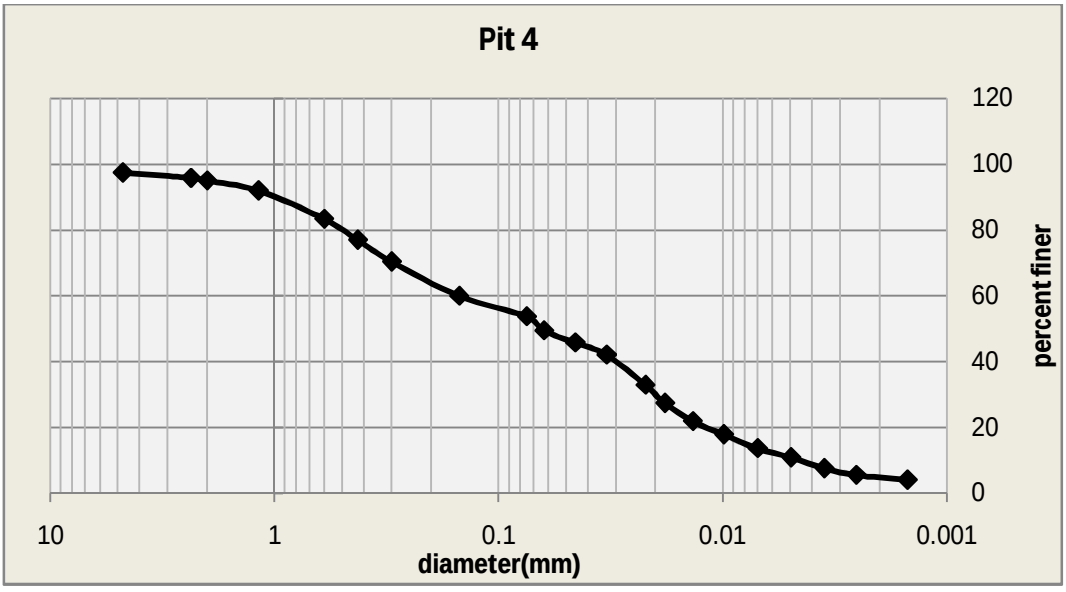
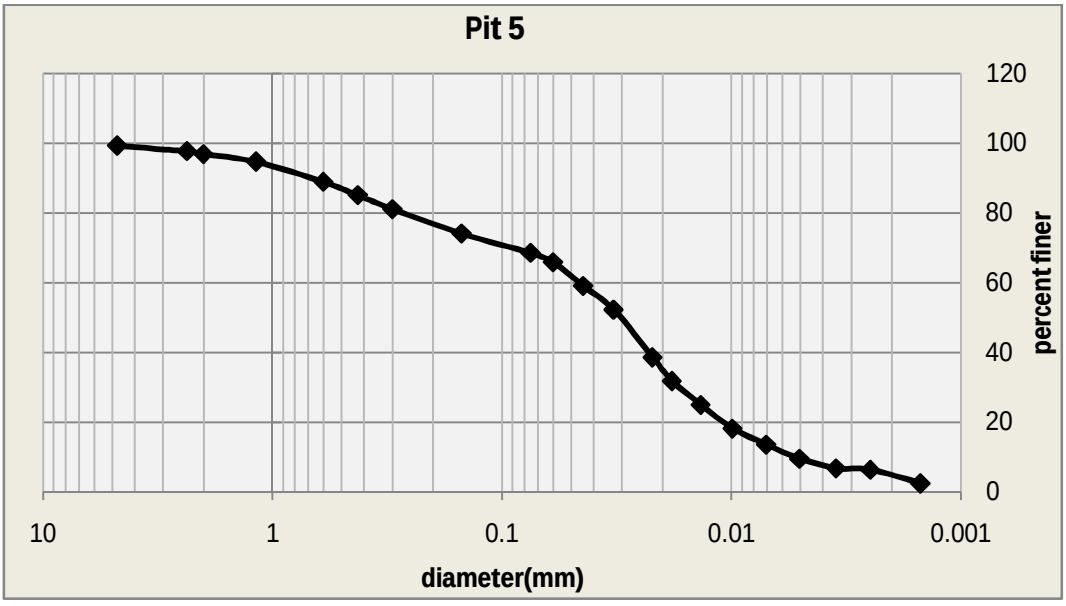


Figure A-2: Liquid limit graphs of oven dried soils of pit 1 and 2



Figures A-3: Grain size distribution curves of pit 1, 2 and 3





Figures A-4: Grain size distribution curves of pit 4 and 5

Appendix – B

Hysteresis loop of the 5th cycles of each test pits

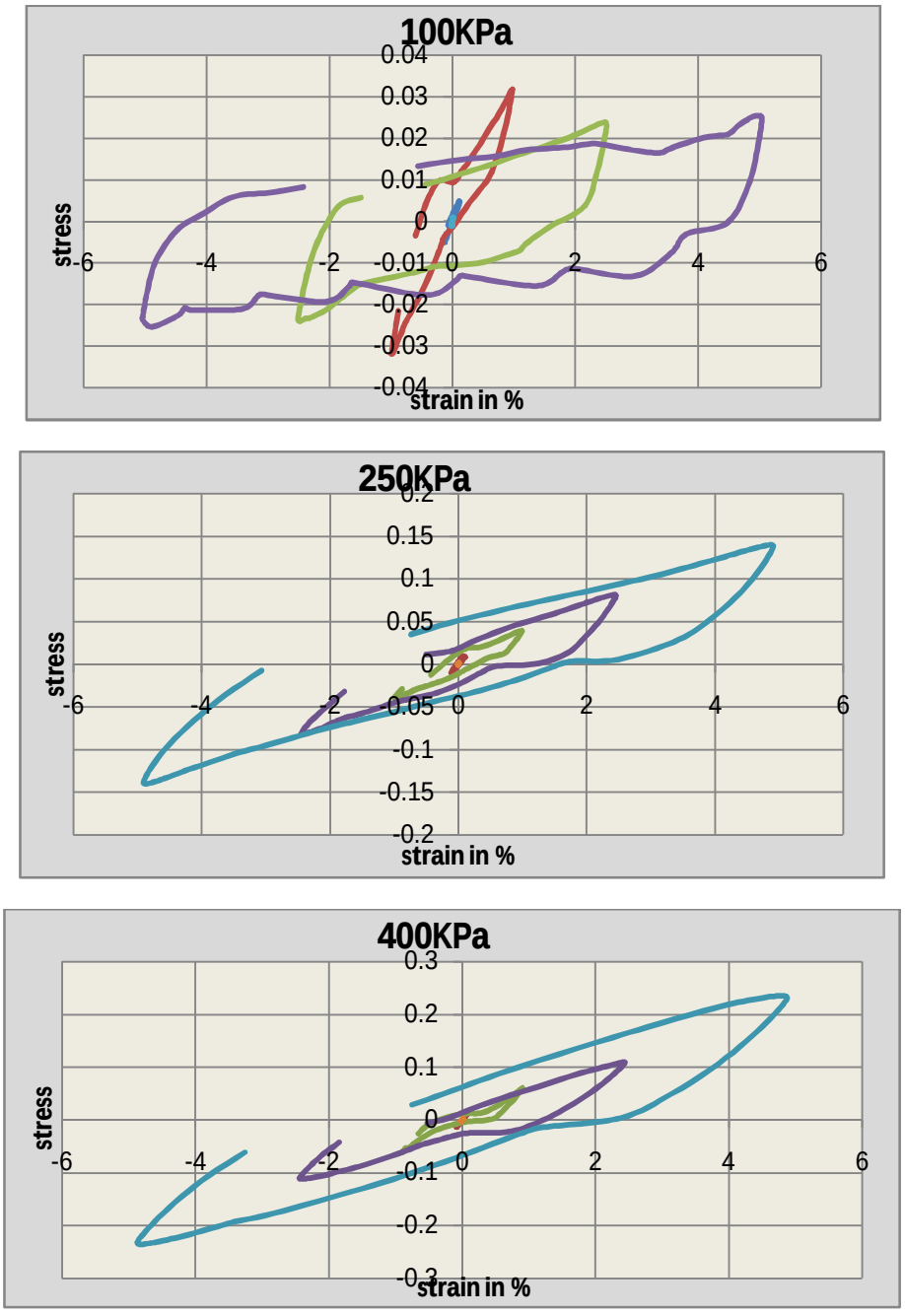


Figure B-1: Hysteresis loops of test pit 2 at each strain levels with axial stresses indicated

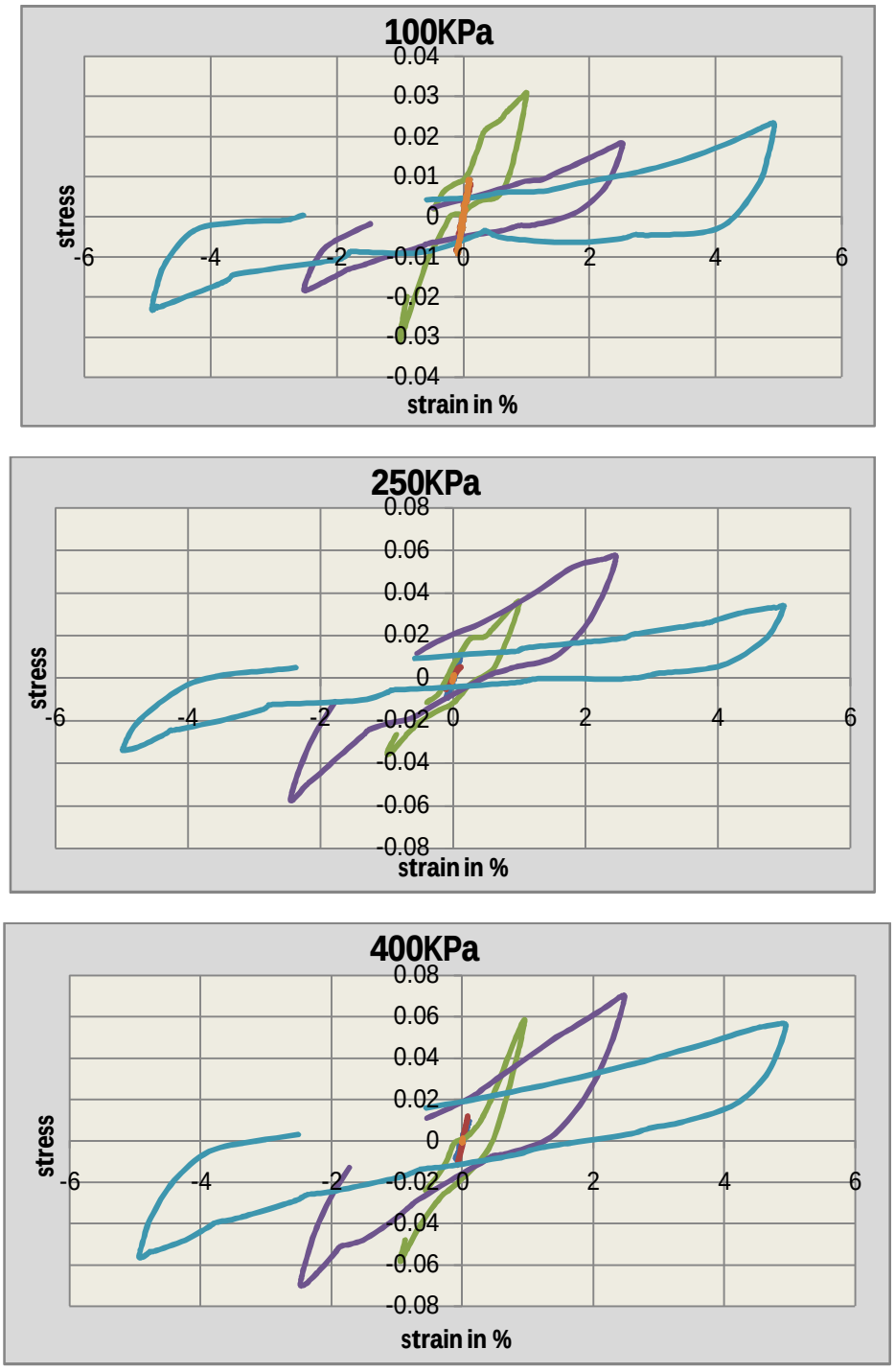


Figure B-2: Hysteresis loops of test pit 3 at each strain levels with axial stresses indicated

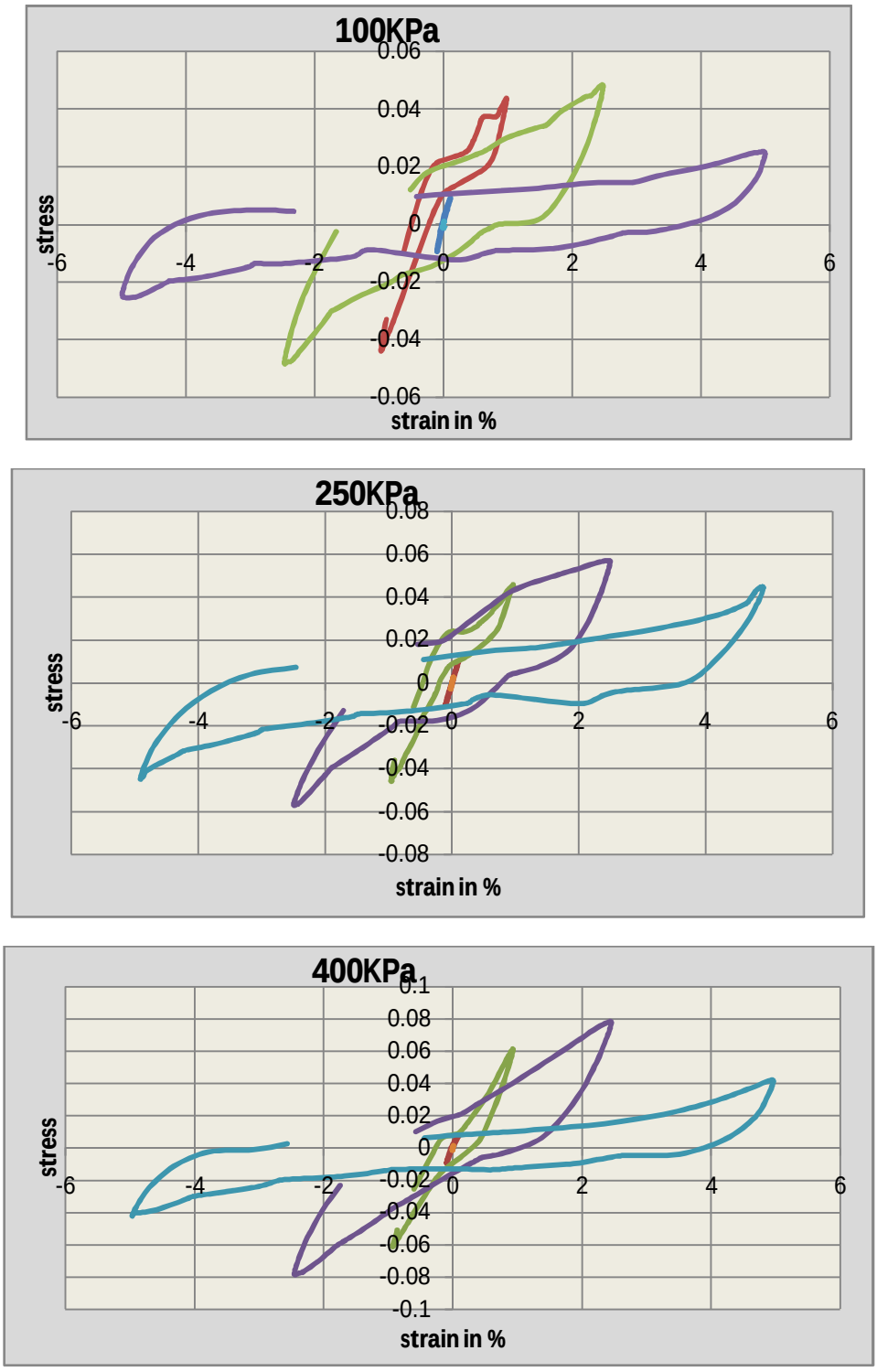


Figure B-3: Hysteresis loops of test pit 4 at each strain levels with axial stresses indicated

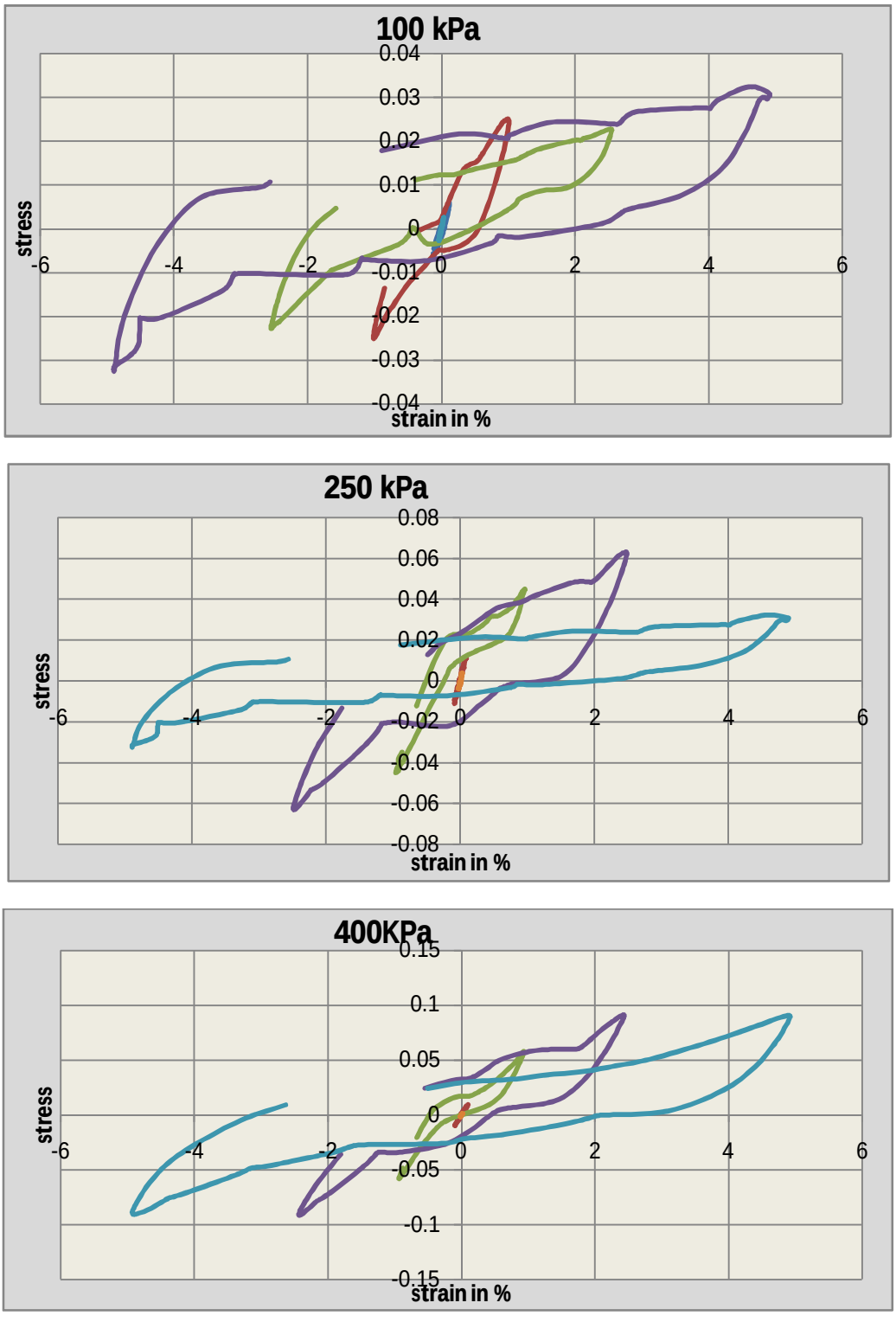


Figure B-4: Hysteresis loops of test pit 5 at each strain levels with axial stresses indicated

Appendix – C

Shear modulus and Damping ratio values of selected cycles

Table C-1: shear modulus values of pit 1

Axial load = 100 KPa					
strain	0.01 %	0.1 %	1 %	2.5 %	5 %
Cycle no	**G** (MPa)				
1	8.163053	6.724797	3.119245	1.261326	0.495292
5	10.33441	7.837673	3.237914	0.874696	0.258264
10	9.73308	7.845756	3.127341	0.784838	0.211439
15	9.796647	7.84444	3.072255	0.736109	0.197426
20	9.730272	7.849305	3.036522	0.70601	0.196802
30	9.873798	7.844839	2.972303	0.657822	0.195205
40	10.46049	7.809312	2.858075	0.639183	0.199589

Axial load = 250 KPa					
strain	0.01 %	0.1 %	1 %	2.5 %	5 %
Cycle no	**G** (MPa)				
1	12.33395	8.58845	6.017933	3.96178	1.724812
5	11.93533	9.16676	5.727093	2.970987	0.982427
10	12.61653	9.08902	5.701755	2.619064	0.645606
15	9.759499	9.124216	5.668311	2.467946	0.580661
20	12.94104	9.072388	5.636883	2.374665	0.520211
30	12.63077	9.002362	5.630322	2.254886	0.46178
40	13.32834	9.126813	5.612373	2.193732	0.423282

Axial load = 400 KPa					
strain	0.01 %	0.1 %	1 %	2.5 %	5 %
Cycle no	**G** (MPa)				
1	14.54529974	11.1253	6.5176	5.188061	3.411347
5	15.73900087	12.99749	6.404153	5.093756	2.918397
10	15.29463871	12.9976	6.248285	4.970487	2.714408
15	16.78116425	12.92135	6.177667	4.864843	2.614947
20	18.69187682	12.85944	6.117193	4.788228	2.545854
30	19.08476207	12.95224	6.074536	4.720619	2.462563
40	18.66600632	12.99164	6.025551	4.638116	2.397244

Table C-2: Damping ratio values of pit 1

Axial load =100 KPa					
strain	0.01 %	0.1 %	1 %	2.5 %	5 %
Cycle no	β (%)				
1	4.637529	5.354921	19.1757	22.02155	35.96186
5	3.222131	8.794258	13.36556	17.2072	30.48569
10	4.96835	8.156158	13.20324	15.50197	33.65178
15	5.441062	7.890709	13.10897	14.61575	34.3028
20	2.262904	7.750649	13.13465	14.07986	34.4126
30	4.847001	7.212529	12.76616	13.60396	33.30541
40	4.01869	7.290493	12.69366	13.20445	34.10537

Axial load = 250 KPa					
strain	0.01 %	0.1 %	1 %	2.5 %	5 %
Cycle no	β (%)				
1	3.945406	8.13037	10.52791	15.21701	29.38898
5	2.677853	7.637718	9.527731	12.752	22.82315
10	1.74185	7.25059	8.880116	13.40293	26.98436
15	2.92733	7.010309	8.384233	13.57254	25.60718
20	0.083169	6.728841	8.279852	13.56988	26.06117
30	2.007452	6.816561	8.353262	14.0059	23.83996
40	2.228879	6.454816	8.100334	14.00477	23.79499

Axial load =400 KPa					
strain	0.01 %	0.1 %	1 %	2.5 %	5 %
Cycle no	β (%)				
1	0.031969207	5.081472	5.75863	14.83554	17.30904
5	0.021886811	2.895212	6.311289	11.41095	13.87044
10	0.053067734	2.599385	5.967793	11.24592	13.32633
15	0.013349427	2.55833	5.759214	10.86053	12.76022
20	0.024910052	2.463451	5.688783	10.18153	12.30795
30	0.031025882	2.592838	5.612728	9.42691	12.10818
40	0.006120762	2.473212	5.536993	9.495243	11.66478

Table C-3: Shear modulus values of pit 2

Axial load =100 KPa					
strain	0.01 %	0.1 %	1 %	2.5 %	5 %
Cycle no	**G** (MPa)				
1	7.609206	3.690763	3.415976	1.977125	0.918114
5	7.085534	3.877635	3.081314	0.905666	0.480586
10	7.757836	3.870588	2.92166	0.742112	0.400798
15	6.320214	3.884063	2.849488	0.657762	0.358417
20	5.562028	3.831812	2.789539	0.603381	0.356076
30	7.340651	3.910284	2.727698	0.536757	0.347656
40	7.706474	3.883882	2.681331	0.499586	0.332991

Axial load =250 KPa					
strain	0.01 %	0.1 %	1 %	2.5 %	5 %
Cycle no	**G** (MPa)				
1	9.338638	6.893226	3.836316	3.211067	2.793659
5	9.342975	8.27555	3.675267	3.083739	2.641168
10	9.850916	8.279879	3.628661	2.762384	2.5117
15	10.77991	8.263978	3.592164	2.565616	2.39454
20	10.66611	8.552165	3.56042	2.426993	2.319151
30	13.61202	8.426004	3.51044	2.237157	2.210881
40	10.22905	8.728434	3.479585	2.121748	2.105055

Axial load = 400 KPa					
strain	0.01 %	0.1 %	1 %	2.5 %	5 %
Cycle no	**G** (MPa)				
1	12.0794	9.72526	4.71208	4.310652	3.523663
5	12.24322	10.3493	4.626171	4.114119	3.293864
10	12.26083	10.47432	4.579604	4.013786	3.260033
15	11.41344	10.4133	4.542549	3.874089	3.182259
20	12.27316	10.42987	4.519643	3.871644	3.137051
30	11.94211	10.52528	4.487427	3.795724	3.111273
40	11.51819	10.45959	4.449814	3.7643	3.085878

Table C-4: Damping ratio values of pit 2

Axial load = 100 KPa					
strain	0.01 %	0.1 %	1 %	2.5 %	5 %
Cycle no	β (%)				
1	6.20288	7.390496	17.55681	29.75788	42.18452
5	10.67349	11.61302	18.34237	31.44542	39.33037
10	6.770848	7.952726	17.98015	28.56578	37.3313
15	4.900383	12.17348	17.98847	28.36392	39.06399
20	10.63501	11.50654	17.72327	28.16217	36.22073
30	4.425313	12.59992	17.65119	27.645	34.12899
40	9.951294	11.71369	17.60169	27.50248	32.63247

Axial load = 250 KPa					
strain	0.01 %	0.1 %	1 %	2.5 %	5 %
Cycle no	β (%)				
1	6.00447	11.31215	14.50146	19.02119	25.27784
5	7.493635	9.8315	13.49193	22.35615	25.66754
10	2.266345	9.604377	13.57033	22.52632	26.56622
15	6.821164	9.341539	13.68218	22.9354	26.84892
20	2.361281	9.504413	13.26031	23.00477	27.02459
30	1.84027	8.602839	13.20673	23.51966	27.90701
40	3.116368	8.667944	13.19507	23.85481	28.22131

Axial load = 400 KPa					
strain	0.01 %	0.1 %	1 %	2.5 %	5 %
Cycle no	β (%)				
1	2.011103	4.652115	4.890435	18.1327	13.91709
5	2.902473	3.401146	7.204337	13.44178	15.86359
10	1.752317	2.904542	6.917578	13.44115	15.90394
15	2.598701	2.685508	6.850097	13.23392	16.12185
20	2.290286	2.669271	6.78177	12.75421	15.90105
30	2.0482	2.765189	6.524989	12.44471	16.0745
40	0.48548	2.800632	6.693792	12.08796	15.68746

Table C-5: Shear modulus values of pit 3

Axial load = 100 KPa					
strain	0.01 %	0.1 %	1 %	2.5 %	5 %
Cycle no	**G** (MPa)				
1	6.549259	5.717456	2.919869	1.133353	1.022714
5	8.322096	6.84235	2.890331	0.683469	0.443766
10	8.319933	6.974446	2.829065	0.536535	0.346053
15	8.055078	6.809528	2.828894	0.465326	0.282534
20	7.97795	6.908884	2.817708	0.423977	0.245037
30	7.937841	7.049638	2.795023	0.375041	0.1976
40	7.818948	6.758322	2.787152	0.364307	0.185512

Axial load = 250 KPa					
strain	0.01 %	0.1 %	1 %	2.5 %	5 %
Cycle no	**G** (MPa)				
1	12.5192	7.632656	3.842567	3.118232	1.143127
5	12.81414	8.465332	3.359753	2.176543	0.630076
10	14.33168	8.301838	3.076358	1.904028	0.516237
15	13.27978	8.333496	2.922562	1.733514	0.457708
20	13.71728	8.312969	2.81484	1.635094	0.423587
30	14.59871	8.29455	2.680446	1.4999	0.377579
40	13.6078	8.287217	2.584476	1.4092	0.343559

Axial load = 400 KPa					
strain	0.01 %	0.1 %	1 %	2.5 %	5 %
Cycle no	**G** (MPa)				
1	13.66491	13.00752	5.952608	3.485732	2.044629
5	13.97201	13.51011	5.591887	2.568915	1.042308
10	14.16587	13.85922	5.352261	2.162189	0.862264
15	14.0707	13.77932	5.201698	1.959621	0.783116
20	15.03634	13.67122	5.107092	1.854428	0.732063
30	14.81657	13.57766	4.962324	1.680173	0.674162
40	14.31146	13.50665	4.856272	1.53141	0.615035

Table C-6: Damping ratio values of pit 3

Axial load = 100 KPa					
strain	0.01 %	0.1 %	1 %	2.5 %	5 %
Cycle no	β (%)				
1	3.912006	4.415296	9.63935	20.95849	25.69025
5	4.50847	6.264213	10.65369	16.17188	18.1014
10	3.997403	4.735659	10.47784	15.63645	15.67163
15	4.539834	6.089821	10.26989	15.27633	15.97069
20	4.239955	6.085475	10.09181	15.01403	15.41483
30	3.950218	4.775816	9.884384	14.21771	15.14506
40	3.498859	3.935996	9.788147	13.70967	16.10746

Axial load = 250 KPa					
strain	0.01 %	0.1 %	1 %	2.5 %	5 %
Cycle no	β (%)				
1	3.215344	3.40528	10.28712	15.92914	29.74676
5	3.914784	5.848287	10.57287	14.41666	15.79186
10	5.57975	5.705991	10.38721	13.95857	14.53434
15	2.301102	5.461301	10.16676	13.28045	13.9426
20	2.873901	5.350233	10.294	12.85972	13.47236
30	2.994148	5.313755	10.40751	12.95165	12.839
40	4.713264	5.442673	10.5392	13.50636	12.13456

Axial load = 400 KPa					
strain	0.01 %	0.1 %	1 %	2.5 %	5 %
Cycle no	β (%)				
1	3.27418	6.49074	7.641203	12.43007	20.6799
5	1.952678	3.108221	7.964973	12.58839	13.77544
10	1.796015	3.171498	7.572469	12.24507	12.15847
15	2.483953	2.592425	7.344859	11.0679	11.57599
20	2.42399	3.044817	7.336634	10.22035	11.29729
30	2.18088	2.926787	6.908831	9.801106	10.81992
40	1.207241	2.831377	7.339934	9.562808	10.97277

Table C-7: Shear modulus values of pit 4

Axial load = 100 KPa					
strain	0.01 %	0.1 %	1 %	2.5 %	5 %
Cycle no	**G** (MPa)				
1	11.36283	5.516192	4.302904	2.676465	1.048291
5	10.44293	8.377485	4.151217	1.813986	0.469917
10	11.56741	8.198064	3.979759	1.518154	0.330881
15	10.05766	8.236976	3.871068	1.355352	0.267788
20	10.55843	8.237408	3.803109	1.268079	0.233613
30	11.42268	8.186329	3.702786	1.169922	0.193523
40	11.92585	8.221583	3.636946	1.067571	0.165353

Axial load = 250 KPa					
strain	0.01 %	0.1 %	1 %	2.5 %	5 %
Cycle no	**G** (MPa)				
1	9.467568	8.689468	4.420028	3.09761	1.574643
5	10.77948	9.150539	4.317506	2.082966	0.833429
10	9.987889	9.231274	4.108483	1.826733	0.594676
15	9.964592	9.186334	3.9581	1.667231	0.532514
20	9.678439	9.133667	3.862797	1.560902	0.484318
30	9.443587	9.004334	3.740796	1.43226	0.413319
40	9.40993	9.359113	3.669823	1.274455	0.370842

Axial load = 400 KPa					
strain	0.01 %	0.1 %	1 %	2.5 %	5 %
Cycle no	**G** (MPa)				
1	10.78091	6.755417	6.33077	3.94327	2.473495
5	12.76928	10.2595	5.968328	2.907914	1.548907
10	12.84136	10.03978	5.709494	2.340649	1.178631
15	11.68748	10.08743	5.565412	1.971192	0.977978
20	11.33524	10.08796	5.443394	1.746665	0.86434
30	12.02753	10.02541	5.280404	1.489237	0.689763
40	10.94157	10.06858	5.171112	1.286202	0.601327

Table C-8: Damping ratio values of pit 4

Axial load =100 KPa					
strain	0.01 %	0.1 %	1 %	2.5 %	5 %
Cycle no	β (%)				
1	9.741761	23.96197	13.46865	23.7967	42.14621
5	7.709677	11.46993	12.94919	24.69151	33.70011
10	7.4451	10.96362	12.22808	25.28271	31.42336
15	10.14753	10.64609	12.0403	25.36664	29.21159
20	10.95051	11.38418	11.8177	26.0691	29.8142
30	10.78753	11.25051	11.79338	25.86793	29.19068
40	9.20673	10.11492	11.53094	24.84123	29.37981

Axial load = 250 KPa					
strain	0.01 %	0.1 %	1 %	2.5 %	5 %
Cycle no	β (%)				
1	4.849091	10.91723	10.51233	17.33503	22.96919
5	6.512455	7.286943	10.46737	20.24607	27.75447
10	6.365699	7.540228	9.877856	19.09866	31.78917
15	3.538063	6.811668	9.067037	17.97357	28.42514
20	3.669417	6.95392	9.489199	17.17578	27.93354
30	3.794972	7.001423	9.42481	16.4791	28.19738
40	3.70343	6.872086	9.528498	16.93551	28.2121

Axial load = 400 KPa					
strain	0.01 %	0.1 %	1 %	2.5 %	5 %
Cycle no	β (%)				
1	5.25637	11.98098	8.962088	15.95669	17.65749
5	5.722598	5.734963	9.393966	16.81744	19.61943
10	5.15287	5.481812	9.173194	16.86032	20.30181
15	5.282905	5.323046	9.300036	16.30937	20.74753
20	5.387261	5.192092	9.134801	16.20993	19.89057
30	4.15646	5.125256	8.934873	15.79112	21.33063
40	4.470221	5.057458	9.019539	16.19516	21.34088

Table C-9: Shear modulus values of pit 5

Axial load = 100 KPa					
strain	0.01 %	0.1 %	1 %	2.5 %	5 %
Cycle no	**G** (MPa)				
1	6.734669	5.750011	2.459303	0.977925	0.499532
5	6.768969	4.963777	2.396017	0.866117	0.402339
10	6.513831	4.827343	2.329792	0.798716	0.371927
15	6.406968	4.877987	2.293449	0.787841	0.690446
20	5.675148	4.778832	2.263058	0.761979	0.582513
30	4.981503	4.783366	2.23864	0.713287	0.671731
40	4.963558	4.788712	2.204249	0.686676	0.590446

Axial load = 250 KPa					
strain	0.01 %	0.1 %	1 %	2.5 %	5 %
Cycle no	**G** (MPa)				
1	6.765141	4.596065	4.362344	2.879627	0.743958
5	8.020729	7.134846	4.31377	2.350146	0.614218
10	8.798097	7.440969	4.149904	2.107254	0.863101
15	8.700723	7.171006	4.04762	1.971397	0.490207
20	9.292732	7.488424	3.988225	1.905131	0.69372
30	8.951849	7.457356	3.900555	1.79475	0.614218
40	8.827611	7.331566	3.828879	1.707259	0.490207

Axial load = 400 KPa					
strain	0.01 %	0.1 %	1 %	2.5 %	5 %
Cycle no	**G** (MPa)				
1	9.906233	6.560184	5.545426	3.915059	2.773006
5	9.572456	8.59492	5.568585	3.367889	1.654079
10	10.87344	8.41666	5.436139	3.099696	1.336413
15	11.02941	8.301154	5.36529	2.934875	1.200742
20	10.1784	8.242758	5.299086	2.81224	1.117899
30	10.04938	8.304032	5.239099	2.667509	1.009414
40	9.559976	8.291013	5.184036	2.571645	0.907153

Table C-10: Damping ratio values of pit 5

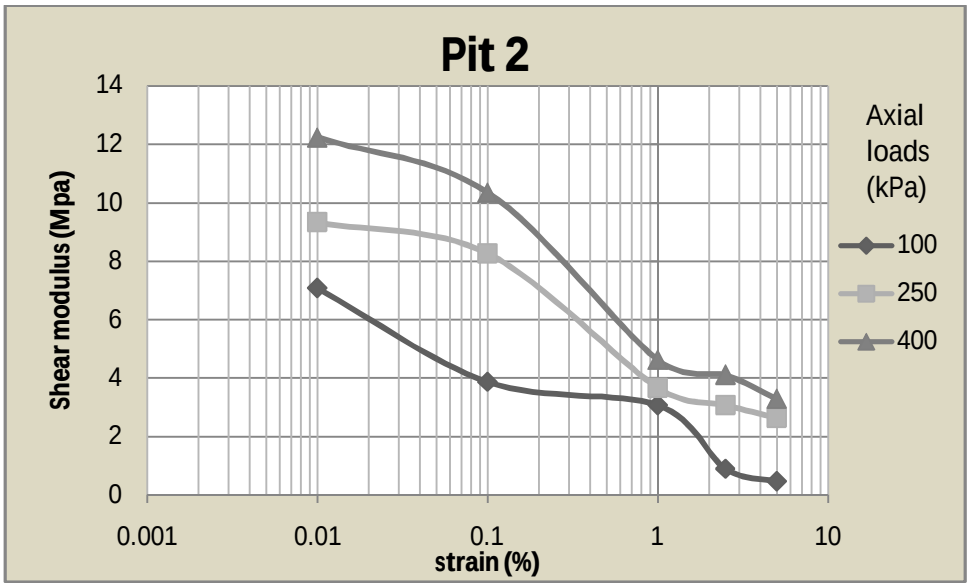
Axial load = 100 KPa					
strain	0.01 %	0.1 %	1 %	2.5 %	5 %
Cycle no	β (%)				
1	3.744505	5.706179	11.41523	14.99019	21.23863
5	6.037806	11.73607	12.5878	16.01777	28.27486
10	7.981241	12.14749	12.54549	15.50845	29.38932
15	7.933652	12.05511	12.4955	14.52498	17.4908
20	9.168573	12.09225	11.92143	13.76951	16.35579
30	10.58036	11.56195	11.75515	14.07837	16.17466
40	10.67745	11.54889	11.64123	13.84135	16.74486

Axial load = 250 KPa					
strain	0.01 %	0.1 %	1 %	2.5 %	5 %
Cycle no	β (%)				
1	4.732435	8.267187	8.267237	20.19467	25.00146
5	5.4812	8.400829	8.590294	15.52547	20.54723
10	2.156666	6.408012	8.030549	16.20387	19.65419
15	1.391844	6.253582	7.950866	16.05295	24.52281
20	1.545528	5.545889	7.894716	15.75363	19.4497
30	1.820146	7.48341	7.707378	16.27231	25.28453
40	2.124281	3.939553	7.662615	15.49741	23.90228

Axial load = 400 KPa					
strain	0.01 %	0.1 %	1 %	2.5 %	5 %
Cycle no	β (%)				
1	8.556932	15.50114	7.79634	14.19921	22.68325
5	3.191744	5.625617	8.02027	12.8188	15.61033
10	3.73706	5.217869	7.640007	12.49016	14.63535
15	2.862177	5.299636	7.380617	12.05412	14.66309
20	2.256931	5.084035	7.414461	12.056	14.3361
30	3.536908	5.013964	7.220822	12.44873	15.23873
40	4.103901	4.986951	7.205993	12.14121	15.33024

Appendix – D

Shear modulus and Damping ratio curves under different axial loads



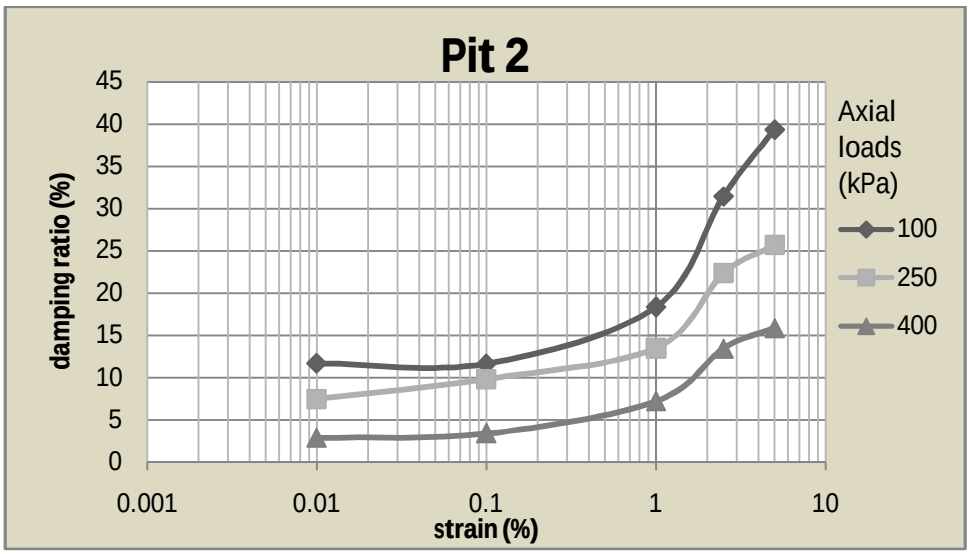
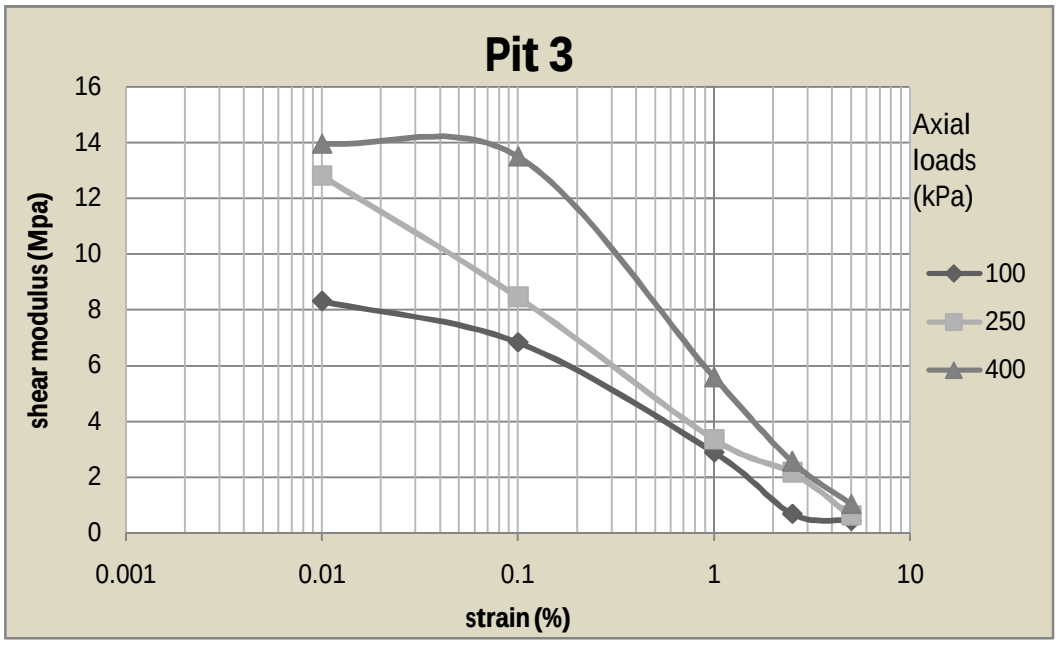


Figure D-1: Shear modulus and Damping ratio curves of pit 2



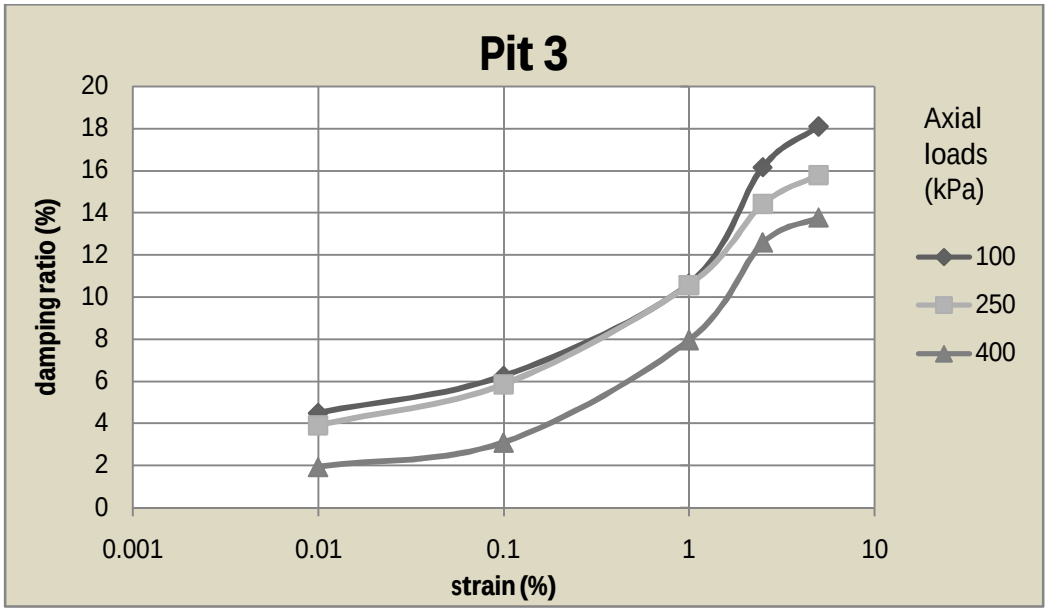


Figure D-2: Shear modulus and Damping ratio curves of pit 3

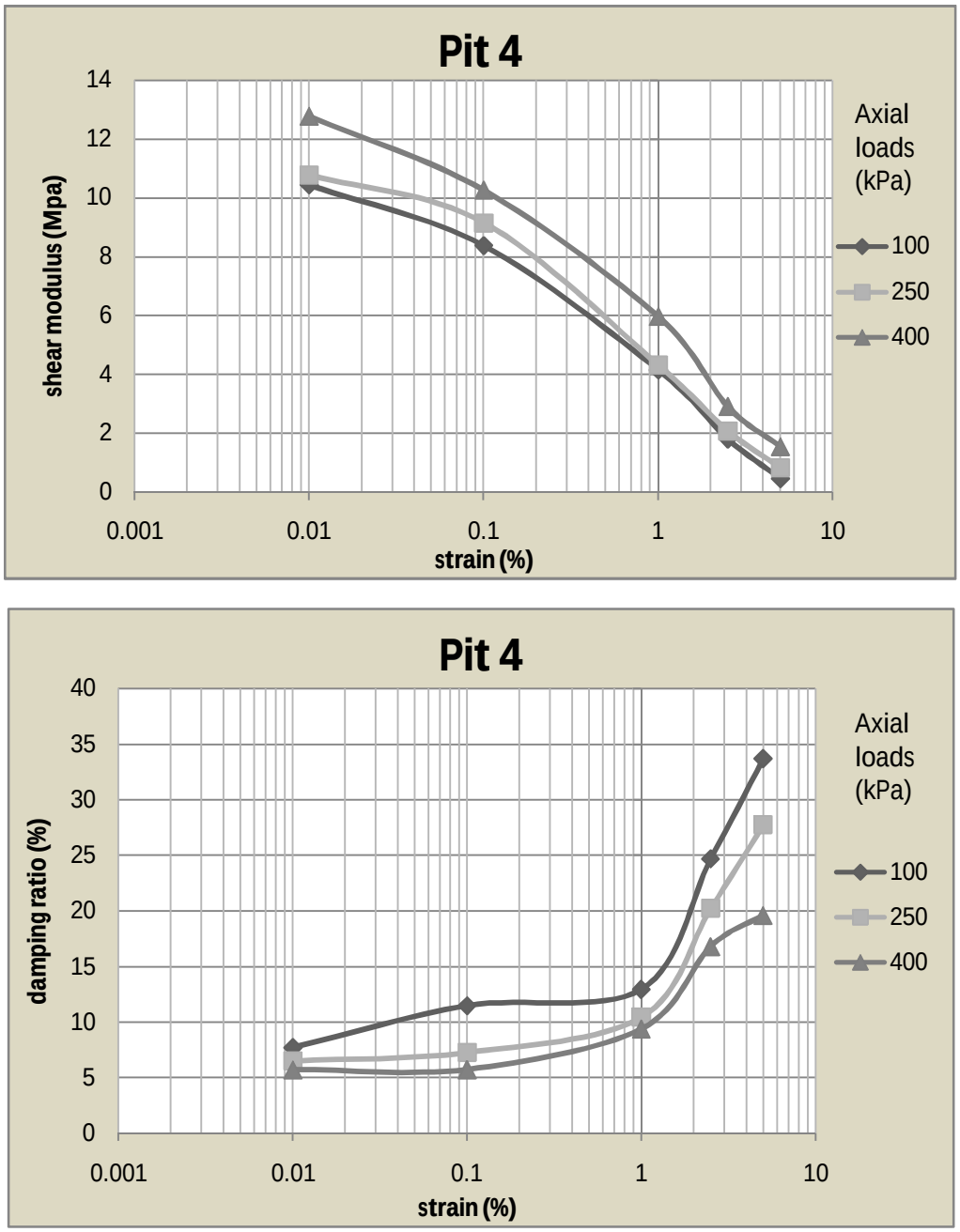
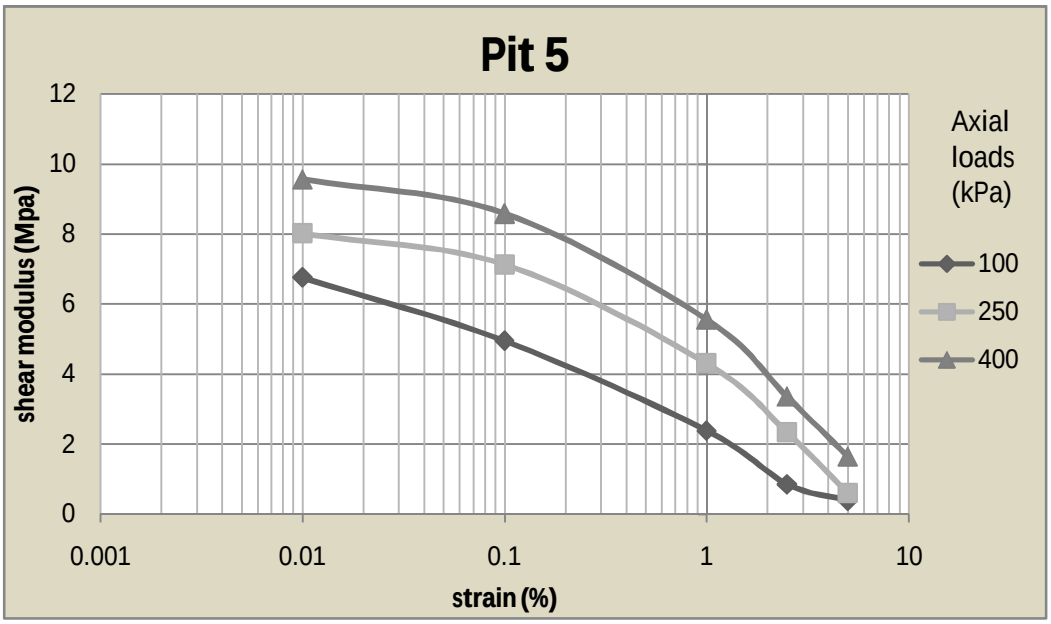


Figure D-3: Shear modulus and Damping ratio curves of pit 4



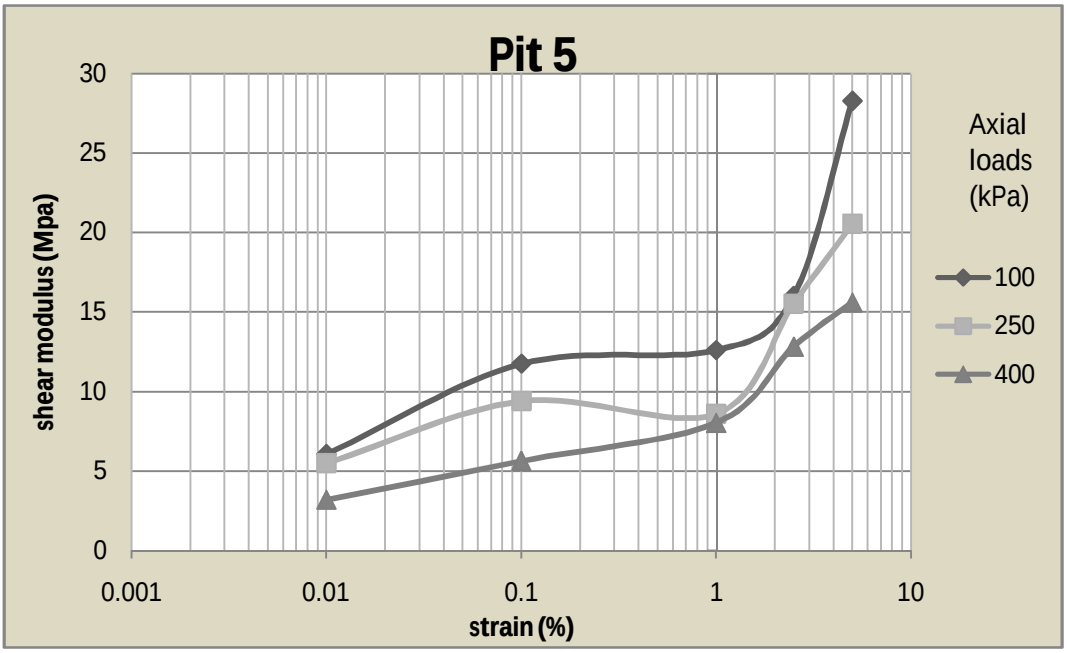
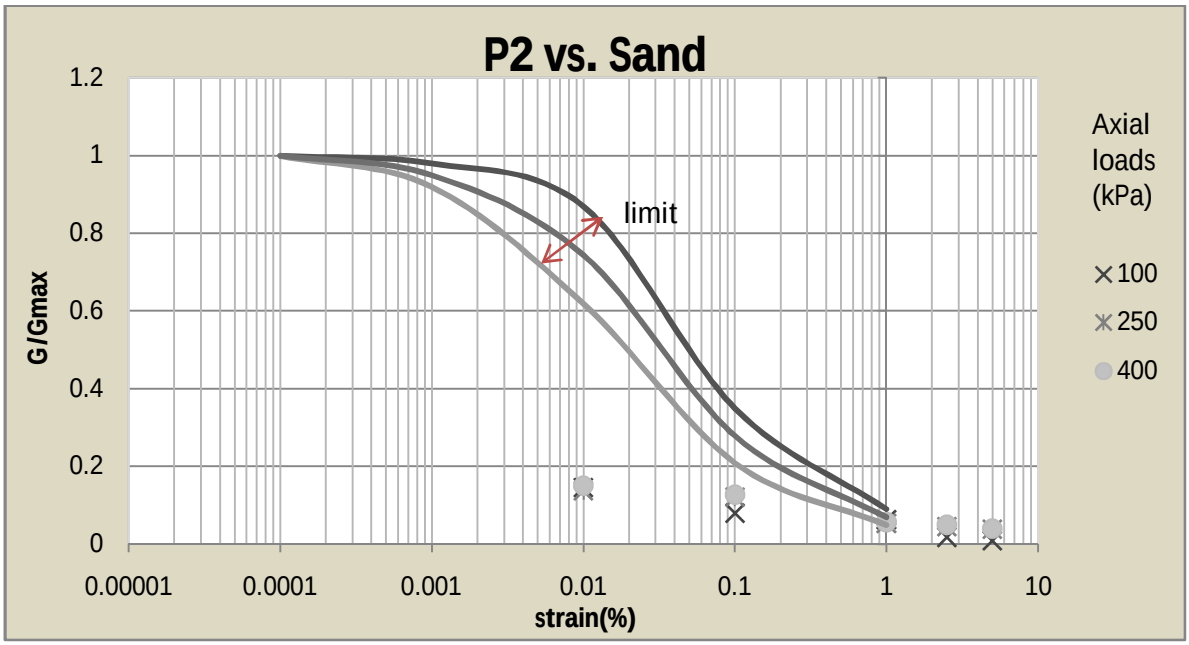


Figure D-4: Shear modulus and Damping ratio curves of pit 5

Appendix – E

Comparison of Shear modulus values with literatures



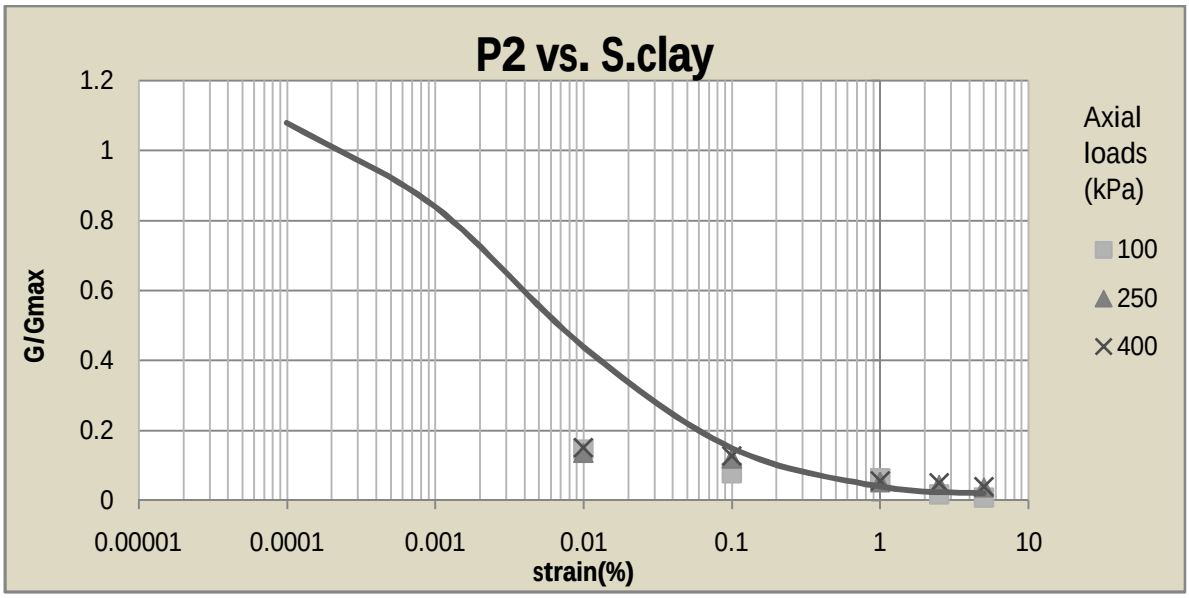
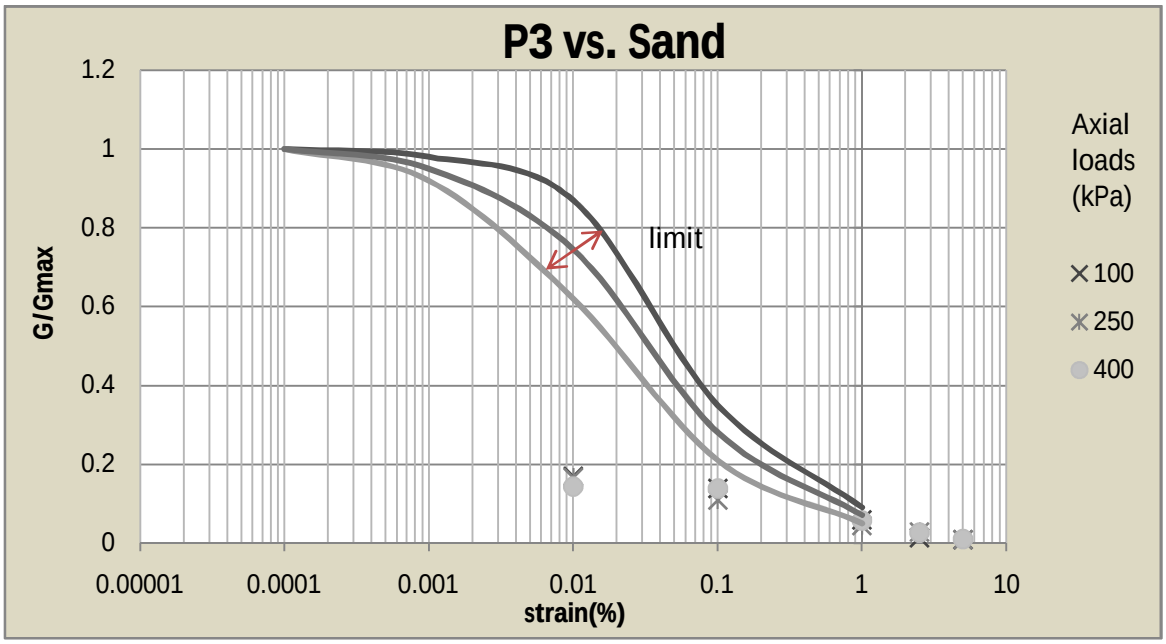


Figure E-1: Comparison of shear modulus ratio of pit 2 with literature curves



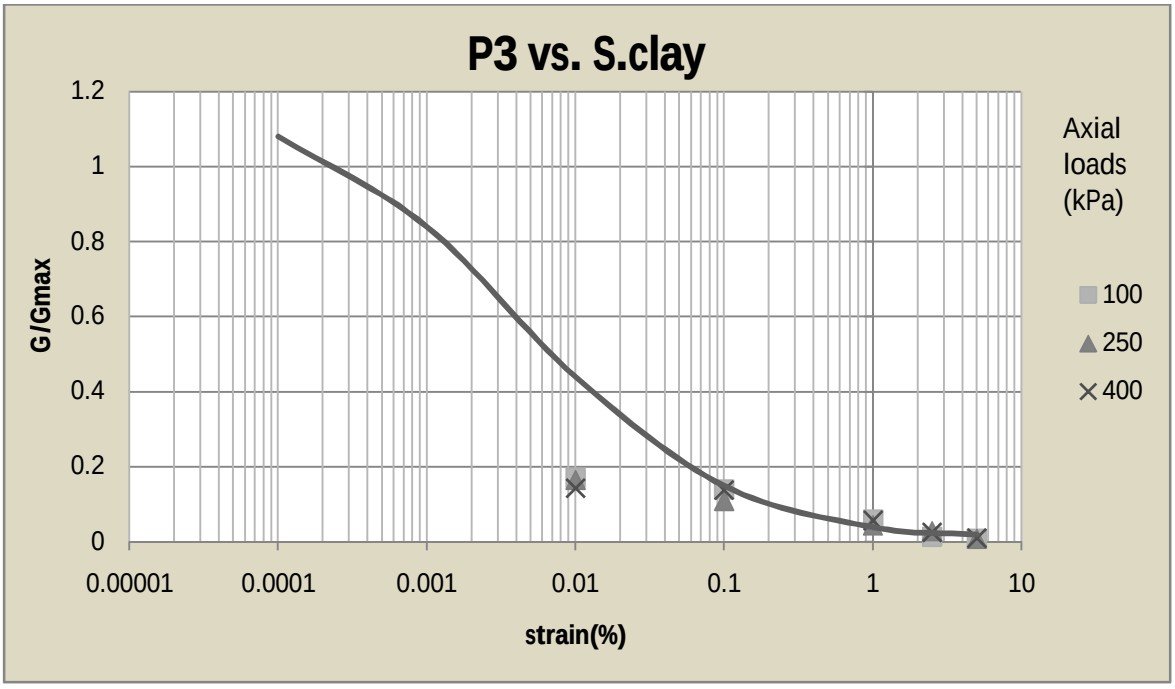
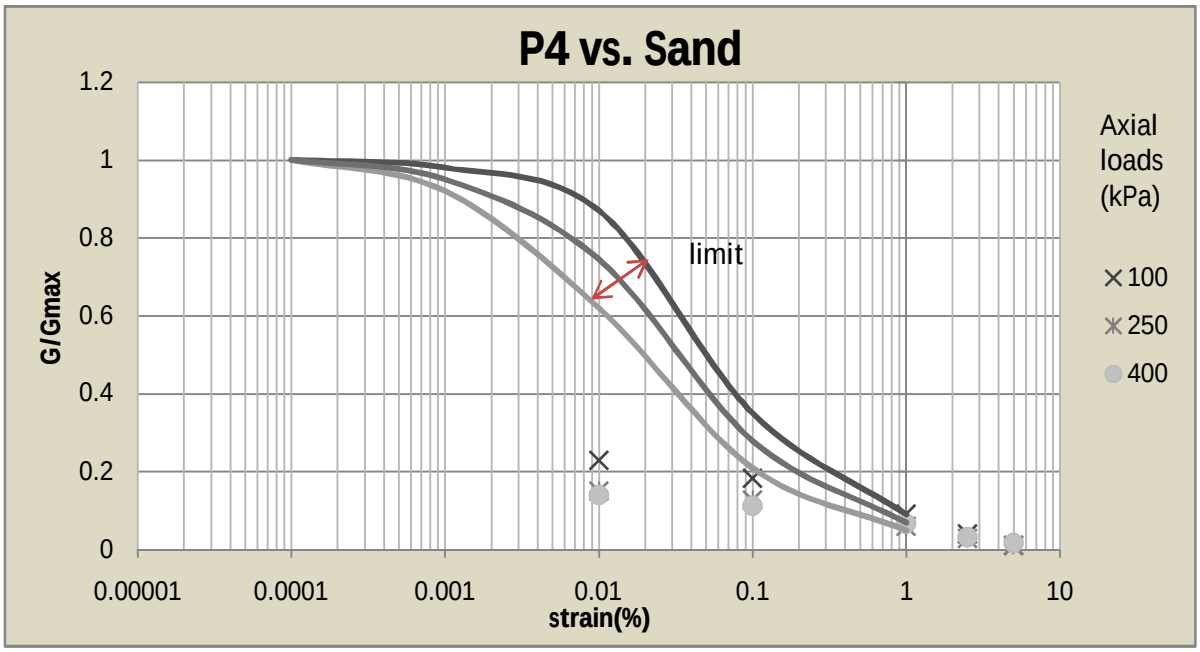


Figure E-2: Comparison of shear modulus of pit 3 with literature curves



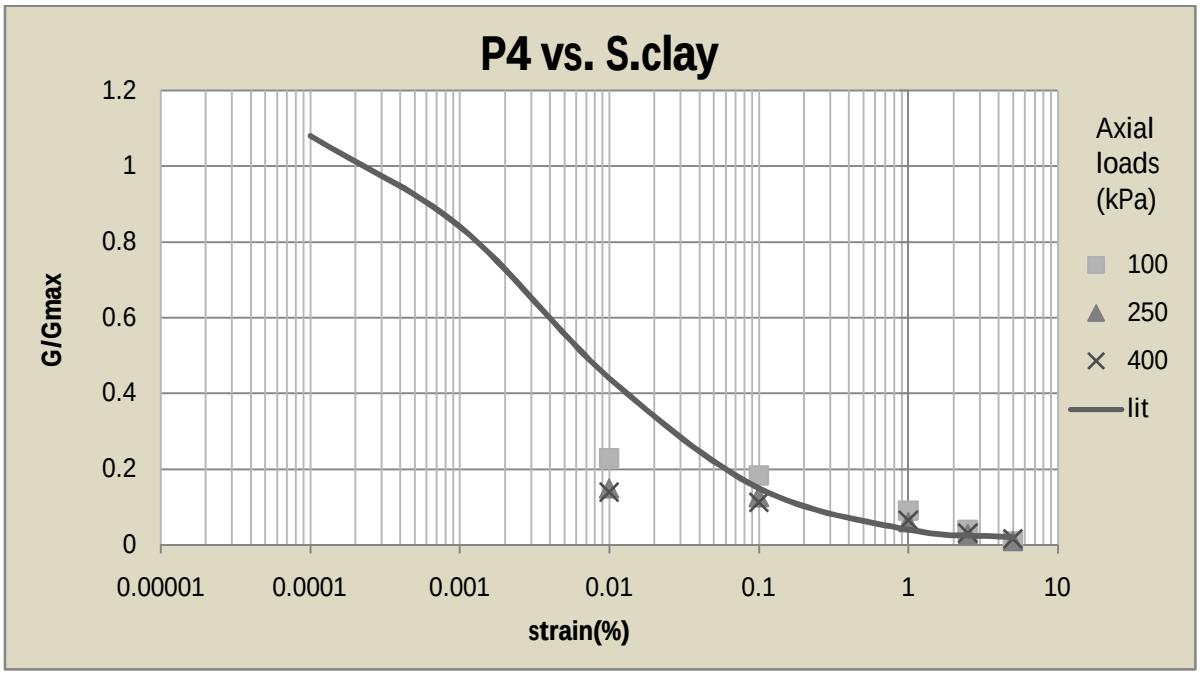
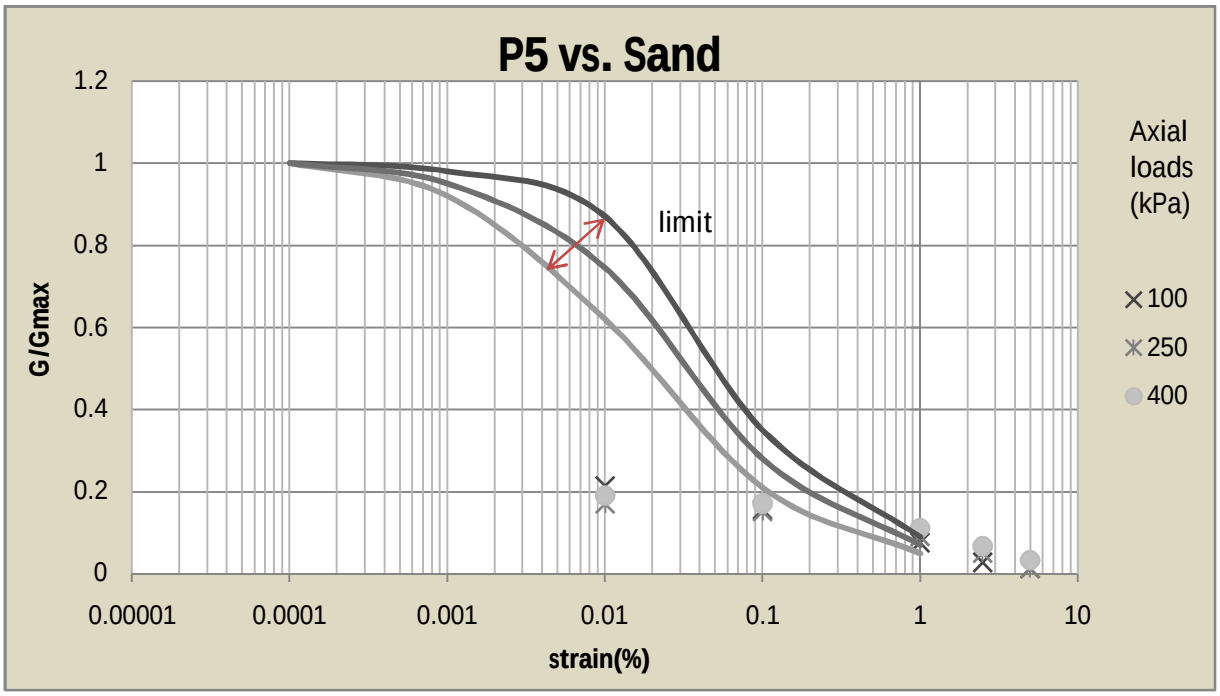


Figure E-3: Comparison of shear modulus ratio of pit 4 with literature curves



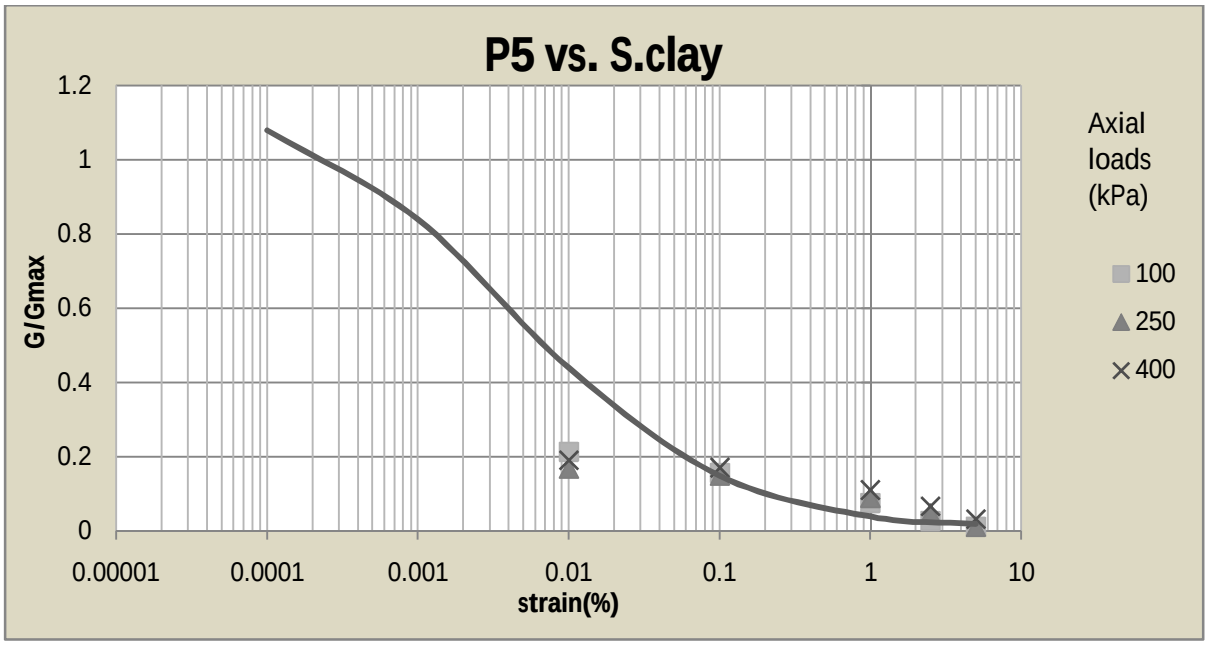
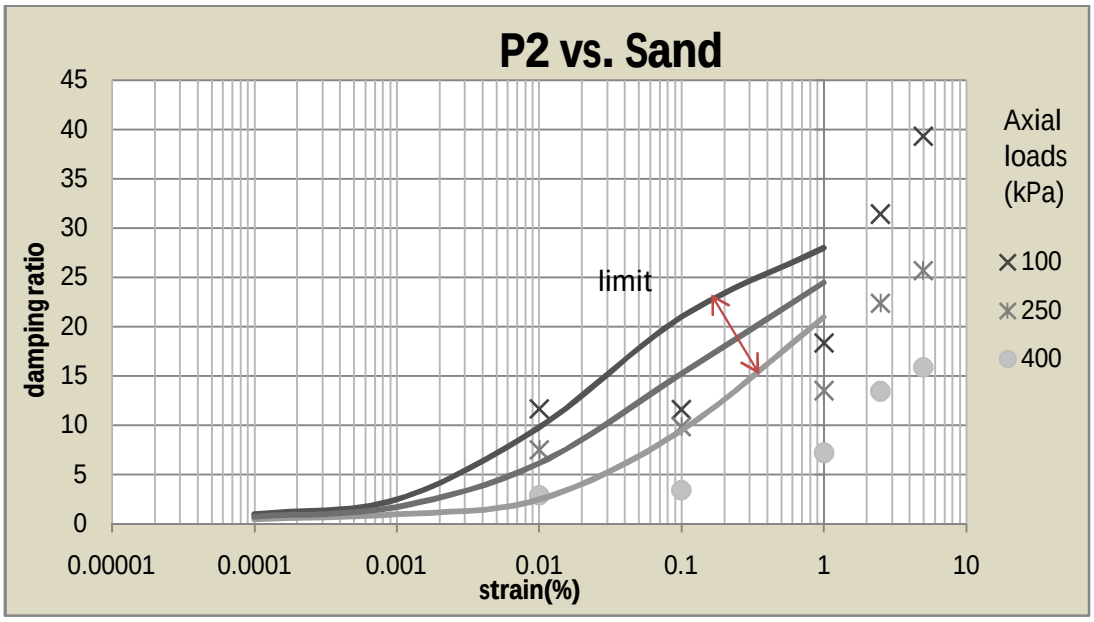


Figure E-4: Comparison of shear modulus ratio of pit 5 with literature curves

Appendix – F

Comparison of damping ratio values with literatures



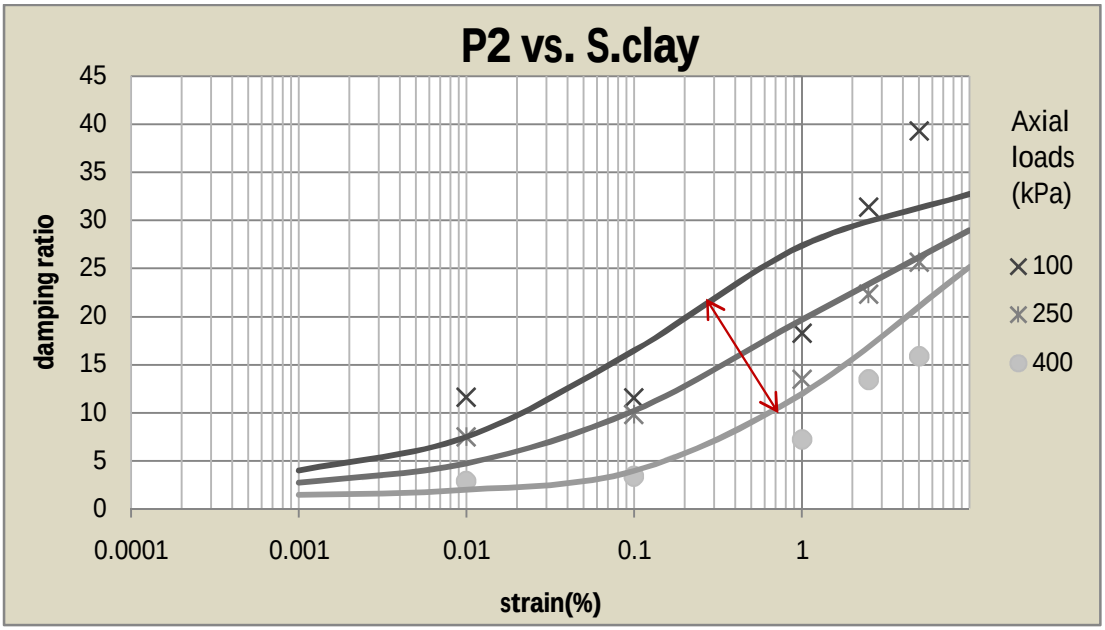
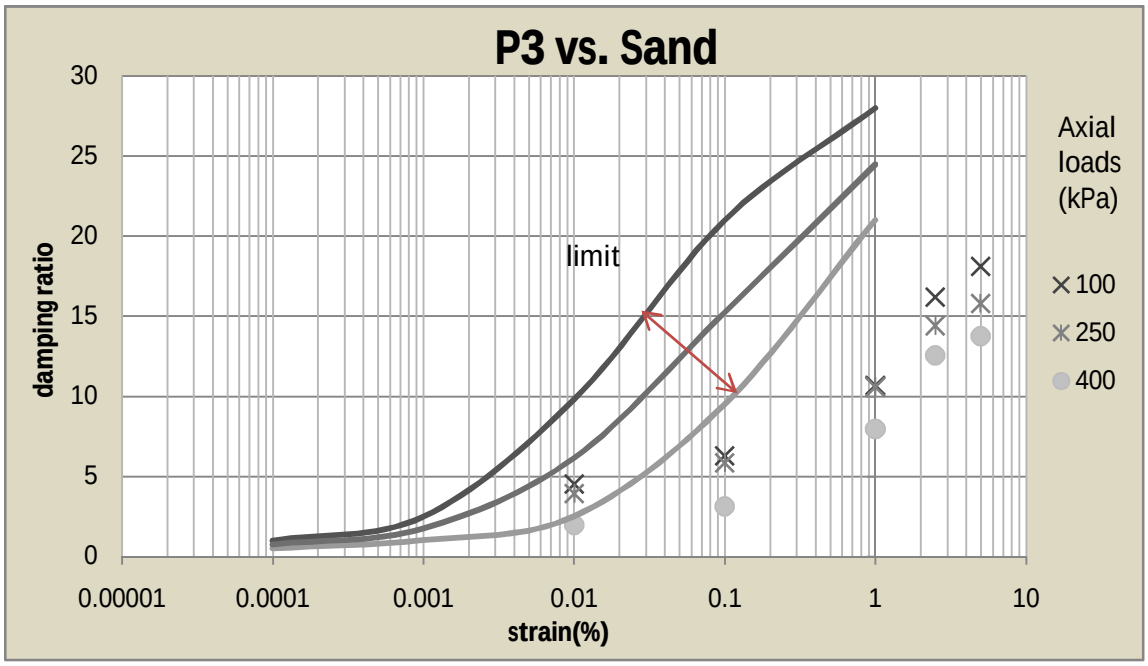


Figure F-1: Comparison of damping ratio of pit 2 with literature curves



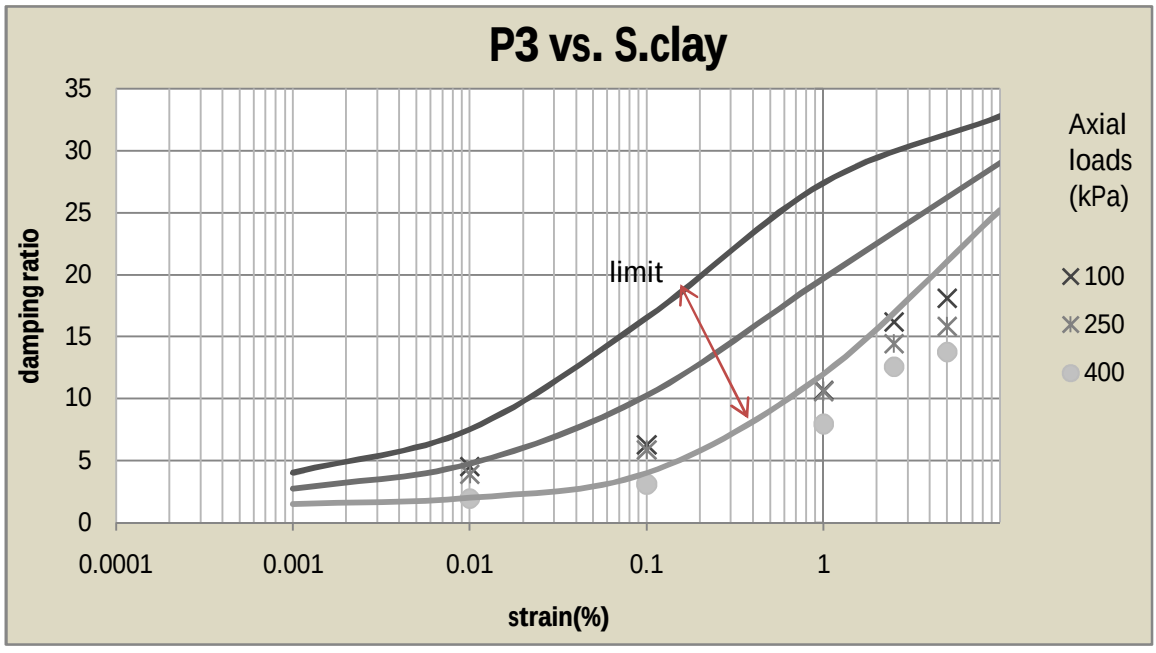
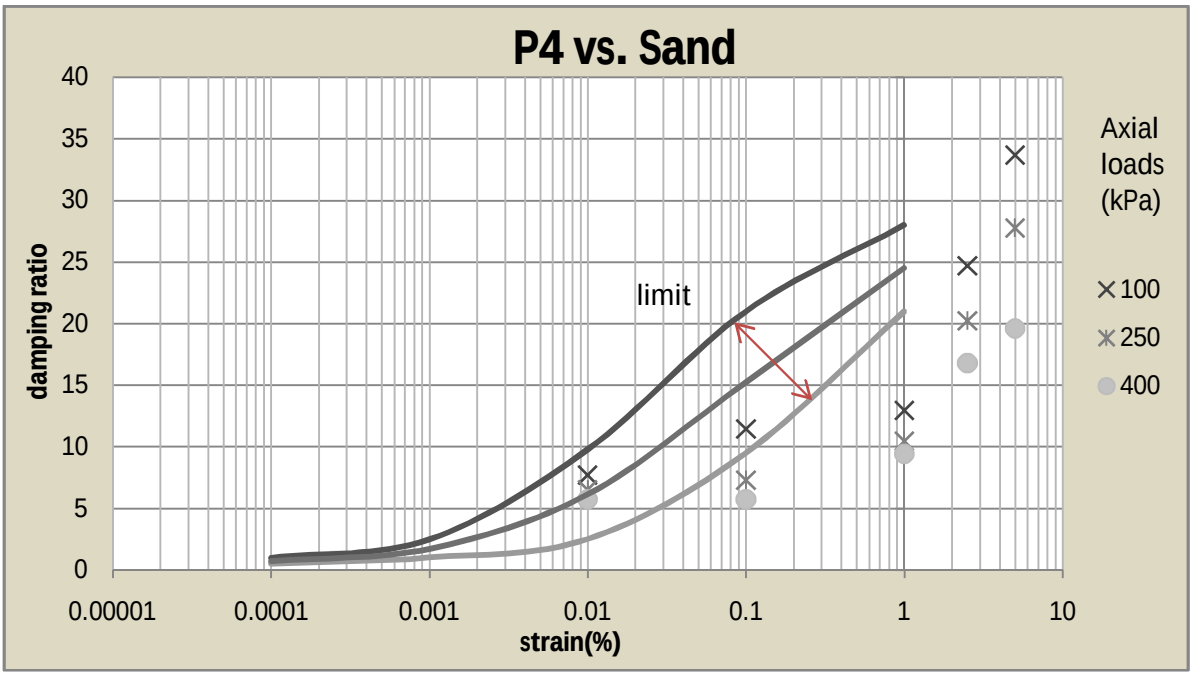


Figure F-2: Comparison of damping ratio of pit 3 with literature curves



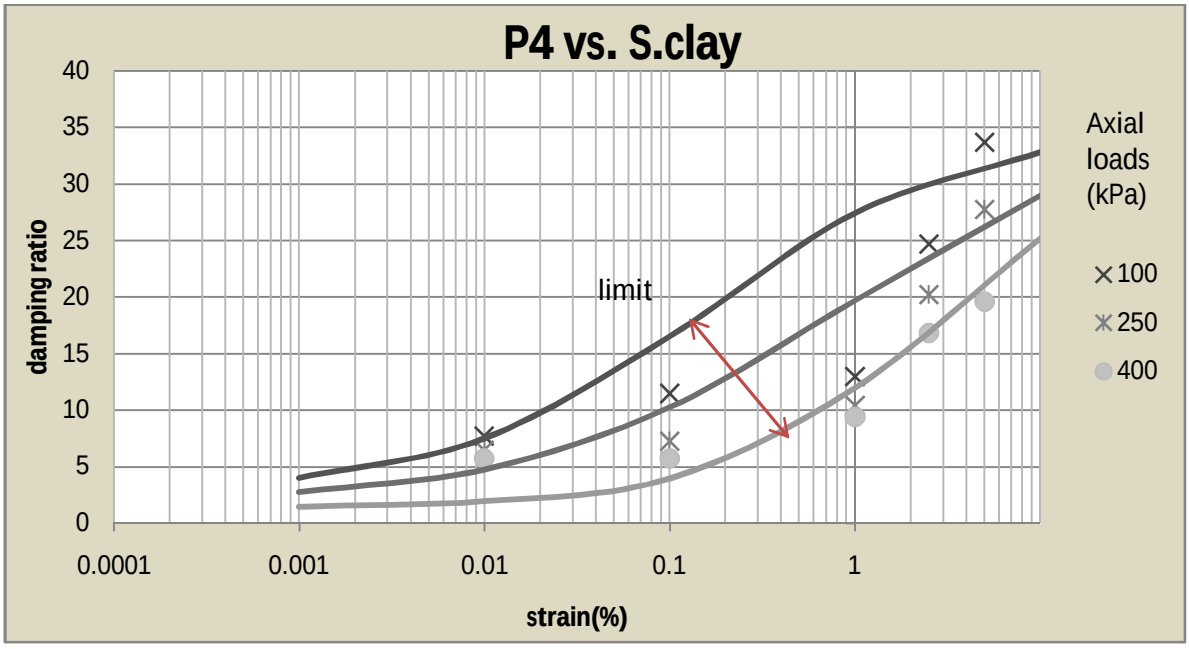
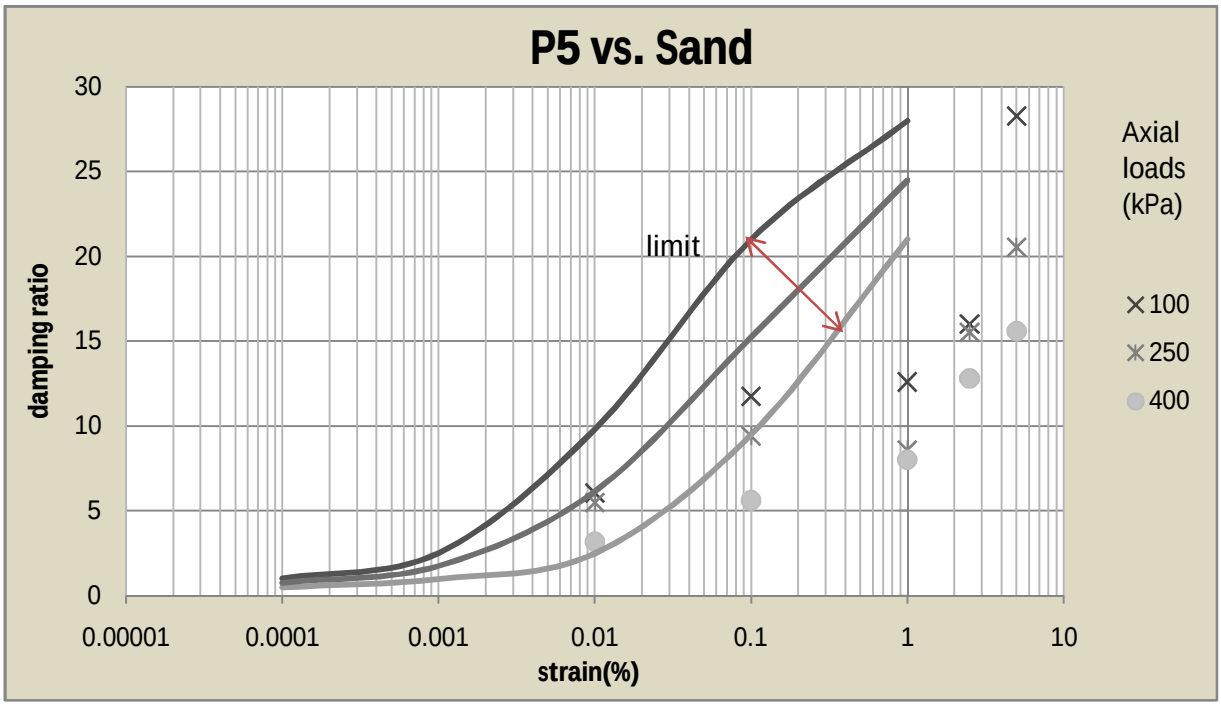


Figure F-3: Comparison of damping ratio of pit 4 with literature curves



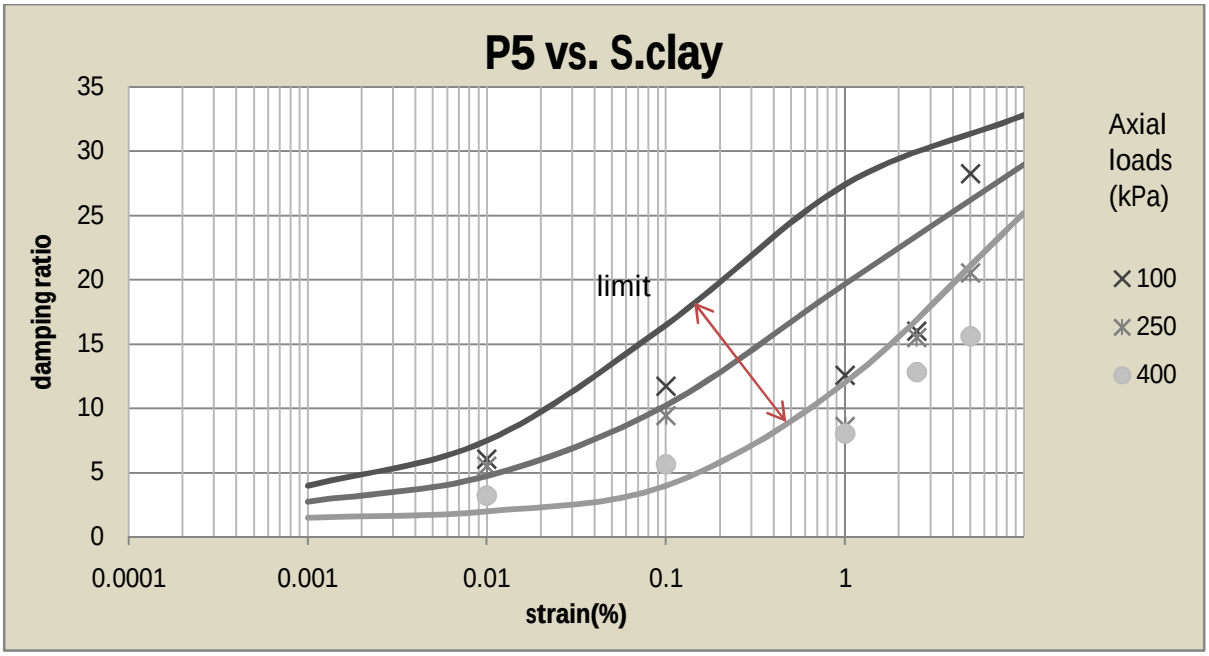


Figure F-4: Comparison of damping ratio of pit 5 with literature curves